NSK Technical Journal

Motion & Control

No.4
1998

NSK

ISSN 1342-3630

MOTION & CONTROL No. 4
NSK Technical Journal
Printed and Published: June 1998
ISSN1342-3630
Publisher: NSK Ltd., Ohsaki, Tokyo, JAPAN
Public Relations Department
TEL +81-3-3779-7051
FAX +81-3-3779-7431
Editor: Kyozaburo FURUMURA
Managing Editor: Yasuhiko MORITA
Design & Typesetting: Fuji Ad. Systems Corp.
Printing: Kuge Printing K.K.

Front cover: Ishibe Plant, NSK Ltd. (Japan)
Bennington Plant, NASTECH (USA)
Newark Plant, RHP Bearings Ltd. (UK)

NSK Technical Journal

Motion & Control

No.4 (1998)

NSK

Contents

Recent Technical Trends in Ball Screws

Mizuho Ninomiya and Kazuo Miyaguchi
Linear Motion Engineering Department,
Precision Machinery & Parts Technology Center

1. Introduction

Ball screws were first utilized as part of automotive steering systems by G.M. in the U.S. in the late 1930's. Twenty years later, the first ball screw was manufactured in Japan by NSK Ltd., and in 1961, NSK delivered its first precision ball screws for machine tools. Since then, as machine tools have become numerically controlled, ball screws have made great progress both in quality and production quantity. Applications for ball screws have been increasing due to their superiority over other linear motion-transmitting elements in terms of the balance between cost and performance, and their being widely recognized as easy to use and control.

In the mechatronics field for semiconductors, LCDs and robots in particular, demand for ball screws has grown to nearly equal that for ball screws used in machine tools. Additionally, demand for ball screws for special environment applications such as in aircraft, outer space and nuclear reactors is rising sharply. Considering this rising demand and broadening range of applications together with users' needs to continually improve their specific applications, the need for improved ball screw performance has no limit.

In this article, recently developed technologies for increasing the operational speed of ball screws and satisfying the diversifying needs of today's market are explained, and related new products are presented.

2. Response to Requirements for Higher Speed

The feed rate of NC machine tools, robots and electronic component-inserting machines has increased greatly in the past ten years, doubling and even tripling in some cases. Thus, the ball screws used in these machines have been and will continue to be required to achieve higher and higher speeds. Table 1 lists some examples of high-speed requirements.

The linear speed achieved by a ball screw is the product of screw lead and rotational speed. Next, we look into these two factors.

Table 1 High-speed requirements

units: m/min

	General high-speed level	Highest speed level	Target speed level for the near future
Machine tools such as machining centers	30 ~ 40	~ 60	80 ~ 100
Robots, punching presses, etc.	60 ~ 80	~ 120	150 ~ 200

2.1 Increasing ball screw lead

A ball screw is a screw mechanism which uses balls to achieve the following functions:

(1) Generating a larger force from a smaller force (torque or force-boosting function)
(2) Converting larger displacement to smaller displacement (speed-reducing function)
(3) Converting rotational motion to linear motion

In the past, ball screws were predominantly used for the speed-reducing function (2) and, in general, their leads were not so long. However, lengthening lead enables a higher feed rate with the same screw rotational speed. Therefore, in response to the need for ever-higher feed rates, there has been a tendency to increase lead length. In recent years, even in machine tools like machining centers, the use of ball screws with leads of around half of their screw shaft diameters, such as those in the HMC Series for high-speed machine tools, has increased. In addition to the HMC Series, NSK has developed several different series for robots and transporting equipment, applications in which function (3) is more important than functions (1) or (2). These include its:

- Triple Lead Series (Photo 1)
- Precision High Helix Lead/ Ultra High Helix Lead Series
- Rolled High Helix/ Ultra High Helix Lead Series
- Miniature High Helix Lead/ Ultra High Helix Lead Series

Triple Lead Series ball screws developed by NSK were

Photo 1 Triple Lead Series

the first in the world to have leads almost three times the screw shaft diameter. In the Miniature High Helix Lead/Ultra High Helix Lead Series, we have successfully developed ball screws in the 8 to 12 mm-diameter range with very long leads previously thought difficult, if not impossible to attain.

In order to make high speed and high precision compatible, it is necessary to maintain a good balance between lead and rotational speed. Improvement of high-speed rotational performance is becoming increasingly important.

2.2 Improvement of high-speed rotational performance

Problems which need to be addressed in order to increase ball screw rotational speed include the following:

(1) Limiting speed determined by d_mN (the revolving speed of the balls)
(2) Limiting speed determined by the critical speed of the screw shaft
(3) Increase in vibration and noise
(4) Increase in temperature and thermal deformation
(5) Increase in load caused by higher speed and higher acceleration/deceleration

Next, these problems and their countermeasures are explained, and related new products are presented.

2.2.1 Limiting speed determined by d_mN

When d_mN (d_m – ball pitch diameter in mm, N – rotational speed of screw in rpm; this represents the revolving speed of the balls) reaches certain levels, the repetitive shocks generated by the balls cause damage to the ball re-circulating mechanism and screw grooves. Therefore, the maximum speed of a ball screw is limited by this value. Fig. 1 illustrates the measuring method used to determine the force exerted on the tongue (pick-up finger) of a ball return tube. Measurement results are shown in Fig. 2. Force was generated by each ball entering the ball return tube; however, it was determined that nearly no force was generated when the balls exited the tube. Fig. 3 is a graph showing the proportional relationship between

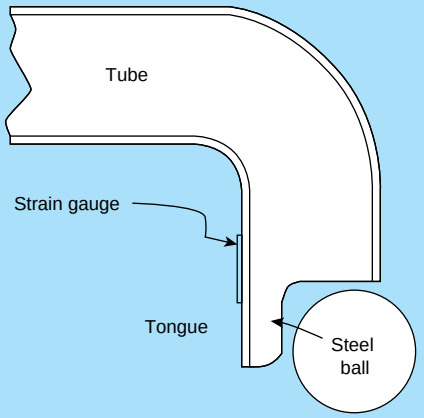

Fig. 1 Method used to measure impact force on ball return tube tongue

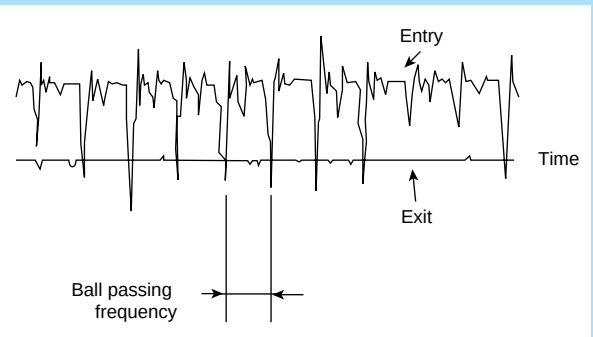

Fig. 2 Measurement results of impact force on tongue

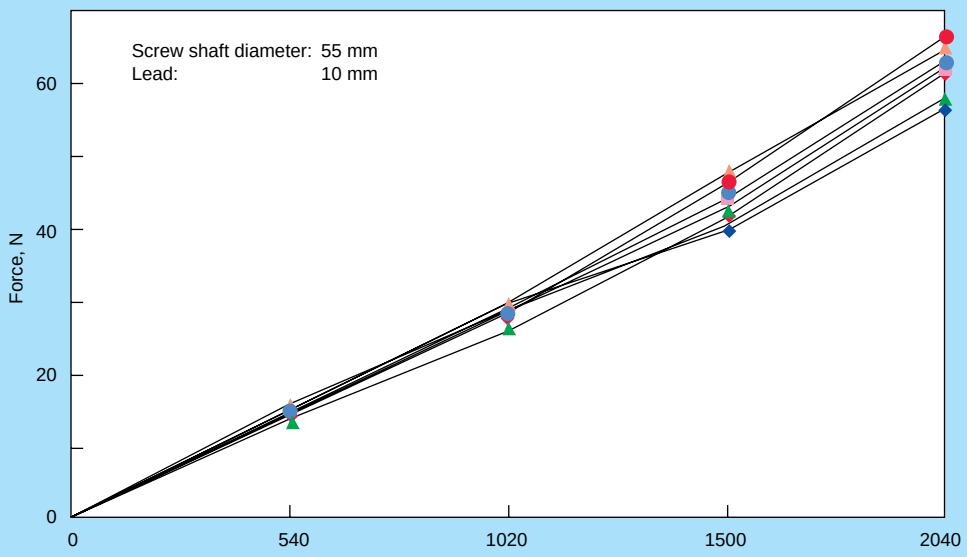

Fig. 3 Rotational speed and impact force

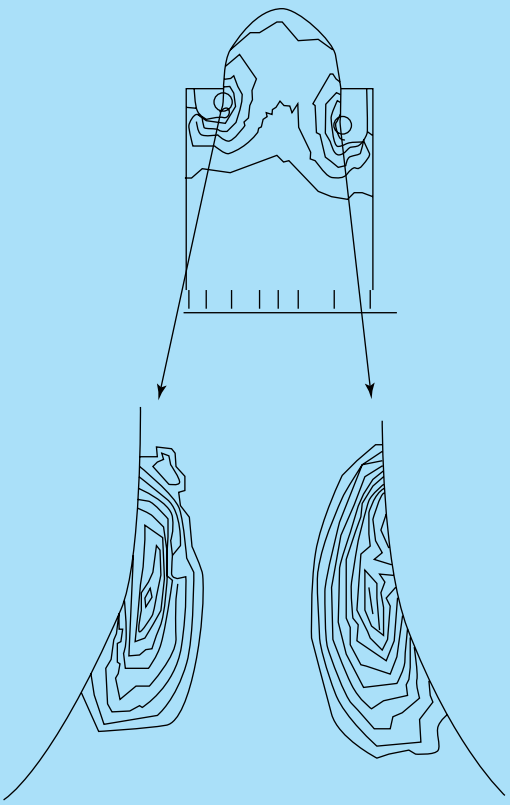

Fig. 4 FEM analysis of stress on ball return tube tongue

ball speed and force magnitude. This supports the theory that the transfer of energy between the balls and the return tube tongue causes deformation of the tongue.

Fig. 4 shows data obtained through FEM (finite element method) analysis of the stress distribution when a ball collides with the return tube tongue. The data in this figure can be used to develop measures to strengthen the return tube tongue.

We are designing and manufacturing ball re-circulating mechanisms which can withstand increasing d_mN values by improving and strengthening the raw materials used in their production and determining the optimum shapes for the ball grooves and tongue of the ball return tube through the analysis of shock force measurements, FEM analysis and high-speed endurance tests.

The ordinary guaranteed d_mN value for ball screws has been 70 000, but we have developed and marketed ball screws with a guaranteed d_mN value of 150 000 through the application of the aforementioned methods, and have conducted high-speed tests exceeding 200 000 d_mN in our laboratory.

2.2.2 Limiting speed determined by the critical speed of the screw shaft

The maximum speed of a ball screw with a long stroke is governed predominantly by the critical speed of the shaft. As these kinds of ball screws have long and narrow shafts supported at both ends, great resonance occurs at high speeds when rotational speed reaches the natural frequency of the shaft. The speed at which this resonance occurs is called the critical speed of the shaft and the effects of this resonance include screw shaft vibration on the order of several millimeters which causes damage to the grooves as well as extreme vibration of the entire machine, excessive noise generation, and instability of the servo system.

As a ball screw is supported at both ends with a moving ball nut in the middle, there are different beams with different natural frequencies on either side of the ball nut. These natural frequencies vary as the nut moves along the shaft. Fig. 5 is a graph showing the relationship between natural frequency, the critical speed of a screw shaft and rotational speed.

The operation of a ball screw with a long stroke at high rotational speed has been considered difficult. The wide-ranging natural frequency of screw shafts is one of the reasons. The countermeasure for this, which is to provide the shaft with intermediate support and increase its natural frequency, had been known for some time, but was not reported on until Tamaki et al[1] explained how they achieved a super high feed rate through the use of this method.

Generally, ball screws are operated with screw shaft rotation; although with a long stroke and when driving several tables with one screw shaft, a rotating ball nut offers advantages in terms of load inertia to driving motors and control. However, problems with critical speed are likely to arise in these cases.

NSK's nut-rotating type ball screw with built-in vibration damper (patent pending) achieved higher speed through the use of a vibration damper as a countermeasure against the critical speed of the shaft. A peculiarity of ball screws, as mentioned above, is that, since the critical speed of the shaft varies as the nut is moved and the shaft frequency changes, the resonance point is reached only momentarily. For this reason, a simple solution - incorporating a vibration damper in the

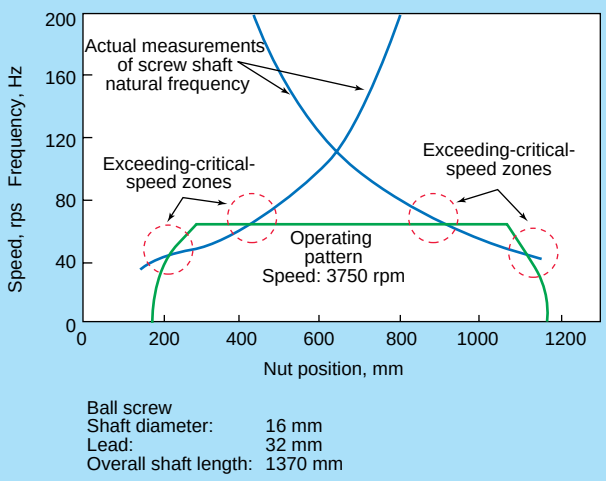

Fig. 5 Natural frequency and critical speed of screw shaft

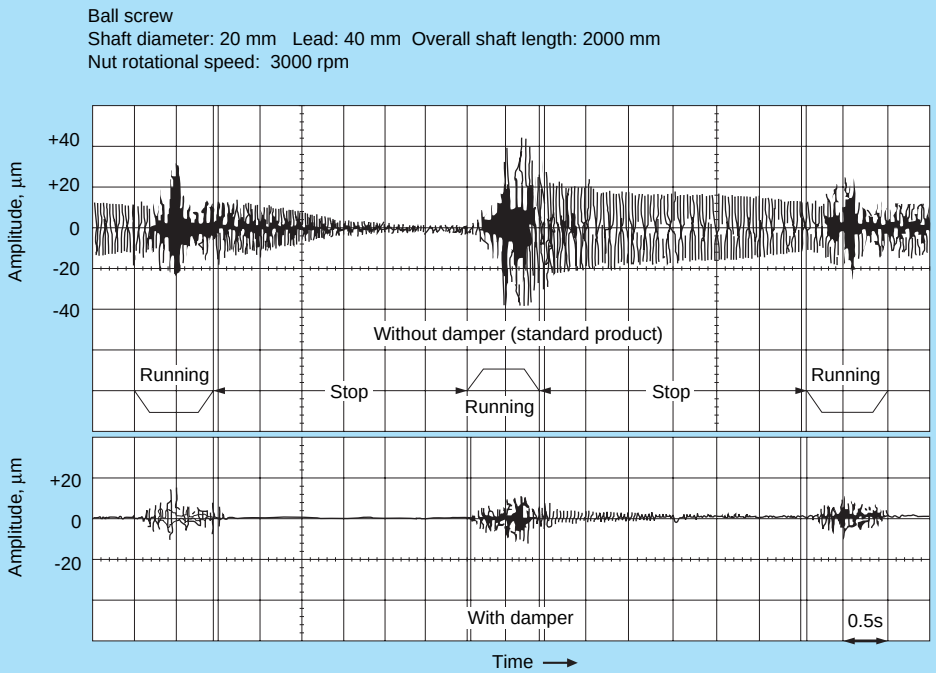

Fig. 6 Effect of damper on screw shaft vibration

hollow screw shaft - achieves outstanding results with only a moderate cost increase and no increase in the ball screw outer dimensions.

Fig. 6 compares the vibration of two screw shafts, one with and one without the vibration damper, at 3 000 rpm. The screw shaft diameter was 20 mm, the lead 40 mm, and the length 2 000 mm. The results clearly demonstrate the efficiency of the vibration damper.

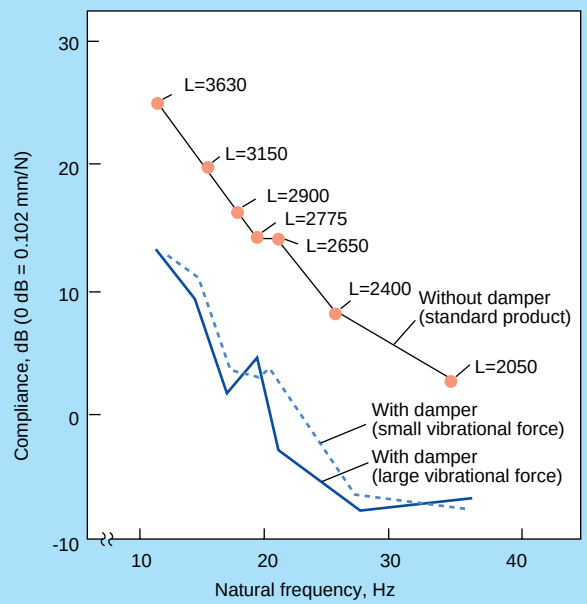

Ball screw
Shaft diameter: 40 mm
Lead: 40 mm
Overall shaft length: 4100 mm
L: Nut position (distance from fixed end in mm)

Fig. 7 Natural frequency and compliance

Fig. 7 shows the results of an experiment done on a screw shaft with a diameter of 40 mm and an overall length of 4 100 mm. The nut was moved and a vibration test was done at each point. The results are arranged based on the natural frequency of each nut position and compliance. Due to the vibration damper, great improvement of dynamic rigidity over a wide frequency range was observed.

Photo 2 is a visual comparison of two ball screws, one with and one without the damper, after high-speed endurance tests during which the critical speed was reached. Flaking of the nut groove was observed on the one without the damper after 2 000 km of operation. However, even after 10 000 km, the ball screw with the damper showed nearly no deterioration.

The efficiency of NSK's ball screw with vibration

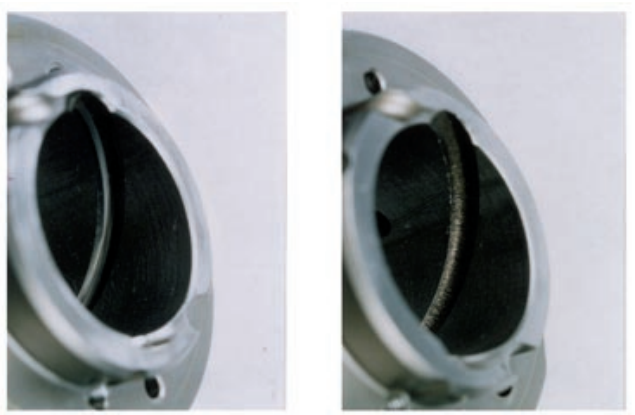

With damper Without damper

(Extent of deterioration of ball nut groove after 5 000 km running)

Photo 2 Effect of damper on ball nut groove endurance

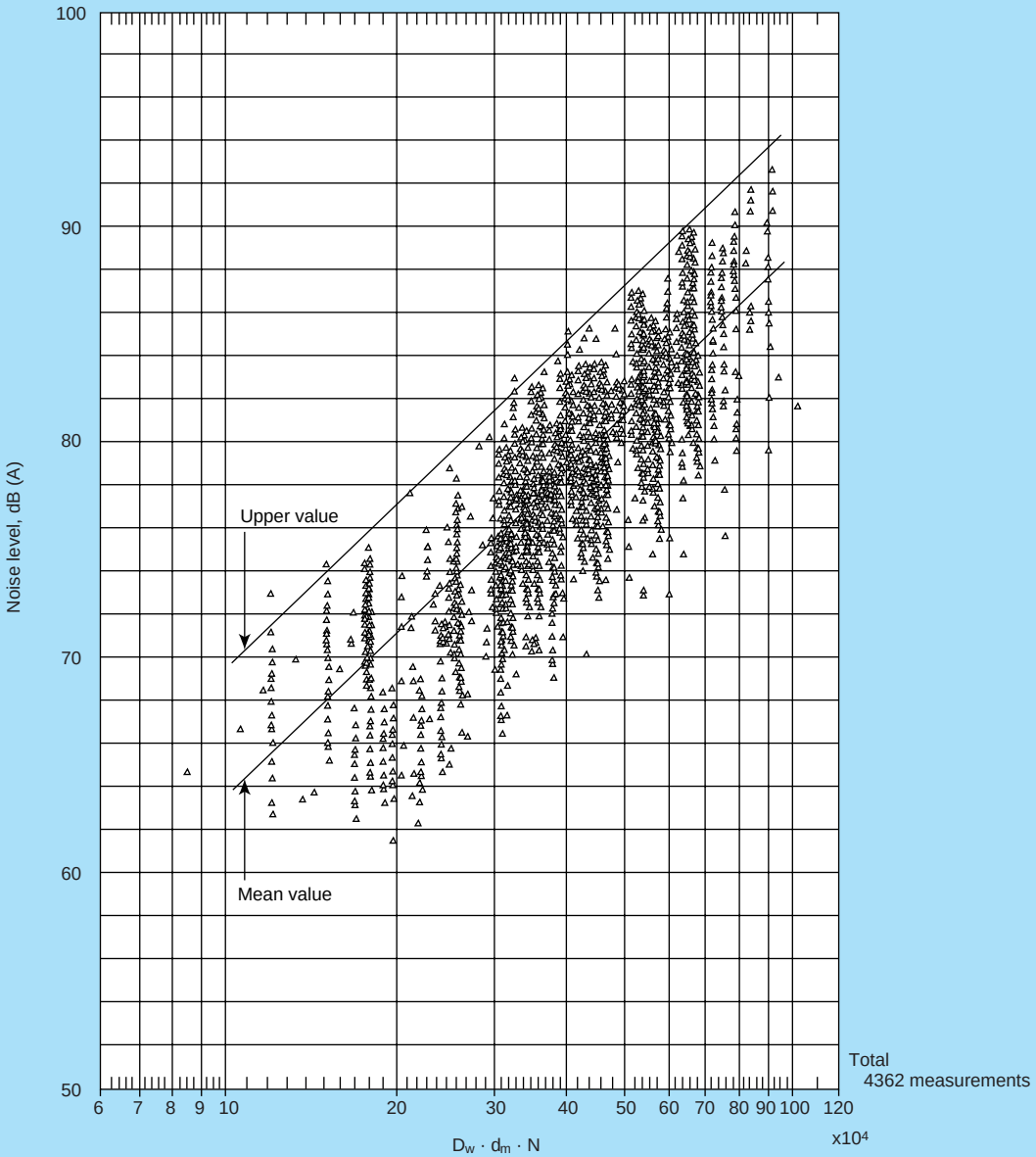

Fig. 8 Noise level data

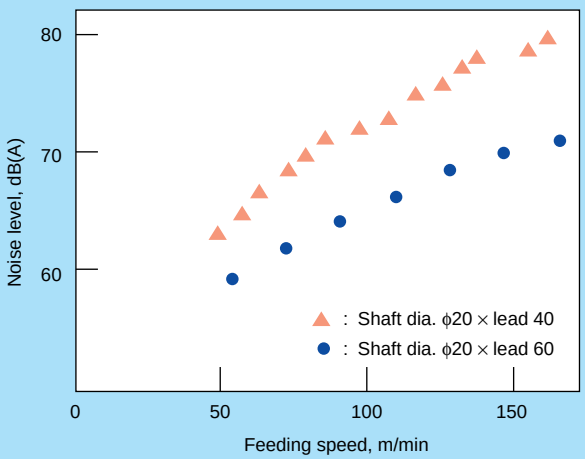

Fig. 9 Noise level and lead

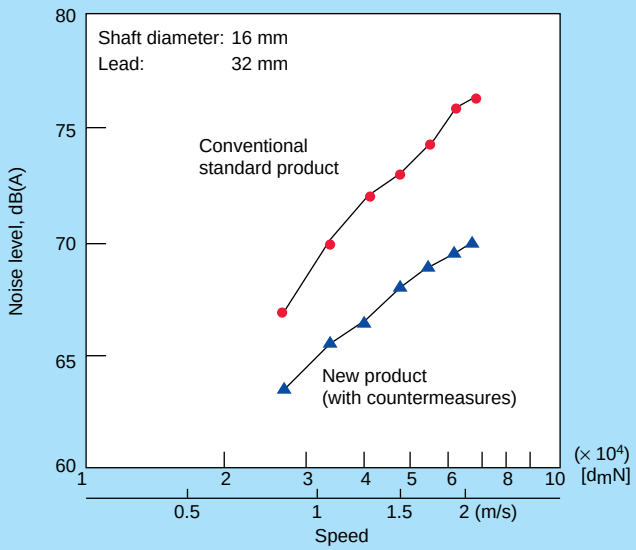

Fig. 10 Effect of product improvement on noise level

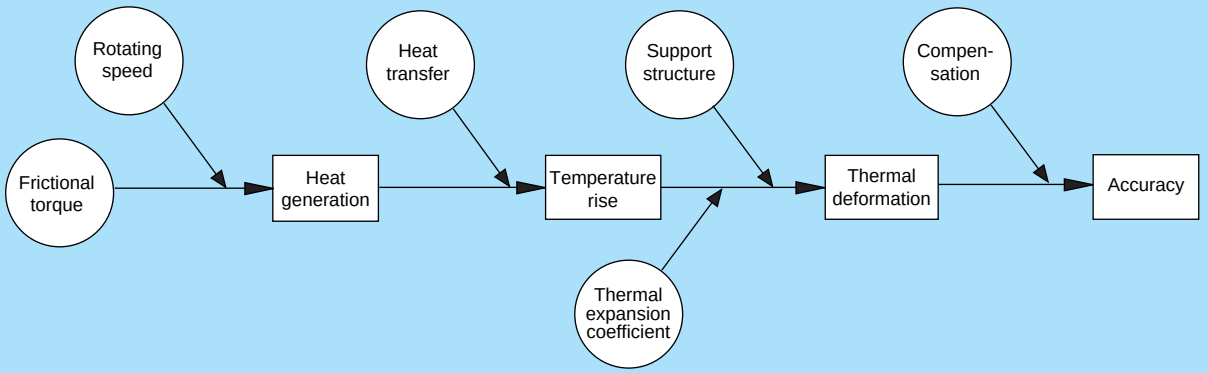

Fig. 11 Factors relating to thermal problems

damper, as illustrated in photo 2, serves to refute previously held notions that high-speed operation of a ball screw with a long stroke was impossible.

2.2.3 Increase in vibration and noise

The balls in a ball screw, since they are constantly being re-circulated by the return tube, generate noise and vibration similar to flaw noise of rolling bearings. After determining that ball diameter, D_w (which reflects mass) and d_mN were the dominant factors, we have come up with an equation for the noise generated by a ball screw through the analysis of 4 362 units of measurement data obtained in diverse experiments involving precision ball screws (please see Fig. 8)[2]. Using the equation, a noise scale was obtained which can predict the influence of high speed on noise, as well as the effects of quality improvement or new design ideas on noise reduction.

Fig. 9 compares noise generated by ball screws with differing leads at the same feed rate. It shows that making lead longer to reduce rotational speed (N) is also one way to reduce noise.

In addition, the quality of the rolling surfaces affects the generation of ball screw noise and vibration. Essentially, higher quality means less noise and vibration. Therefore, methods to improve surface accuracy, such as superfinishing of the screw grooves, have been developed and advanced technology has been applied to the design and manufacturing of ball screw rolling surfaces. In Fig. 10, the noise generated by a single axis table with a ball screw incorporating the above improvements is compared with that of a single axis table with a standard ball screw. As is apparent, significant noise reduction has been achieved.

2.2.4 Increase in temperature and thermal deformation

As ball screw speed increases, so too do temperature and thermal deformation. Fundamentally, the ball screw is a feeding screw which uses rolling contact, in place of sliding contact, to reduce friction. For this reason, even though a certain degree of preload is applied to insure high precision, heat generation due to friction is not so high. Nonetheless, heat generation has become an important problem for ball screws for the following reasons:

(1) Ball screws directly affect machine positioning accuracy and are required to be highly precise in the longitudinal direction over their entire length.
(2) Although the ball screw is an integral part of a machine, most of its surface is exposed to the air making heat transfer with other parts limited.

For this reason, we believe it is important to discuss thermal problems separately from others.

Fig. 11 shows how various factors affect and relate to thermal problems and various countermeasures. Next, these factors and countermeasures will be discussed.

The heat generated by a ball screw is the product of frictional torque and speed:

$$Q = 0.12\pi NT$$

Where, Q: heating quantity per unit of time (kJ/hr)
N: rotational speed (rpm)
T: frictional torque (N·m)

The temperature rise is determined by the difference between the heating quantity and the heat transfer value, including forced cooling:

$$\theta = (Q/\beta)\,[1 - \exp\{-(\beta/CM)\cdot t\}]$$

Where, θ: temperature rise (K)
β: heat transfer value per unit of time, unit temperature difference (kJ/hr/K)
CM: heat capacity (kJ/K)
t: time (hr)

The right part of the equation in brackets, [ ], represents secular change and reflects that the amount of time until temperature stabilization occurs is related inversely to the heat transfer value.

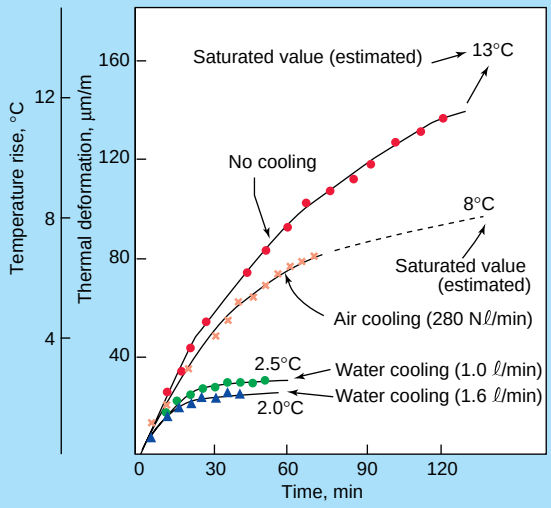

Screw shaft diameter:	70 mm
Lead:	20 mm
Average speed:	177 rpm
Nut stroke:	1800 mm

Fig. 12 Effects of various cooling methods on a hollow ball screw shaft

Thermal deformation is determined by the temperature rise, a thermal expansion coefficient and the overall rigidity of the ball screw's surrounding structure, including support bearings, housing, connecting parts, etc. The extent to which machine accuracy is affected by thermal deformation is decided by how well it is compensated for through closed loop control.

Methods for reducing heat generation in ball screws include limiting screw rotational speed by increasing lead length and reducing frictional torque by applying appropriate preloads. Recent efforts on this problem at NSK have produced a ball screw with adjustable preload for which a patent is pending[3].

A very efficient method for increasing heat transfer in ball screws is forced cooling[4]. NSK's hollow shaft ball screw series, which features holes in the shaft to allow for efficient coolant flow, uses this method and is becoming increasingly popular in the market. Fig. 12 shows how various cooling methods affect the temperature rise and saturation point of a hollow shaft ball screw. As can be seen, temperature rise and the amount of time until temperature saturation occurs have both been reduced. Among coolants, water is ten times more effective than oil and several thousand times more effective than air because of its lower viscosity and higher thermal conductivity, specific heat and density.

Additionally, many methods focusing on controlling and compensating for thermal deformation, rather than reducing it through cooling, have been developed, including special arrangements of ball screw shaft support and digital compensation via numerical controllers.

2.2.5 Increase in load caused by higher speed and higher acceleration/deceleration

To realize true high speed, it is imperative to increase not only maximum speed, but acceleration/deceleration as well. Especially when driving a heavy mass at high speed and high acceleration/deceleration, such as in a machining center, ball screw load and momentum per unit time increase, necessitating higher load capacity and rigidity. In response to this challenge, NSK developed its HMC Series ball screws for high-speed machine tools (Photo 3), which incorporate numerous high-speed countermeasures and achieve higher load capacity and rigidity. The HMC Series has the following features:

(1) Its maximum feed rate of 72 m/min was achieved by lengthening the lead, not increasing rotational speed. (lead/screw shaft diameter ≅ 1/2)
(2) Its high-speed endurance limit was increased through improvements in the design of the ball re-circulating mechanism and ball screw grooves.
(3) As a countermeasure to temperature rise and thermal expansion, its hollow shaft enables high accuracy.
(4) While load capacity and rigidity are normally adversely

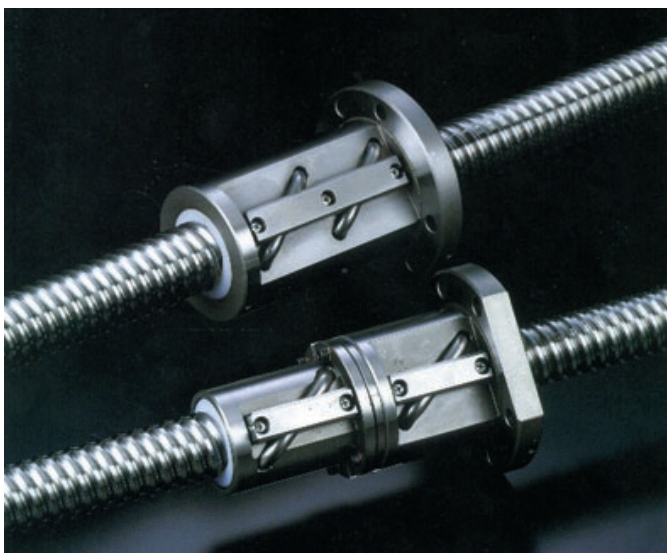

Photo 3 HMC Series ball screws for high-speed machine tools

Photo 4 Endurance test of high-speed and high-acceleration/deceleration work table

Table 2 Comparison of HMC Series with conventional products
(Screw shaft diameter: 45 mm, effective turns: 5)

Specifications		HMC Series		Conventional products
		Standard type	Compact type	
Lead	(mm)	25	25	12
Maximum feed speed	(m/min)	67	57	19
Rigidity*	(N/μm)	1 430	1 430	1 240
Dynamic load rating	(N)	77 200	77 200	64 140
Nut length	(mm)	228.5	228.5	227
Nut outside diameter	(mm)	101	92	90

* Rigidity value when the preload is 5% of the dynamic load rating.

Table 3 Test conditions of high-speed and high-acceleration/deceleration work table

Ball screw	HMC Series (HDF5030-5, shaft diameter: 50, lead: 30)
Linear guide	LA Series (LA45)
Weight to be loaded	19.6 kN (2000 kgf)
Acceleration/deceleration	1.3 G
Maximum speed	60 m/min (2000 rpm)
Running pattern	Step feeding, 100 mm/step
Stroke	600 mm

affected by the reduction in effective turns of the balls resulting from lengthening the lead, its double-threaded screw, optimum groove design and ideal ball diameter effectively counteract this effect and achieve high load capacity and rigidity.

(5) By utilizing single nut “thread off-set" preload, the ball nut is more compact than a double-nut configuration.

Table 2 compares major specifications of the HMC Series with ordinary series.

Photo 4 shows a high-speed and high-acceleration/deceleration work table with a feeding system constructed using an HMC Series ball screw and a new LA Series linear guide for machine tools. (Please see “LA Series Linear Guides” in the New Products section of this journal.) We are presently conducting an endurance test of this work table under very high acceleration/deceleration, repeating high-frequency short-stroke operation. The conditions of this test are outlined in Table 3. Encouraged by the progress shown by the HMC Series in endurance and functional characteristics tests, we are continuing development with our sights set on the next target: achieving a feed rate of 100 m/min.

3. Responses to Diverse Needs

3.1 High-load drive applications

High-load drive applications utilizing the force-boosting function of the ball screw are increasing. As electrically-powered numerical control replaces hydraulic cylinders in injection molding machines, presses and other machines, the use of ball screws is growing. There are cases in which ball screws are used in injection molding machines to control forces exceeding 50 tons. The requirements for such applications include super-high load capacity and durability, along with a short stroke. To fulfill such requirements, it is necessary to develop ball screws with load capacities higher than ever before, and also to establish technology for selecting the correct ball screw for a given application.

“HTF Series” ball screws (Photo 5) are NSK’s response to market demand for ball screws capable of driving heavy loads. Their super-high load capacity was realized through the following specifications which were made possible by the application of new production and machining techniques:

- Specially-designed groove profile, ideal groove dimensions and optimum ball diameter.
- The return tubes, rather than side by side, are on opposite sides of the nut making the load balanced in the circumferential direction.

Table 4 compares the load capacity of HTF Series ball screws with previous high-load ball screws. Table 5 and Photo 6 compare the results of severe endurance tests done on the HTF Series and previous high-load ball screws. The test results confirm that the durability of the

Photo 5 HTF Series ball screws for high-load drive

Table 4 Comparison of HTF Series with conventional products

Nut model		Screw shaft diameter (mm)	Permissible dynamic load (N) (target)	Basic static load rating C_{0a} (N)	Basic dynamic load rating C_a (N)
HTF Series	HTF8020-7.5	80	230 400	1690 000	511 000
Conventional products	Stand. spec. SFT8020-7.5	80	110 000	874 000	230 000
	Special spec. 8020-7.5	80	173 600	1440 000	445 000
	Special spec. 10020-7.5	100	225 500	1820 000	500 000

Conventional product
Flaking occurred after 1.3×10^6 shots

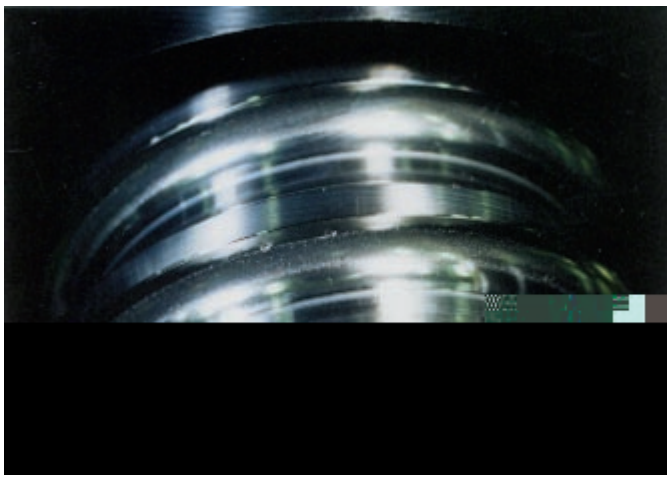

HTF Series
No abnormality after 6.5×10^6 shots

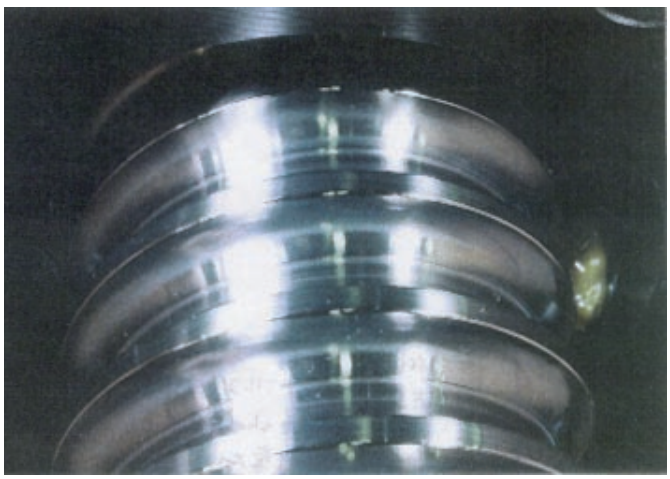

Photo 6 Screw shaft appearance after severe endurance test

Table 5 Results of severe endurance test

	Conventional products		HTF Series	
Sample No.	1	2	3	4
Ball screw specifications	Screw shaft diameter: 80 mm, lead: 20 mm, 2.5 turns, 3 circuits			
Maximum axial load	283 kN			
Maximum contact surface pressure	2 300 MPa		2 180 MPa	
Stroke	100 mm	50 mm		
Lubrication	Conventional grease			Recommended grease
No. of shots until flaking	1.3×10^6	1.05×10^6	2.5×10^6	8.0×10^6 continuing
Total no. of shots	2.0×10^6	1.2×10^6	4.2×10^6	No abnormality

HTF Series is 2 to 3 times higher than previous high-load ball screws which were specially designed for their particular applications.

While developing the HTF Series, we conducted durability tests on a ball screw suitable for high-load/short-stroke applications. During these tests, load and stroke were varied. Using the results, we have come up with a life-estimating equation based on the general rating fatigue life equation, but modified with surface pressure and stroke coefficients:

$$L = \{ C_a/(F_a \cdot f_w \cdot f_c \cdot f_L) \}^3 \times 10^6$$

Where, L: Rating fatigue life (rev.)
C_a: Basic dynamic load rating (N)
F_a: Axial load (N)
f_w: Load factor
f_c: Surface pressure coefficient $f_c = (P_{max}/1961)^3$
provided that when $P_{max} \leq 1961$, $f_c = 1$
P_{max}: Maximum contact surface pressure (MPa)
f_L: Stroke coefficient $f_L = 2/S^{1/2}$
provided that when $S \geq 4$, $f_L = 1$
S: Stroke (rev.)

Especially under such severe conditions, the selection of a suitable lubricant is very important for high durability. NSK provides assistance in selecting suitable greases for high-load ball screws.

3.2 Maintenance-free

In an effort to greatly increase maintenance intervals, NSK has developed Molded Oil and used it to create its "NSK K1 Seal™", compact lubricant-supplying units for ball screws and linear guides. As a detailed account of the development and testing of Molded Oil and the K1 Seal has already been given in "Motion and Control" No. 2 ("Development of "Molded Oil" and Its Application to NSK Linear Guides"), in this article we focus specifically on K1 Seal ball screw applications. Fig. 13 shows the structure of a ball screw with a K1 Seal. Fig. 14 compares test results on the durability of a ball screw for light load transporting with a K1 Seal and one without any lubrication. The test results confirm the high lubricating effectiveness of the K1 Seal. Additionally, durability tests on high-load ball screws for machine tools with grease and K1 Seal lubrication were performed. (The test rig is shown in Photo 7.)

The test conditions were as follows:

Shaft diameter:	40 mm
Lead:	20 mm
No. of effective turns:	2.5×1
Axial load:	4 700 N (Upper limit for this application)
Stroke:	450 mm
Speed:	2 000 rpm (40 m/min)
Lubrication:	AV2 grease and K1 Seal (Initially packed AV2 grease was not replenished)

After 5 600 km of operation (exceeding the target of 5 000 km), the results were as follows:

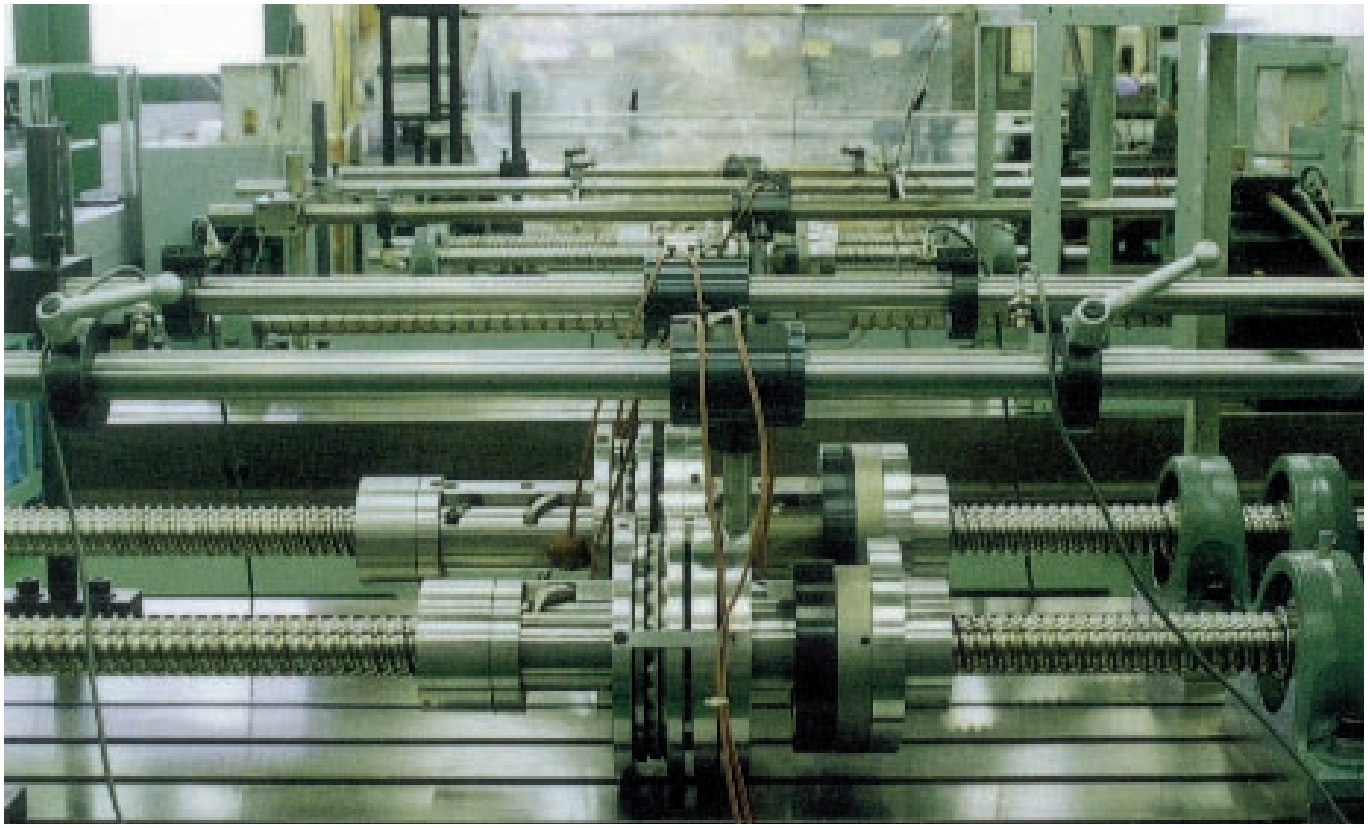

Photo 7 Endurance test of ball screws with K1 Seals

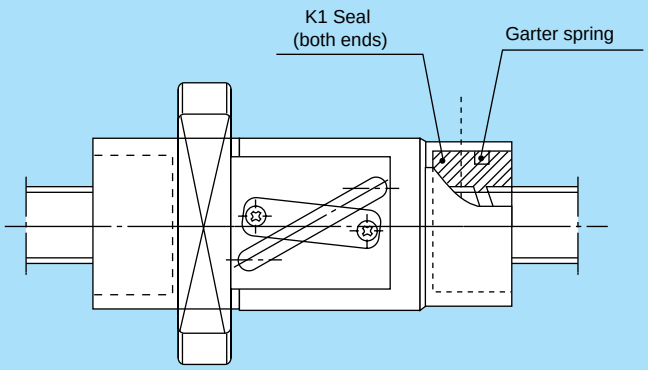

Fig. 13 Structure of ball screw with K1 Seal

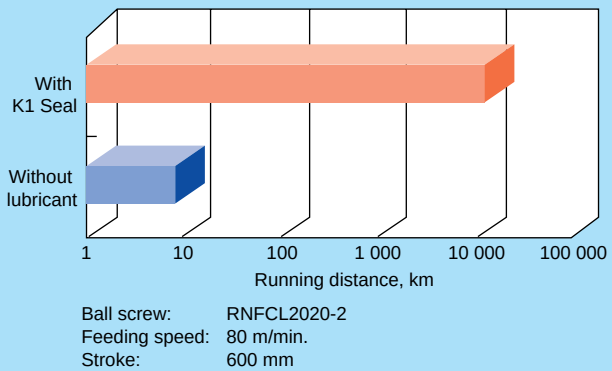

Fig. 14 Ball screw running test with K1 Seal

(1) Upon visual inspection, running traces of the balls were observed in the grooves, but no abnormality was present.
(2) The total wear of the balls and grooves was evaluated by measuring the clearance between the balls and nut before and after the test with the preload released. The variation in clearance between before and after the test was minimal, less than 0.5 µm.
(3) Other analyses conducted on torque and various components of the ball screw revealed nearly no variations.

A similar durability test under high-load conditions like those of a machine tool with only a K1 Seal for lubrication was conducted in order to assess and improve the maintenance-free attribute of the K1 Seal. After 3 500 km of operation (exceeding the target of 3 000 km), results like those explained above were obtained.

Through the outstanding results of these and other tests, we have confirmed the high efficiency of the K1 Seal in lubricating ball screws, particularly those operating in the high-load conditions of machine tools. In our further efforts, we will focus on accumulating research data to assist in the improvement of the maintenance-free attribute of the K1 Seal.

3.3 Clean environments

Semiconductor and LCD production must be carried out in an extremely clean environment. Therefore, the minuscule particles generated by the lubricant when the ball screw rotates must be minimized.

Generally, the amount of particles generated increases

tenfold when ball screw speed doubles, though this varies greatly depending on the type of grease. Fluorine-based grease, while usually used for vacuum environments, is used under normal atmospheric pressure conditions when high cleanliness is required due to its low particle generation. However, it presents the following problems:

(1) As speed increases, the frictional torque caused by lubrication resistance increases markedly causing heat generation and motor overload.
(2) Compared to ordinary grease, fluorine-based grease is inferior in terms of wear resistance, durability and anti-corrosive properties.

Table 6 Comparison of grease characteristics

Characteristics	LG2	Grease A	Grease B	Grease C	Grease D
Thickener	Lithium soap	Lithium soap	Fluorine compound	Lithium soap	Fluorine compound
Consistency (60 W)	207	273	265	270	250
Type of base oil	Mineral oil and synthetic hydrocarbon	Mineral oil	Fluorine oil	Ester oil and mineral oil	Fluorine oil
Kinematic viscosity of base oil (mm^2/s, 40°C)	30	130	240	15	350

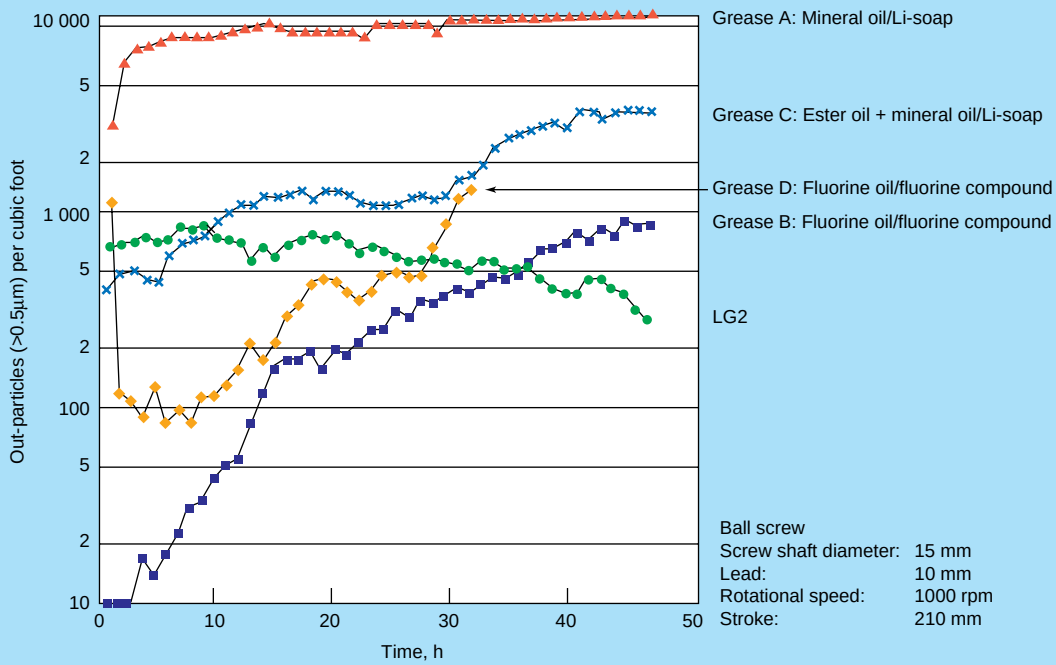

Fig. 15 Particle generation by grease

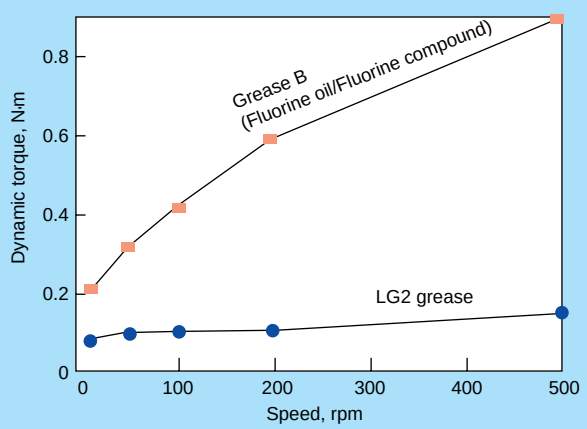

Fig. 16 Dynamic torque by grease type

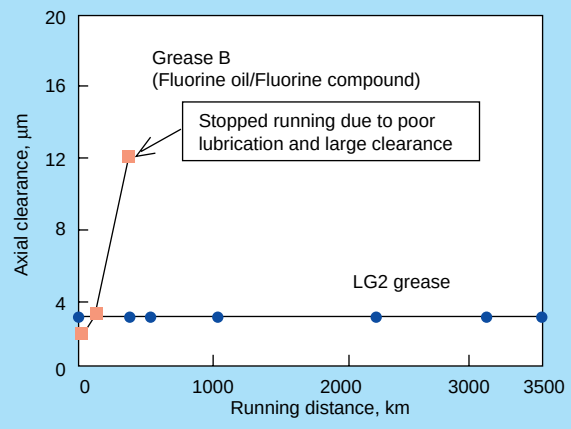

Fig. 17 Effect on wear by grease type

To overcome these problems, NSK developed LG2 clean grease, a low particle-generating grease which retains the positive characteristics of ordinary grease. Table 6 compares basic characteristics of LG2 with four other greases. Test results on particle generation are shown in Fig. 15. They show that different greases generate varying amounts of particles just after being packed. And, more importantly, the test results demonstrate that, after running-in, LG2 is very stable and generates the fewest particles. Additionally, comparative tests were done on LG2 grease and a fluorine-based grease for vacuum environments. Fig. 16 shows test results on dynamic torque and Fig. 17 shows test results on wear resistance. The anti-corrosive properties of LG2 and two other greases are compared visually in Photo 8. As all of the test results indicate, LG2 is clearly superior to competing products.

Presently, NSK is working on the development of a clean grease with better overall characteristics for high-temperature and vacuum environments.

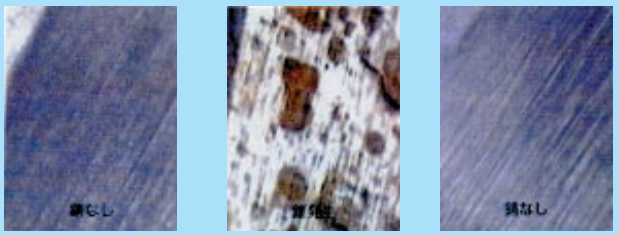

LG2 grease coating | Grease B coating (fluorine-based grease) | Grease C coating (general grease)

Test conditions
Humidity: 95%
Temperature: 70°C
Time: After 96 hours

Photo 8 Anti-corrosive properties of grease

4. Conclusion

As mentioned in the beginning of this article, with the range of applications for ball screws widening, demand for higher-performance ball screws is diversifying and increasing. In this article, we have presented just a part of the technologies and products NSK has developed in response to the requirements of today's market.

Other recently developed products include:

1. a series of ball screws with low-inertia rotatable nuts (with reduced outer dimensions of the nut housing and ball bearings installed on the ball nut)
2. "Robotte™": a series of products combining ball screws and splines (utilizing the same ball nut construction of the low-inertia rotatable nut series)
3. low-priced VFA Series precision ball screws for factory automation
4. RMA and RMS Series miniature rolled ball screws.

Goals for future technology development include:

1. a solid lubricant for outer space and vacuum applications
2. countermeasures for special environments, such as in aircraft and nuclear reactors
3. highly effective sealing technology for preventing dust penetration
4. surface treatment technology for rust prevention and chemical resistance
5. improved stainless steel and nonmagnetic material technology
6. optimum lubrication technology for every specific application.

We will report on the above products and technologies in more detail at another time.

References:

1) Tamaki, A., "Elements for ultra-high speed/low noise linear motion table," Mechanical Automation, Vol.25, No.3 (1993), 43. [in Japanese]
2) Kajita, T., Ishikawa, A., "Noise Level of Precision Ball Screw," "Motion & Control," NSK Ltd., No.1, (1996), 37.
3) Yamaguchi, T., "Technology in Improving Ball Screw Functions," J.JSPE, Vol.61, No.3, (1995), 333. [in Japanese]
4) Ninomiya, M., "Temperature Rise and Its Countermeasures of Ball Screw," Machine Tool & Machine Technology, Vol.28, No.4 (1987), 98. [in Japanese]

Mizuho Ninomiya

Kazuo Miyaguchi

Research and Development of Bearings for Special Environments

Hiroyuki Ito
Basic Technology Research and Development Center
Shigeki Matsunaga
Precision Bearing Technology Department, Bearing Technology Center

1. Introduction

For about 10 years, NSK has produced and supplied rolling bearings, ball screws and linear guides which support the state-of-the-art machinery and instruments used in special environments like outer space, and those required for the production of semiconductors, liquid-crystal panels and hard disks[1].

Resulting from recent technical innovation in the computer, aerospace and other industries, bearings used in clean environments, such as those found on semiconductor and liquid-crystal panel production lines, are strictly required to meet the limitations set for the number and size of out-particles they generate in operation. Additionally, bearings used in cleaning equipment, where solutions are more caustic than ever before, are required to be increasingly corrosion-resistant. Thus, the requirements of bearings for special environments have become more demanding from year to year.

To meet these advancing, state-of-the-art requirements, NSK has developed its own tribological, material, surface treatment, and evaluation technologies, and applied them to developing and improving the bearings, ball screws, and linear guides in its "SPACEA Series" for clean, vacuum, and corrosive environments (Photo 1). SPACEA Series products meet the strict industrial requirements that are the result of ever-advancing technology. In this article, the technologies behind the SPACEA Series are explained, and SPACEA Series products and their features are presented.

Photo 1 SPACEA Series

2. New NSK Technologies

2.1 Technologies for reducing out-particle generation

2.1.1 Clean grease

Bearings, ball screws and linear guides used in diffusion furnaces and steppers that must be kept clean, must not generate grease and wear particles. (Note: Both grease and wear particles are collectively referred to as out-particles throughout this report.) For applications such as these, whether in vacuum or normal atmospheric conditions, various types of commercially available, relatively low out-particle-generating fluorine grease have been conventionally used[2]. However, fluorine grease presents problems with its high torque, strong tendency to cause corrosion and wear, and high cost.

Ahead of other bearing manufacturers, NSK, applying its wide-ranging knowledge of and experience with grease, has developed very low out-particle-generating clean greases which solve the problems associated with conventional fluorine grease[3]. Table 1 lists the properties of these clean greases, and Fig. 1 shows their application ranges.

LG2 grease is a lithium soap grease with very low out-particle generation. It can be used in temperatures up to 70°C. LGU grease is a urea-based grease which can be used in moderately high temperatures not exceeding 120°C. LGF grease is a long-life fluorine grease for vacuum applications.

Out-particle generation by bearings lubricated with LGU, LG2 and other commercially available greases is compared in Fig. 2. LGU grease generates slightly more out-particles than LG2 grease does, but much fewer than the commercially available greases do. LGU grease does not contain sulfur, salt or metals like lithium and sodium.

Table 1 Properties of clean greases

	Clean greases		Wear-resistant fluorine grease
	LG2	LGU	LGF
Base oil	Mineral oil and synthetic hydrocarbon oil	Synthetic hydrocarbon oil	PFPE
Thickener	Li-soap	Urea	PTFE
Kinematic viscosity of base oil (mm^2/s, 40°C)	30	94.8	200
Consistency (60W)	207	209	280

Out-particle generation by ball screws lubricated with LG2 and other commercially available greases is compared in Fig. 3[3]. The fluorine greases B and D, whose out-particle generation is relatively limited when compared to other commercial greases, tend to generate more out-particles with time. In contrast, LG2 grease tends to generate fewer with time.

LG2 grease, formulated with mineral oil and synthetic hydrocarbon oil, and LGU grease, formulated with synthetic hydrocarbon oil, have better lubrication and rustproof properties as well as lower torque, and are less costly than fluorine grease.

Table 2 compares the life and out-particle generation of LGF grease with other greases. LGF grease, while comparable to commercially available fluorine grease in out-particle generation, lasts about 5 to 10 times as long in bearings in vacuum conditions. This long life of LGF grease has been attained by treating a fluorine grease with an optimum wear-resistant additive developed through NSK's superior additive formulation technology.

2.1.2 Special low out-particle-generating fluororesin coating (LDF coating)

The temperature and the degree of vacuum conditions bearings are exposed to in sputtering and CVD equipment on semiconductor and liquid-crystal panel production lines have been increasingly higher as production lines have been producing larger-scale integrated circuits and larger panels. In response, solid lubricants are replacing vacuum grease in such bearing applications. Bearings coated with

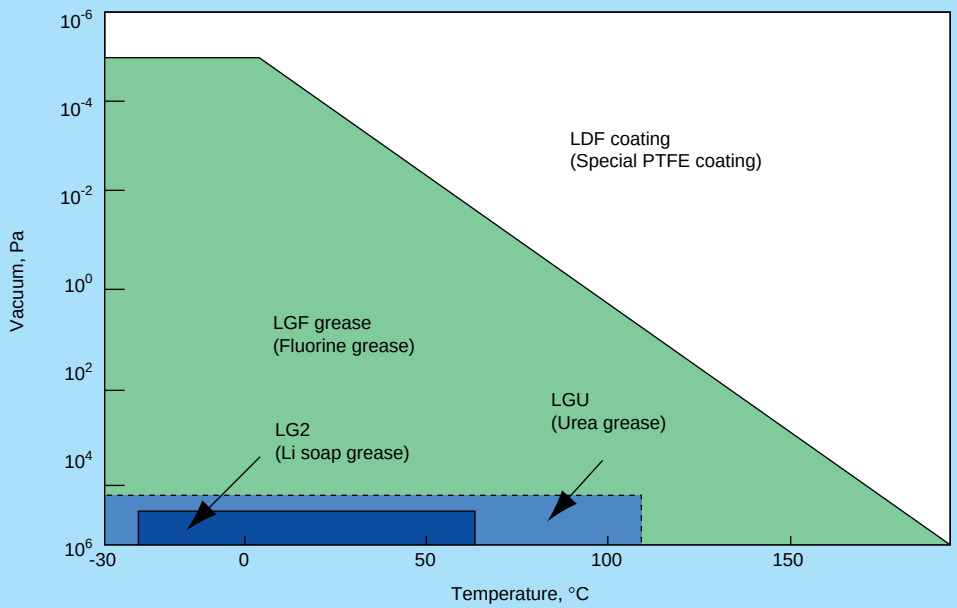

Fig. 1 Clean grease application ranges

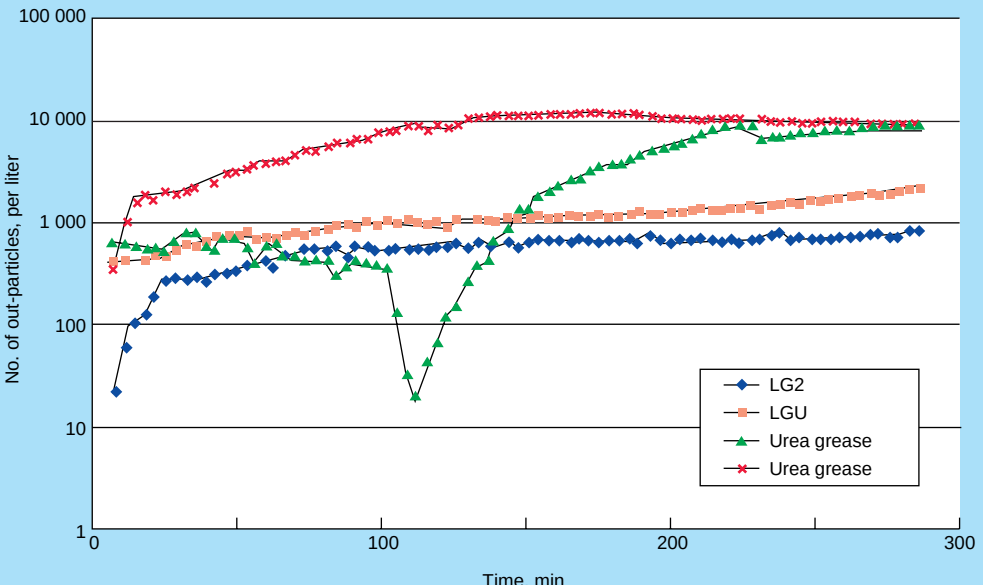

Fig. 2 Bearing out-particle generation with clean greases

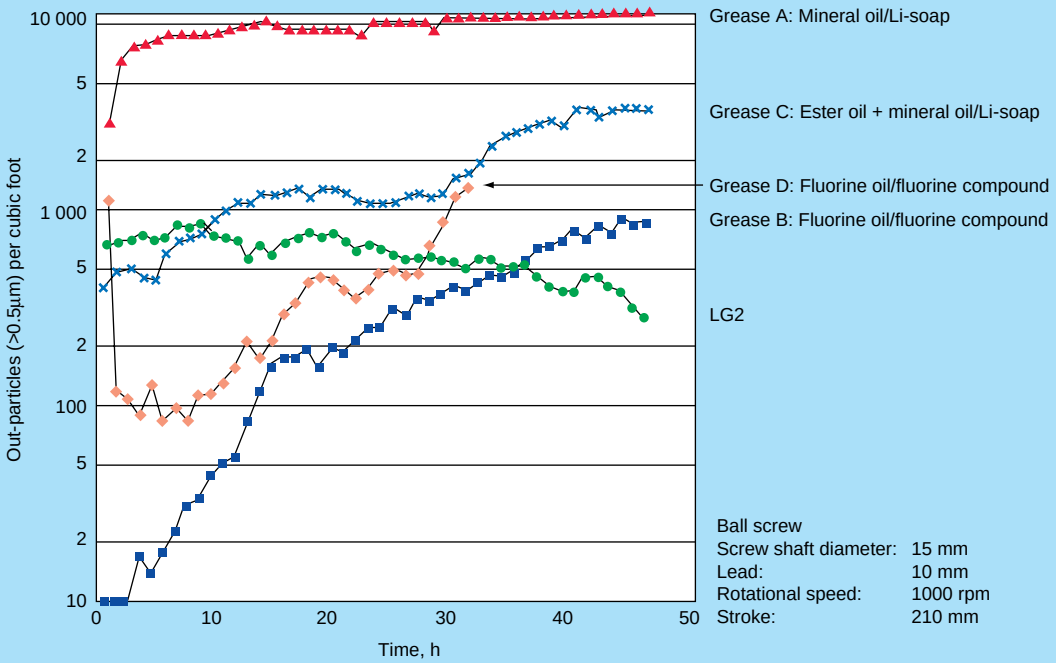

Fig. 3 Ball screw out-particle generation with greases

Table 2 Comparison of out-particle generation and life of LGF and other greases

Grease	Torque life (hrs)	Out-particling, p/(54 × 10³ rev)
LGF	390	4
Demnum L200	80	5
Krytox 240AC	40	13
Fomblin YVAC3	50	7

gold, silver, MoS_2, fluororesin or other solid lubricants[4),5)], as well as ion-implanted bearings[6)], are highly regarded for their low out-particle generation.

Many of the fluororesin coatings are applied employing a binder and may cause problems at high temperatures or under high loads because of their lubrication and out-particle-generating properties. NSK has developed a special low out-particle-generating fluororesin coating (LDF coating) which can be applied without a binder through a special coating treatment[7)].

The relationship between out-particle generation and rotational speed of bearings lubricated with different solid lubricants is shown in Fig. 4. As this figure shows, LDF-coated bearings produce a small quantity of one or two out-particles/hr at all running speeds, while the sintered polytetrafluoroethylene (PTFE)-coated and silver-coated bearings tend to produce more as the running speed increases.

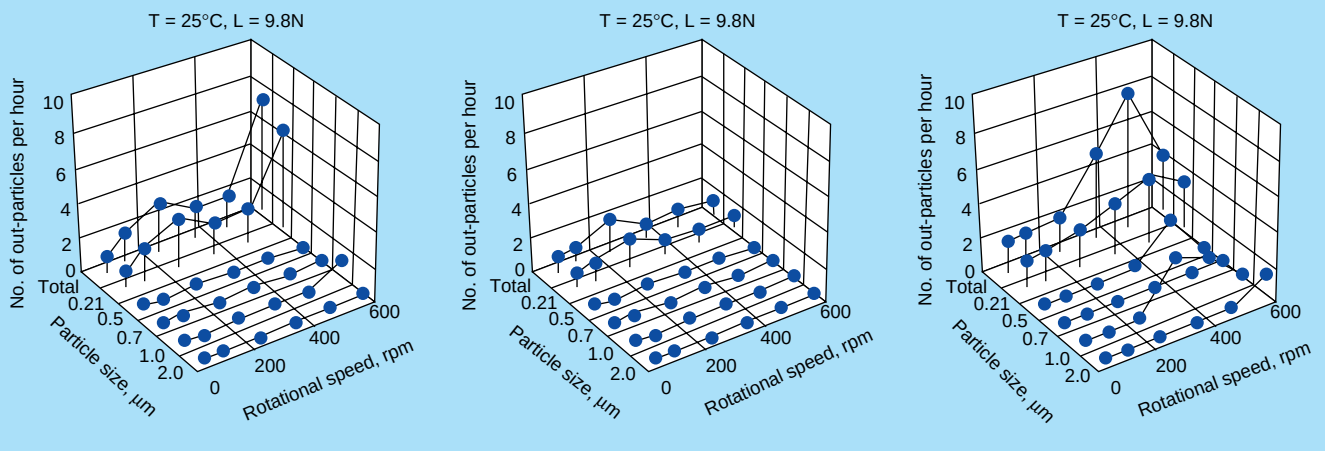

(a) Sintered PTFE-coated bearing (b) LDF-coated bearing (c) Silver-coated bearing

Fig. 4 Out-particle generation by solid-lubricated bearings

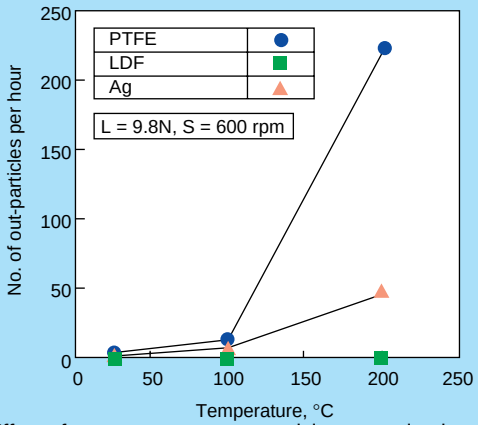

Fig. 5 Effect of temperature on out-particle generation by solid-lubricated bearings

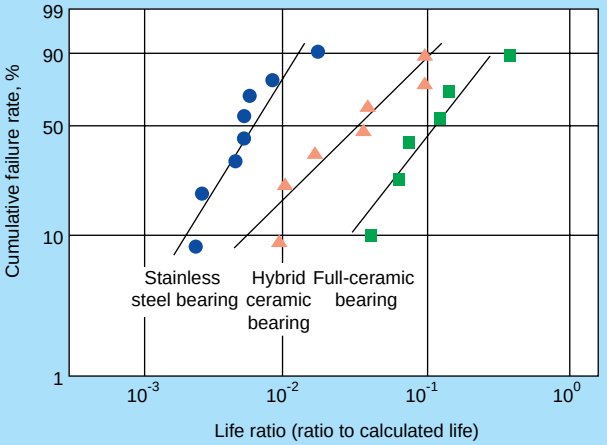

Fig. 6 Life of bearings in water

Fig. 5 shows the effect of temperature on out-particle generation. LDF-coated bearings produce a very small quantity of one out-particle/hr regardless of temperature, while the sintered PTFE- and silver-coated bearings generate more with increasing temperature. Particularly, the out-particle production of bearings with the sintered PTFE coating sharply increases at 200°C and up because of the binder used in its application.

The out-particle-generating properties of the LDF coating, which employs no binder, are less influenced by temperature, and the coating has a longer life than the others.

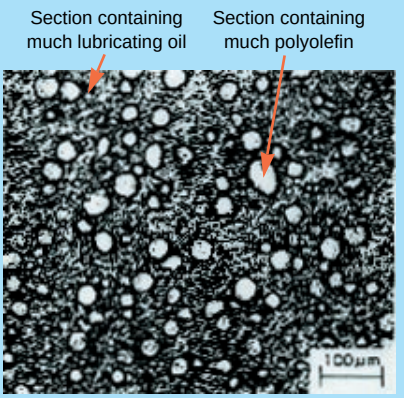

Photo 2 Structure of Molded Oil

Table 3 Corrosion resistance of rustproof coatings

		SUS440C	Hard Cr coating	Cr-fluororesin coating	Ni-alloy coating
Water		×	△	○	○
Chloric acid	(1 N)	×	○	○	○
Chloric acid	(5 N)	×	○	△	○
Sulfuric acid	(5 N)	×	×	○	○
Nitric acid	(10 N)	○	○	○	○
Fluoric acid	(1 N)	×	△	△	○
Hydrogen peroxide	(1 N)	○	○	○	○
Cost		—	Moderate	Low	Moderate

Note: Nitric acid (5 N) corrodes all of the coatings and SUS440C ○: No corrosion △: Partly corroded ×: Corroded

Table 4 Properties of highly corrosion-resistant ceramics

		Silicon nitride	Carbide-based ceramic	Oxide-based ceramic	Bearing steel
Density	(g/cm^3)	3.23	3.14	5.9	7.8
Young's modulus	(GPa)	330	390	210	208
Poisson's ratio		0.27	0.14	0.31	0.3
Fracture toughness	($MPa \cdot m^{1/2}$)	6.0	2.5	7.5	18
Vickers hardness	(H_V)	1500	≧2000	1300	700
Thermal expansion coefficient	(10^{-6}/°C)	2.8	4.3	10.5	12.5
Thermal conductivity	(W/m•K)	31	60	3	50
Bending strength	(MPa)	900	600	1100	≧2500
Running in water		◎	△	○	×
Running in acid solution		△	◎	○	×
Cost		Moderate	Moderate	Low	Lowest

◎: Excellent ○: Good △: Fair ×: Poor

2.2 Corrosion prevention technologies

2.2.1 Rustproof coatings

Ceramic bearings and other corrosion-resistant bearings with rustproof coatings are used in wafer and hard disk cleaning machines. Ceramic bearings are highly corrosion-resistant, but costly. Rustproof coatings often used for these bearings are electroless nickel and chrome, but these have a drawback in that they are susceptible to corrosion by acids such as hydrochloric acid, sulfuric acid and hydrofluoric acid. In view of this, NSK has developed a chrome fluororesin coating and a nickel alloy coating.

The corrosion resistance of these rustproof coatings is summarized in Table 3. The chrome fluororesin is a low-cost rustproof coating with excellent lubrication properties and is frequently used in bearings and linear guides.

The nickel alloy coating has higher corrosion resistance than the chrome fluororesin coating, and is frequently used in bearings. Additional commercial applications for this coating should develop in the future.

2.2.2 Highly corrosion-resistant ceramics

Silicon nitride bearings have a fatigue life about 10 times longer than stainless steel bearings, and are used in water or other corrosive environments (Fig. 6). However, in etching equipment or cleaning machines where very corrosive solutions are used, even highly corrosion-resistant silicon nitride ceramic bearings[8] (with improved corrosion resistance over conventional silicon nitride bearings) can have problems with short life as a result of the dissolution of their binder by the corrosive solution. In response to this, NSK has developed a highly corrosion-resistant ceramic and a low-cost ceramic for corrosive environments. Their properties are listed in Table 4.

Carbide-based ceramics have corrosion resistance superior to that of silicon nitride ceramics. And, as they have longer life in corrosive solutions than other ceramic bearings, they are commonly used in etching equipment and cleaning machines.

Oxide-based ceramics are low-cost and corrosion-resistant. They have a longer service life in water than carbide ceramic bearings[9] and are used widely in cleaning machines.

2.3 Lubricant-developing technology: Molded Oil (NSK K1 Seal™)

Molded Oil is a solid compound consisting of lubricating oil and a polyolefin resin with an affinity for oil. While commercially available oleoplastics contain only 2 or 3 percent oil by weight, Molded Oil contains not less than 50% lubricating oil by weight. In Photo 2 of Molded Oil, the polyolefin is the structure within which the lubricating oil is retained.

NSK K1 Seals for linear guides are made of this Molded Oil, a remarkable material capable of both sealing and continuously providing lubrication[10]. The K1 Seal has allowed linear guides to be used without requiring maintenance for extended periods in environments where they are exposed to water and dust, and where it was otherwise difficult to keep them efficiently lubricated. In addition, as only a small quantity of this sealing lubricant is sufficient, it helps keep equipment clean.

Fig. 7 shows changes with distance traveled in the lubricating oil supply and frictional force of a linear guide lubricated with a K1 Seal. Immediately after the linear guide is degreased, the frictional force of the linear guide increases sharply, but as it is operated several times, the frictional force decreases and the linear guide operates normally. This means that the lubricating oil supply from the K1 Seal begins to flow soon after degreasing to ensure smooth and stable operation of the linear guide.

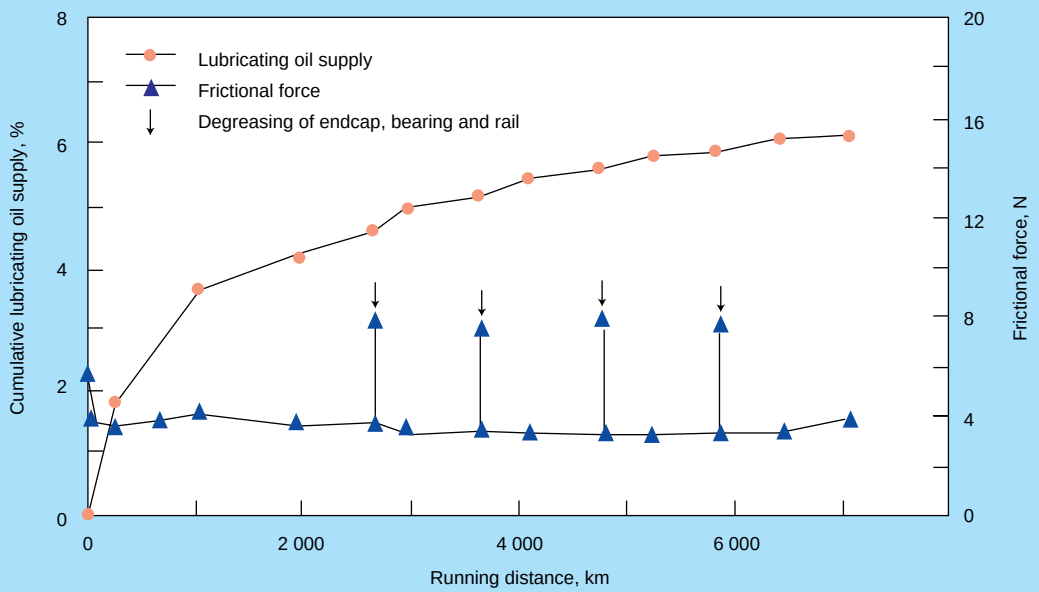

Fig. 7 Change in lubricating oil supply and frictional force with distance traveled by a linear guide

Table 6 Typical applications of SPACEA bearings

Special conditions	Major applications
Clean environment	Liquid crystal, semiconductor, and hard disk mfg. equipment; food processing and medical equipment
Vacuum	Space equipment, vacuum equipment, stepping motors, vacuum deposition equipment, electronic device mfg. equipment, X-ray tubes, turbo-molecular pumps
Corrosive environment	Liquid crystal, semiconductor, and hard disk mfg. equipment; food processing, film mfg. and cleaning equipment; molten plating tanks
High temperature	Heat treatment furnace roller conveyors, kiln cars
Nonmagnetic	Semiconductor mfg. equipment, medical inspection equipment
Low temperature	Liquid fuel turbo-pumps, liquefied gas submerged pumps
Radiation	Nuclear reactors, nuclear fusion reactors, accelerators
High speed	Machine tools, jet engines, turbo-chargers

2.4 Evaluation technology

Bearings for special environments are used in various applications, and bearing performance needs to be evaluated under test conditions simulating actual application conditions as far as possible. For vacuum-related applications, for example, we use X-ray tube bearing testers, aerospace equipment bearing testers, turbo-molecular pump touch-down bearing testers, ball screw and linear guide testers, and out-particle generation testers to determine, evaluate and predict bearing life, out-particle generation, torque and other factors under actual conditions.

2.5 Life equations for bearings in special environments

Based on the extensive database we have compiled through bearing life testing, we have developed life equations for solid lubricant-coated and ceramic bearings. With these equations, we can calculate the life of bearings for special environments.

1) Life Equation for Solid Lubricant-Coated (silver, lead, molybdenum disulfide) Bearings:

$$L = a_{SL} \cdot a_{SV} \cdot (C_r/P)^d$$

where,

L: rating fatigue life (90% reliability), 10^6 rev

C_r: basic dynamic load rating of steel bearing with same dimensions, N (× 0.85 for stainless steel bearing)

P: dynamic equivalent load, N

a_{SL}: lubrication factor (1 for Ag, 0.7 for Pb, 1 for MoS_2)

a_{SV}: velocity factor (1 for MoS_2; 2 when below 100 rpm, 3 when above 100 rpm, for Ag and Pb)

d: 0.5 for Ag, Pb; 2 for MoS_2

2) Ceramic Bearing Life Equation:

$$L = a_{CL} \cdot a_{CM} \cdot (C_r/P)^3$$

where,

L: rating fatigue life (90% reliability), 10^6 rev

C_r: basic dynamic load rating of steel bearing with same dimensions, N

P: dynamic equivalent load, N

a_{CL}: lubrication factor

a_{CM}: velocity factor

Lubricating condition	a_{CL}	Type of bearing	a_{CM}
Oil or grease	1	Hybrid bearings	4
		Full-ceramic bearings	1
Water	0.02	Hybrid bearings	0.1
		Full-ceramic bearings	1

3. "SPACEA Series" Bearings

Specifications and typical applications of "SPACEA Series" bearings developed utilizing the aforementioned NSK technologies are listed in Tables 5 and 6 respectively. The following sections describe the main features of the bearings in the SPACEA Series.

3.1 Bearings for clean environments

The bearings for clean environments can be divided into two groups: one lubricated with clean grease, and the other lubricated with fluororesin. For the selection of appropriate bearings for particular applications, the technology for low out-particle generation described in Section 2.1 above should be taken into consideration. In addition to generating few out-particles, ceramic bearings have corrosion-resistant, nonmagnetic and insulating properties. As illustrated in Fig. 8, bearings lubricated with clean grease are used in wafer transfer robots operated on semiconductor production lines. As shown in Fig. 9, LDF-coated bearings are used for substrate carriages operated in vacuum and high-temperature environments in sputtering equipment.

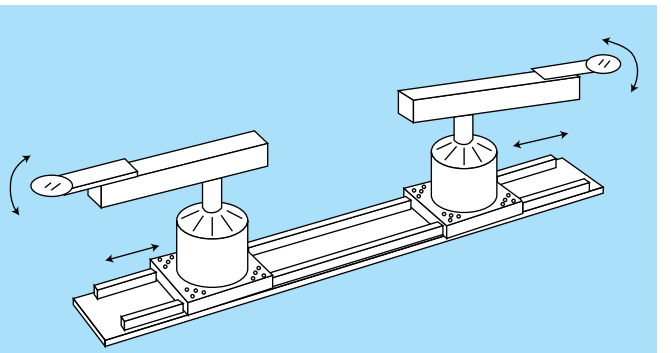

Fig. 8 Silicone wafer transfer robot

Table 5 Specifications of SPACEA Bearings

	Operating conditions					Requirements	Bearing conditions			Lubricant
	Temperature	Air	Vacuum	Corrosive conditions	Magnetic fields		Inner ring/ Outer ring	Balls	Cages	
Bearing for clean environments	Room temperature	○				Low dust	Martensite stainless steel	Martensite stainless steel	Austenite stainless steel or resin	Clean grease
	Room temperature	○	○			Low dust	Martensite stainless steel	Martensite stainless steel	Austenite stainless steel or resin	Clean grease
	Up to 200°C	○	○			Low dust	Martensite stainless steel	Martensite stainless steel	Austenite stainless steel	Fluorine grease
	Up to 200°C	○	○			Low dust, Corrosion resistance, Non-magnetism, Insulation	Martensite stainless steel or ceramics	Martensite stainless steel or ceramics	Fluororesin	—
	Up to 250°C	○	○			Low dust, Corrosion resistance, Non-magnetism, Insulation	Martensite stainless steel or ceramics	Martensite stainless steel or ceramics	Austenite stainless steel + special fluororesin coating	—
	Up to 300°C	○	○			Low dust, Corrosion resistance, Non-magnetism, Insulation	Martensite stainless steel or ceramics	Martensite stainless steel or ceramics	High-temperature self-lubricating resin	—
Bearings for vacuum conditions	Room temperature		○			Lubricity	Martensite stainless steel	Martensite stainless steel	Austenite stainless steel	Fluorine grease
	Up to 300°C	○	○			Lubricity, Heat resistance	Martensite stainless steel	Martensite stainless steel + molybdenum disulfide coating	Austenite stainless steel + molybdenum disulfide coating	—
	Up to 300°C		○			Lubricity, Heat resistance	Martensite stainless steel	Martensite stainless steel + lead coating	Austenite stainless steel	—
	up to 400°C		○			Lubricity, Heat resistance	Martensite stainless steel	Martensite stainless steel + silver coating	Austenite stainless steel	—
Bearings for corrosive environments	Room temperature	○		○		Corrosion resistance	Martensite stainless steel	Martensite stainless steel or ceramics	Austenite stainless steel or fluororesin	Waterproof grease
	Up to 200°C	○	○	○		Corrosion resistance	Martensite stainless steel	Martensite stainless steel or ceramics	Austenite stainless steel or fluororesin	—
	Up to 200°C	○	○	○		Corrosion resistance	Martensite stainless-steel + corrosion-resistant coating	Martensite stainless-steel + corrosion-resistant coating or ceramics	Fluororesin	—
	Up to 200°C	○	○	○		Corrosion resistance	Precipitation hardened stainless steel	Ceramics	Fluororesin	—
	Up to 200°C	○	○	○	○	Corrosion resistance	Ceramics	Ceramics	Fluororesin	—
Bearings for high temperatures	Up to 400°C	○				Heat resistance	Martensite stainless steel	Martensite stainless steel or ceramics	Graphite-based self-lubricating material	—
	Up to 500°C	○				Heat resistance	Ceramics	Ceramics	Graphite-based self-lubricating material	—
Nonmagnetic bearings	Room temperature	○	○		○	Non-magnetism	Nonmagnetic materials	Ceramics	Austenite stainless steel or resin	Fluorine grease
	Up to 200°C	○	○	○	○	Non-magnetism	Ceramics	Ceramics	Fluororesin	—
Bearings for low temperatures	down to -270°C	○				Lubricity	Martensite stainless steel	Martensite stainless steel	Fluororesin	—
Radiation resistant bearings	Up to 120°C	○				Radiation resistance	Bearing steel	Bearing steel	Cold-rolled steel	Radiation-resistant grease
Bearings for high speeds	Room temperature	○				High-speed tolerance	Bearing steel or Martensite stainless steel	Ceramics	Resin	High-speed grease, Oil-air or oil jet

<Note:> The parts of the bearing coated with special fluororesin coating, molybdenum disulfide, lead, or silver vary according to the conditions in which the bearing is to be used. For details, please contact NSK.

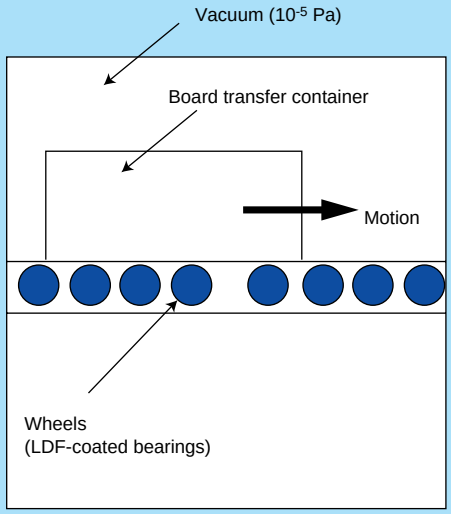

Fig. 9 Substrate carriage in sputtering system

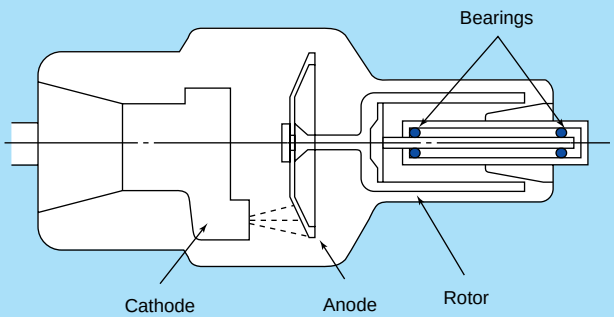

Fig. 10 X-ray tube

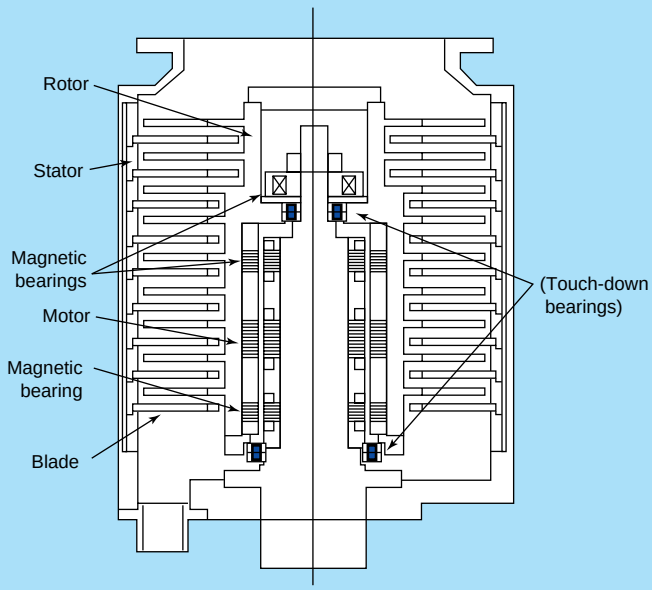

Fig. 11 Turbo-molecular pump

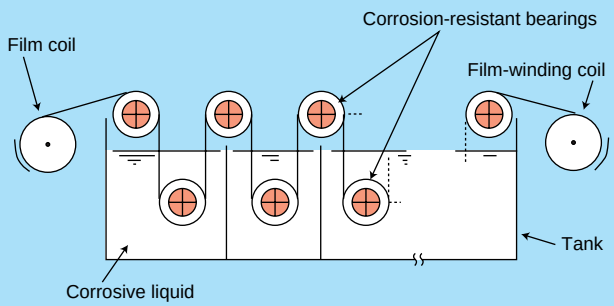

Fig. 12 Film cleaning system

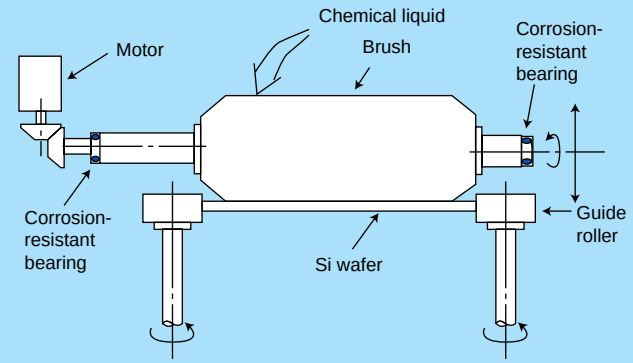

Fig. 13 Semiconductor polisher

3.2 Bearings for vacuum environments

For operation in vacuum environments where ambient temperatures are not high, bearings may be lubricated with a fluorine grease of low vapor pressure. However, where ambient temperatures are high and may cause fluorine grease to vaporize, bearings need to be lubricated with a solid lubricant. For over the last 10 years, silver-, lead- or molybdenum disulfide-coated bearings have been used in X-ray tubes like the one shown in Fig. 10, and turbo-molecular pumps like the one in Fig. 11. They have also been used in vacuum equipment and aerospace instruments and machines.

Under vacuum, high-temperature and high-speed operating conditions, hybrid bearings with molybdenum disulfide-coated outer and inner rings, ceramic balls, and self-lubricating cages have proved in actual service to have a long life of no fewer than 10^9 revolutions[11].

3.3 Corrosion-resistant bearings

Corrosion-resistant bearings include several types of rustproof film-covered bearings and several types of ceramic bearings. The corrosion resistance and rotational performance of corrosion-resistant bearings can vary depending on the environmental conditions under which they are operated. For selection of the appropriate corrosion-resistant bearings for specific applications, reference should be made to Section 2.2, Corrosion Prevention Technologies. Rustproof film-covered bearings are used in cleaning machines on hard disk and semiconductor production lines. Ceramic bearings are used in film cleaning systems (Fig. 12) and semiconductor polishers (Fig. 13).

3.4 Bearings for high and low temperatures

Bearings for high temperatures employ a self-lubricating graphite lubricant and can be used at temperatures up to 500°C. They are made of stainless steel or ceramics depending on operating conditions. The radial clearance of bearings for high temperatures is made larger than that of general bearings in order to ensure their long life.

Bearings for low temperatures are lubricated with a very low-viscosity liquid lubricant, and their cages are lubricated with fluororesin. They can be used without maintenance over a long period.

3.5 Nonmagnetic and radiation-resistant bearings

Nonmagnetic bearings are made of either nonmagnetic stainless steel or ceramic. They are lubricated with either grease or fluororesin.

Lubricant selection is important for radiation-resistant bearings. They are lubricated with standard grease for service at permissible radiation doses up to 10^6 rad, and with radiation-resistant grease for up to 10^9 rad.

3.6 High-speed bearings

Bearings used for high-speed applications are hybrid bearings whose balls are made of ceramic. Because of the lower friction between the balls and raceways than steel ball bearings, hybrid bearings have lower temperature rise during high-speed operation[12]. For this reason, hybrid bearings are used in machine tool spindles. Recently, NSK created Neo-Brid bearings for machine tool spindles by changing the material of the inner ring of the hybrid bearing from bearing steel to stainless steel[13]. This change resulted in 30% better high-speed performance than conventional hybrid bearings.

Hybrid bearings also have excellent seizure-resistance. Bearings for jet engines are required to have strong resistance to seizure, particularly in an emergency. In a 30-second oil shut-off test where steel bearings seize, hybrid bearings do not seize owing to the very low cohesiveness between their dissimilar materials and their low expansion coefficient which limits increases in preload[14].

4. Conclusion

Focusing on the technologies behind the SPACEA Series, current research and development of bearings for special environments has been described in the foregoing sections. As bearing operating environments are expected to become even more severe and demanding in the future, the development and improvement of the SPACEA Series is ongoing.

References:

1) For example, NSK Technical Journal No. 648 (1988). [in Japanese]
2) Miyake, S., "Bearings for Clean Environments," Precision Engineering Association Paper, 57, 4 (1991) 27.
3) Naka, M. et al, "Practical Performance of Low Out-Particle Grease, LG2," NSK Technical Journal No. 663 (1997) 32. [in Japanese]
4) Miyake, S., Takahashi, S., "Small-Angle Oscillatory Performance of Solid-Lubricant Film-Coated Ball Bearings for Vacuum Applications," ASLE Trans., 30, 2 (1987) 248.
5) Ito, H., "Dust Generation Characteristics of Ceramic and Solid Lubricant Coated Bearings," NSK Technical Journal No. 658, (1994) 26. [in Japanese]
6) Hirano, M., "Minute Oscillation Characteristics of Ion Implanted Ball Bearings," Tribologist, 34, 1 (1989) 58. [in Japanese]
7) Yamamoto, T. et al, "Dust Generation Characteristics of Bearings Lubricated with Solid Lubricant under Vacuum," Preliminary Print for Tribology Conference, (Kita-Kyushu, 1996-10) 306. [in Japanese]
8) Niizeki, S. et al, "Reliability and Corrosion Resistance Concerning Rolling Fatigue of Silicon Nitride Ceramic Balls," Preliminary Print for Tribology Conference, (Fukuoka, 1991-10) 67. [in Japanese]
9) Yamamoto, T. et al, "Rotating Capability of Ceramic Bearings under Water Lubrication," Preliminary Print for Tribology Conference, (Osaka, 1997-11). [in Japanese]
10) Yabe, T. et al, "Development of "KOKEIYU" and Its Application to NSK Linear Guide," NSK Technical Journal No. 661, (1996) 36. [in Japanese]
11) Ogawa, T., et al, "Development of Ball Bearings with Solid Film for High-Vacuum, High-Temperature, High-Speed Applications," NSK Technical Journal No. 656, (1993) 22.
12) Aramaki, H. et al, "The Performance of Ball Bearings with Silicon Nitride Ceramic Balls in High-Speed Spindles for Machine Tools," Trans. ASME, J. Tribology, 110 (1988) 693.
13) "Neo-Brid Angular Contact Ball Bearing," NSK Technical Journal No. 660, (1995) 54. [in Japanese]
14) Shoda, Y., "Hybrid Ceramic Rolling Bearings," NSK Technical Journal No. 653 (1992) 33. [in Japanese]

Hiroyuki Ito

Shigeki Matsunaga

Performance of Large-size Spherical Thrust Roller Bearings at High Speed

Tomoyuki Aizawa and Yukio Satoh
Roller Bearing Technology Department, Bearing Technology Center

ABSTRACT

Spherical thrust roller bearings can endure shaft distortion and are not restricted by the mounting dimensions in the axial direction. On the other hand, their design makes it difficult to supply enough lubricant to all the sliding and rolling surfaces resulting in poor high-speed capability. Recently, requirements for higher speeds exceeding conventional limiting speeds and for heavier loads beyond those of conventional bearings of this type have been increasing. To satisfy these requirements, NSK has studied and tested large-size spherical thrust roller bearings which are designed with the newest high-speed countermeasures for use at high speeds. The test results showed that it is possible to use large bearings at higher speeds than conventional bearings. This report describes test results and recent trends in large-size spherical thrust roller bearings.

1. Introduction

Spherical thrust roller bearings use convex rollers, run under high axial load and commonly encounter shaft deflection and mounting error. They are used in places where a large mounting axial dimension or large bearing width will not fit. Applications include boat propeller shafts, main spindles in vertical pumps and vertical motors, and refiner spindles which are used in preprocessing during paper manufacture.

This type of bearing, however, in comparison with tapered roller bearings, has not accumulated a large database of proven performance at high speeds. It is often said that it is unsuitable for high-speed rotation since it is difficult to make a design so that lubrication can easily circulate to each section of the bearing, and the sliding speed is large between the rib and roller ends on account of the large inner-ring rib[1].

As far as supporting high-speed rotation, however, the demand for spherical thrust roller bearings may grow in the future because the restrictions on their mounting dimensions are few and they have good endurance under heavy axial loads. For example, recently attention has been paid to water jet pumps in the propeller device for high-speed boats such as jet foils like Mitsubishi Heavy Industries' Techno-Super-Liner (Photo 1) [2), 3), 4)]. As for the thrust bearing used in the main spindle of such water jet pumps, it is desirable to have increased axial load capacity and high speed in the performance of the spherical thrust roller bearing. Also, higher-speed performance is

Photo 1
Techno-Super-Liner (courtesy of Mitsubishi Heavy Industries)

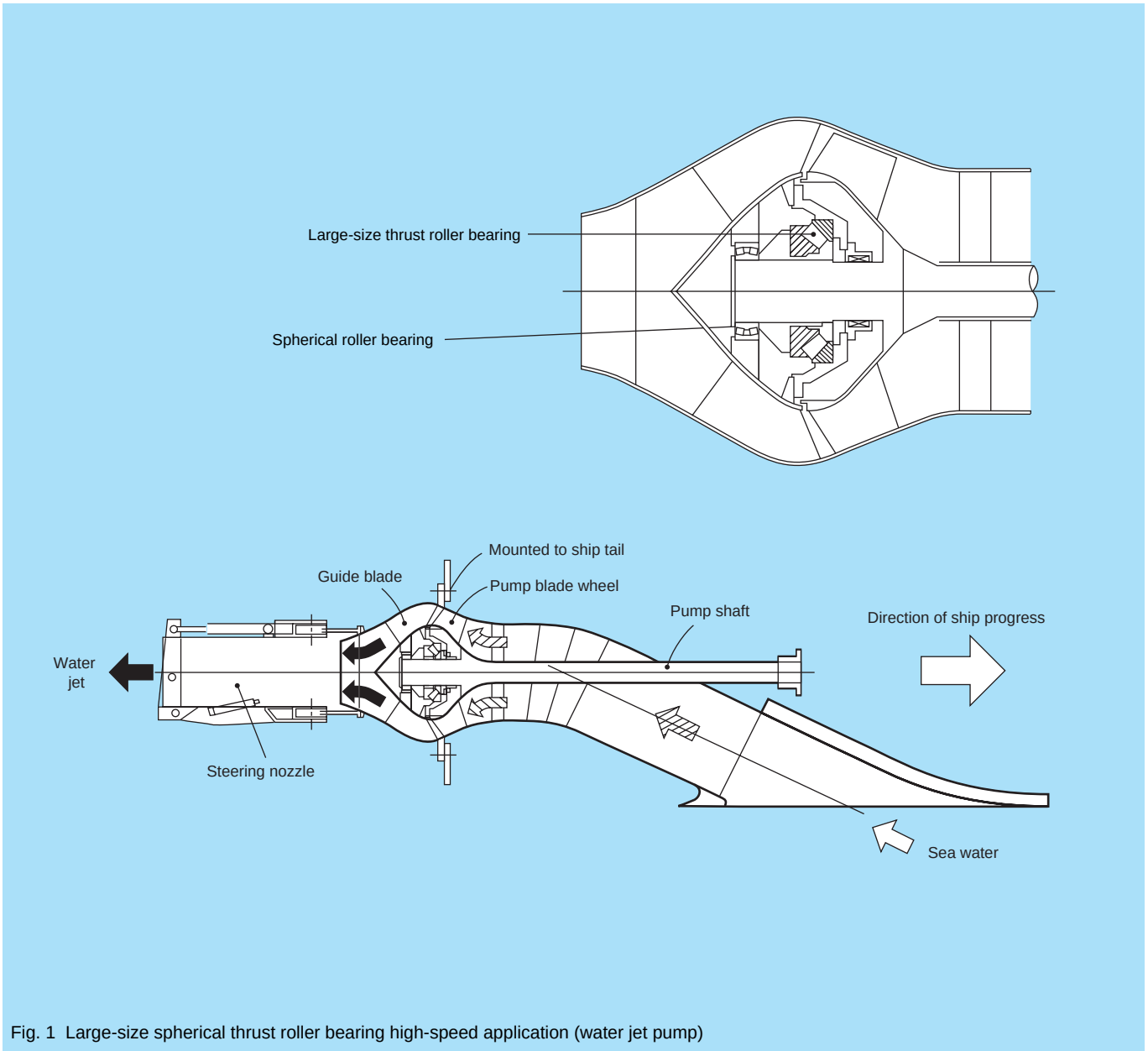

Fig. 1 Large-size spherical thrust roller bearing high-speed application (water jet pump)

Table 1 Actual results for large-size spherical thrust roller bearings

Use location	Brg. No.	Bore × Outside diameter × Assembled height (mm)	$\sqrt{DH}$ (mm)	N_{max} (rpm)	$F_{a\,max}$ (kN)	$\sqrt{DH}\cdot N/f_1$ (mm · rpm)	PV (MPa · m/s)
Vertical-type motor main shaft	29430M	$\phi150\times\phi300\times90$	164.3	900	75.2	159×10^3	274.4
Vertical-type pump main shaft	29420H	$\phi100\times\phi210\times67$	118.6	1 770	59.7	219×10^3	494.9
Boat propeller shaft	29318M	$\phi90\times\phi210\times67$	77.7	1 750	—	138×10^3	—
	29320M	$\phi100\times\phi170\times42$	84.5	1 450	41.1	125×10^3	216.5
	29322H	$\phi110\times\phi190\times48$	99.5	1 450	52.7	142×10^3	312.6
	29328M	$\phi140\times\phi240\times60$	120	1 160	62.1	145×10^3	252.2
	29336M	$\phi180\times\phi300\times73$	148	880	89.7	138×10^3	231
	29336M	$\phi180\times\phi300\times73$	148	354	6.9	56×10^3	95.3
	29340M	$\phi200\times\phi340\times85$	170	349	157.3	64×10^3	128.5
	29444M	$\phi220\times\phi420\times122$	226.4	276	193.9	70×10^3	123.1
	29436M	$\phi180\times\phi360\times109$	198.1	319	149.5	69×10^3	127.8
	29438M	$\phi190\times\phi380\times115$	209	321	76.4	74×10^3	147.3
Bench test results (use in a refiner main shaft)	29434M	$\phi170\times\phi340\times103$	187	1 500	78.2	305×10^3	530.2

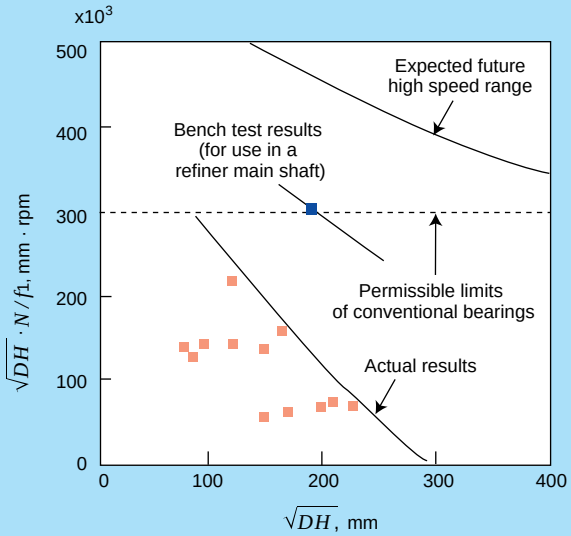

Fig. 2 Expected and actual results for large-size spherical thrust roller bearings

demanded in thrust bearings for refiner main spindles.

As for an example of a high-speed application, Fig. 1 shows a schematic of a water jet pump. A compact design is obtained by the use of spherical thrust bearings in the propulsion system which provides propulsion power from a jet and pressurized water sucked from below the water surface. To answer these demands for higher speeds, NSK has tested and studied improved large-size spherical thrust roller bearings at higher speeds than the normal rated speed zone.

This report discusses the investigation results and tests in high-speed regions, and reports on trends related to large-size spherical thrust roller bearings.

2. Actual Results and Expectations of Large-size Spherical Thrust Roller Bearings at High Speed

Table 1 and Fig. 2 show the high-speed range and conditions that future water jet pumps are expected to satisfy and the accumulated results (including bench tests) of large-size spherical thrust roller bearings for boat propeller shafts, main spindles of vertical-type motors and pumps, and refiner main spindles.

Conventional NSK spherical thrust roller bearings normally achieve rating rotational speeds of $(DH)^{0.5} \cdot N/f_1 \leq 300 \times 10^3$. The highest recorded value is slightly over $(DH)^{0.5} \cdot N/f_1 = 300 \times 10^3$. In this case, the size of the bearing was $(DH)^{0.5} = 187$ and D = 340 mm. Also, the PV value for seizure of the sliding contact surface was a record-setting value for this kind of bearing at about 500 MPa·m/s.

In contrast to these records, future expectations are for axial loads of over 250 kN at rotational speeds of 2 000 rpm or more and for axial loads of over 650 kN at speeds of over 800 rpm. These expectations show the need for high-speed and heavy-load performance. When these conditions are applied to bearings selected based on the above levels of axial load, it is necessary to consider the following factors: $(DH)^{0.5} = 200$ (D = 350 mm) at $(DH)^{0.5} \cdot N/f_1 = 450 \times 10^3$, and PV = 1000 or more; or on the other hand, $(DH)^{0.5} = 400$ (D = 800 mm) at $(DH)^{0.5} \cdot N/f_1 = 350 \times 10^3$, and PV = 600 or more. These performance levels greatly surpass previous records in rotational speed for conventional bearings while operating under conditions of high speed and heavy load.

Here, the quantity labeled as $(DH)^{0.5} \cdot N/f_1$ represents a parameter that shows the spherical thrust roller bearing's limiting speed; it corresponds to $d_m N$ for radial bearings. Similarly, $(DH)^{0.5}$ is a basic property that corresponds to the pitch diameter d_m of the rolling elements of radial bearings. D represents the bearing outside diameter, H the bearing height, N the rotational speed, and f_1 the compensation factor.

At high speeds, besides it being necessary to investigate seizure and abnormal wear of the cage, it is also necessary to consider bearing temperature and bearing dynamic power loss. Seizure occurs between the rib surface and roller end faces and is attributed to lubrication conditions and the PV value, which is a combination of the pressure (P) and the sliding speed (V). Abnormal cage wear problems occur when cage runout is large at high speed, especially with horizontal shafts in which the proper contact and formation of oil film among the cage, rollers, and guide surfaces is difficult to maintain. It is important to preserve lubrication conditions and proper cage positioning to prevent damage.

Also, for large bearings, the rotation limit is frequently determined by the temperature limit before the seizure limit in terms of $(DH)^{0.5} \cdot /f_1$ and PV value. In the case of forced oil circulation, the bearing temperature is determined by the amount of heat removed from the bearing by the oil. Therefore, the estimation of bearing heat generation (dynamic power loss) is vital in order to select the lubrication system (oil supply rate, cooling capacity). Also, for large bearings especially during high-speed rotation, the bearing dynamic power loss becomes large to such an extent that the manufacture's design and recommendation for the dynamic power source is influenced. For these various reasons, the estimation of the bearing dynamic friction torque (hereafter called dynamic torque) is a vital item which requires extensive investigation by the user.

3. High-Speed Rotation Tests

To respond to the demands for greater speeds, NSK has conducted high-speed tests with large-size spherical thrust roller bearings. In the bearing tests, the latest high-speed rotation countermeasures were implemented for the spherical thrust roller bearings, 29434M ($\phi 170 \times \phi 340 \times 103$) and 29480M ($\phi 400 \times \phi 710 \times 185$) including upgrading the precision of each part and modifying the dimensions for the improvement of the maintenance of oil film and

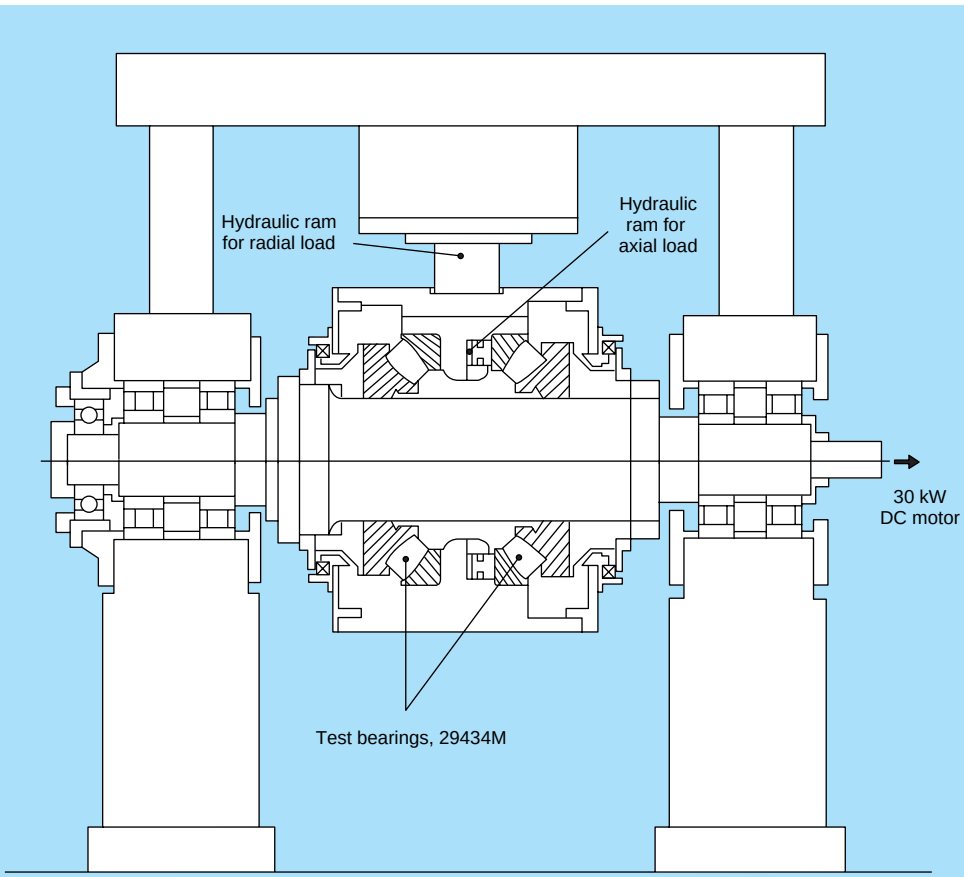

Fig. 3 Schematic diagram of test rig (29434M test)

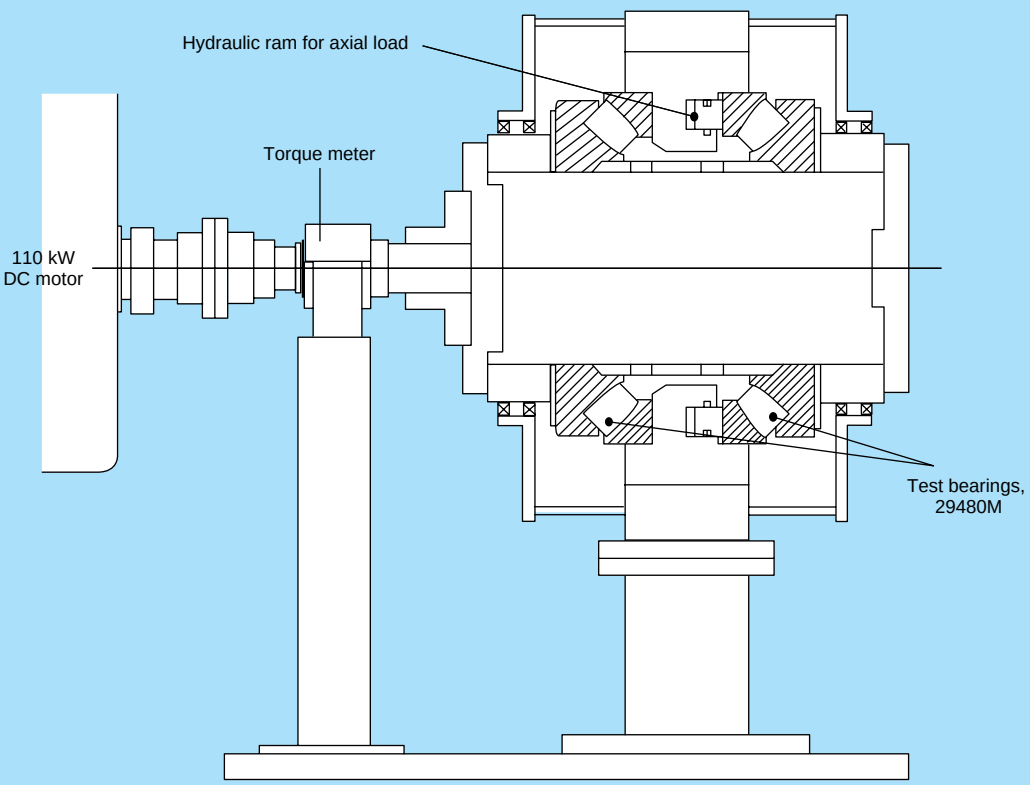

Fig. 4 Schematic diagram of test rig (29480M test)

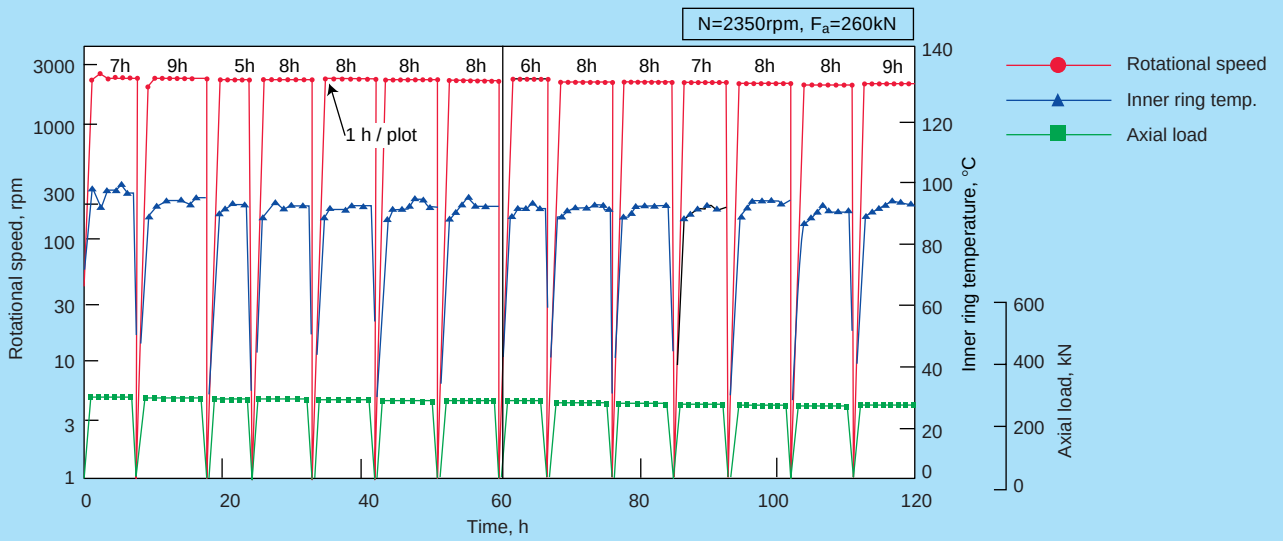

Fig. 5 Variation of bearing inner ring temperature (29434M test)

cage positioning stabilization.

The 29434M test was a high-speed rotation test under the following conditions:

$(DH)^{0.5}$ = 187 (D = 340 mm), $(DH)^{0.5} \cdot N/f_{1(max)} = 480 \times 10^3$, $PV_{(max)}$ = 1230

The 29480M test was a high-speed rotation test under the following conditions:

$(DH)^{0.5}$ = 362 (D = 710 mm), $(DH)^{0.5} \cdot N/f_{1(max)} = 355 \times 10^3$, $PV_{(max)}$ = 629

Through these tests, large-size spherical thrust roller bearings incorporating the latest high-speed countermeasures were analyzed for the possibility of attaining higher speeds than those of conventional bearings, and examined to determine effective lubrication methods and placement of the oil drain ports. Additionally, calculations were performed to estimate the dynamic torque.

3.1 Test methods

Figs. 3 and 4 show schematic diagrams of the test rigs. Two test bearings are installed back-to-back inside the bearing housing. The design enables axial loading to be applied to the bearing by means of oil pressure from the housing's cylinder. The design also enables the measurement of the dynamic torque of both test bearings without the necessity of a support bearing by means of omitting the radial load capacity using the 29480M test rig. The maximum rotation for the 29434M test was $N_{(max)}$ = 2350 rpm ($(DH)^{0.5} \cdot N/f_{1(max)} = 480 \times 10^3$), the maximum load was $F_{a(max)}$ = 255 kN {26 tonf} and the endurance test time was approximately 100 hours. The lubrication was forced oil recirculation using lubrication oil ISO VG 46 for gears, with an oil supply rate of 10 liters/min/brg and a target temperature of 40°C.

The conditions for the 29480M performance test were N = 300 ~ 800 rpm ($(DH)^{0.5} \cdot N/f_{1(max)} = 355 \times 10^3$) with load of F_a = 196 ~ 686 kN {20 ~ 70 tonf}. The lubrication in the forced oil recirculation system had the oil level adjusted inside the housing by the oil drain port. As for the oil drain ports, there were three types: one in which oil is drained from the upper part of the bearing and the upper drain port, another in which oil is drained from the center of the bearing and the middle drain port, and another in which oil is drained from the height of the lowest roller pitch diameter and the lower drain port. As for the upper drain port, a valve is installed so that the oil level is always full inside the housing. Further, the supplied oil is carried at the height of the center of the lowest roller, which is at the same height as the lower side drain oil port. The lubrication oil was made of two gear oils which were equivalent to ISO VG 46 and VG100, and it was supplied at a rate of 15 ~ 40 liters/min/brg with a target temperature of 40°C.

3.2 Test results

During the tests with 29434M and 29480M, no abnormal

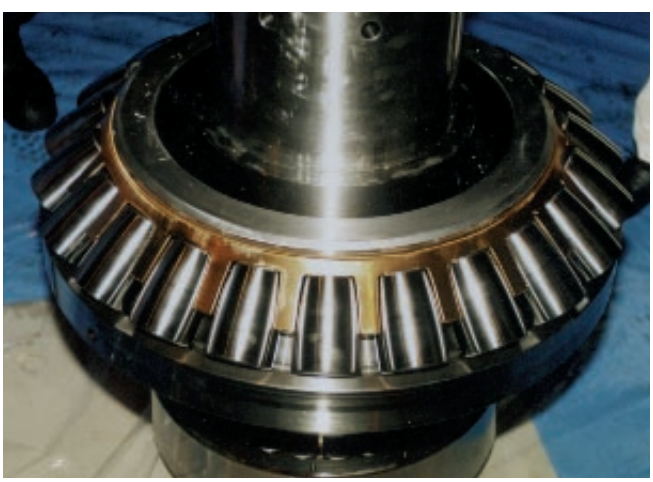

Photo 2 Spherical thrust roller bearing after test

vibrations and temperature variations were observed. As a result of post-test observation of the bearings' interior and analysis of the bearings, the conditions were found to be satisfactory without any dents or abnormal wear (Photo 2). Also, no abnormalities were found during the lubrication oil inspection nor when measuring the cross-section profile of the inner and outer-ring raceways and the inner-ring rib.

Fig. 5 shows the results of the 29434M test. Table 2 shows the measurement results on temperature and dynamic torque in the 29480M test under maximum conditions. In Figs. 6 to 8, dynamic torque and temperature are related to speed, axial load and oil supply rate respectively. In the figures, the inner ring temperature is used for the bearings with lower oil drain ports while the oil drain port temperature is used for bearings with upper and middle drain ports. In the test:

For bearings with upper and middle oil drain ports:
drain oil temperature > inner ring temperature > outer ring temperature;
For bearings with lower oil drain ports:
Inner ring temperature > drain oil temperature > outer ring temperature.

When comparing the dynamic torque and bearing temperature of the bearings with the three types of oil drain ports, there is a trend as follows: upper oil drain

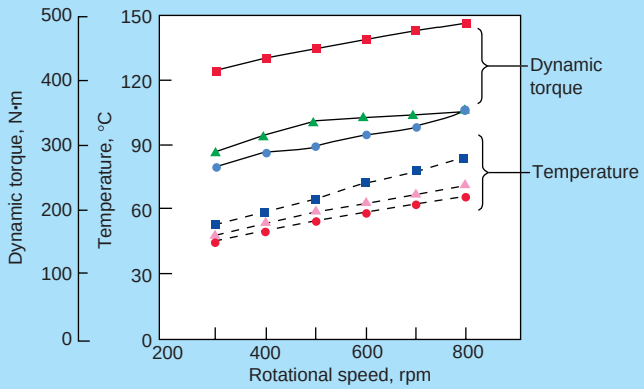

Bearing: 29480M Axial load: 392 kN Oil: VG100 Oil rate: 25 ℓ/min Oil temp.: 40°C		Drain port		
		Upper	Middle	Lower
	Dynamic torque			
	Drain temperature			

Fig. 6 Dynamic torque and temp. vs. speed (29480M test)

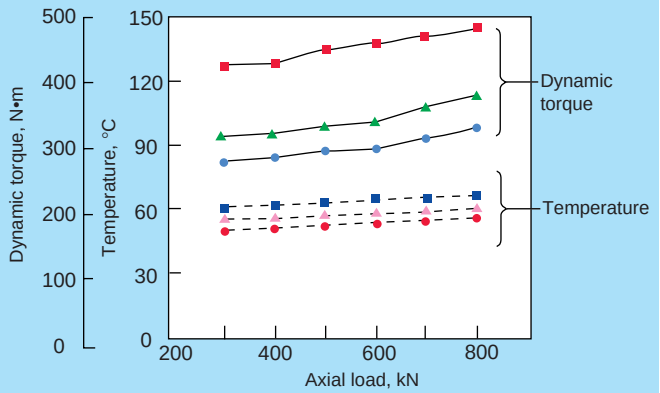

Bearing: 29480M Rotating speed: 500 rpm Oil: VG100 Oil rate: 25 ℓ/min Oil temp.: 40°C		Drain port		
		Upper	Middle	Lower
	Dynamic torque			
	Drain temperature			

Fig. 7 Dynamic torque and temp. vs. axial load (29480M test)

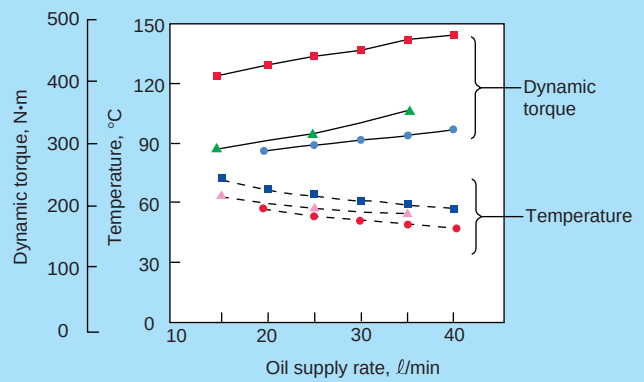

Bearing: 29480M Axial load: 392 kN Rotating speed: 500 rpm Oil: VG100 Oil temp.: 40°C		Drain port		
		Upper	Middle	Lower
	Dynamic torque			
	Drain temperature			

Fig. 8 Dynamic torque and temp. vs. oil supply rate (29480M test)

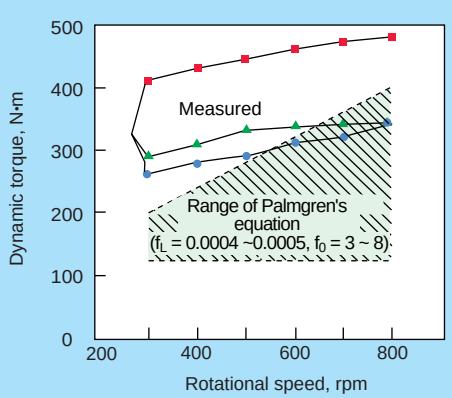

Brg. No.: 29480M Axial load : 392 kN Lubrication oil: VG100 Oil rate: 25 ℓ/min Oil temp.: 40°C		Drain port		
		Upper	Middle	Lower
	Dynamic torque			

Fig. 9 Comparison between measured and calculated (Palmgren) dynamic torque (29480M test)

port-type > middle oil drain port-type > lower oil drain port-type. Under the maximum rotation conditions, however, the bearings with middle and lower oil drain ports have nearly the same bearing temperature and dynamic torque.

Under the maximum conditions, the difference in dynamic torque between the bearings with the upper oil drain ports and those with both the middle and lower oil drain ports was 165 N·m (upper oil drain port : middle and lower oil drain ports = 1.5 : 1), and the difference in temperature was about 20°C.

4. Review

4.1 Use of large-size spherical thrust roller bearings at high speed

From the results of tests on 29434M and 29480M, it is deemed feasible to operate bearings at high speeds exceeding conventional limiting speeds. The new thrust roller bearings with high-speed rotation specifications are being used at high speeds: $(DH)^{0.5}$ = 187 size bearing at $(DH)^{0.5}\cdot N/f_1 = 480 \times 10^3$ and $(DH)^{0.5}$ = 362 size bearing at $(DH)^{0.5}\cdot N/f_1 = 355 \times 10^3$

Table 2 Test results in maximum condition (29480M test)
(F_a = 686 kN, N = 800 rpm, Q = 25 liters/min/brg.)

Drain port	Lower oil drain		Middle oil drain	Upper oil drain	
Lubricating oil	VG46	VG100	VG100	VG46	VG100
Inner ring temp. (°C)	69.8	72.5	62.6	69.3	78.9
Outer ring temp. (°C)	58.5	61	63.1	74.9	83.7
Drain oil temp. (°C)	63.9	66.8	69.9	80.2	88.6
Torque (N·m)	304	362.8	371.7	470.7	532.5
Oil supply temp. (°C)	40.3	40.5	39.5	40.2	44.7
Internal pressure (MPa)	—	—	—	0.2	0.2
Atm. temp. (°C)	23	22.9	22.7	24.5	24.3

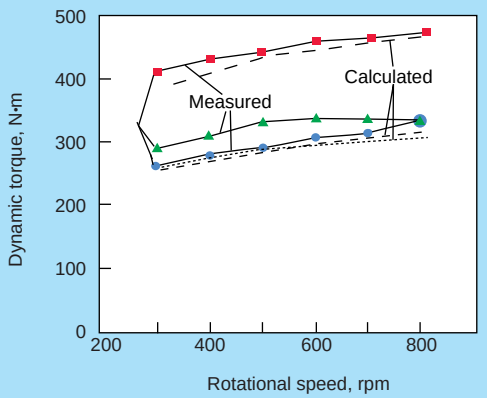

Brg No.: 29480M Axial load: 392 kN Lubrication oil: VG100 Supplied oil: 25 ℓ/min Oil supply temp.: 40°C		Drain port		
		Upper	Middle	Lower
	Measured values	—■—	—▲—	—●—
	Calculated values	— —	·····	- - -

Fig. 10 Comparison between measured and calculated dynamic torque (29480M test)

4.2 Lubrication method (drain location)

Based on test results, it is believed that a sufficient oil film is formed by the three types of lubrication methods. Under conditions of high-speed rotation, the measured maximum bearing temperature along with the dynamic torque develop as follows:
upper oil drain port > middle oil drain port ≈ lower oil drain port.

The reason is that with high-speed rotation, oil drainage is promoted by centrifugal force in the bearing with the middle oil drain port and the oil level inside the bearing is lowered. When comparing the temperature of the oil ports, however, the middle oil drain port temperature > lower oil drain port temperature, and the middle oil drain port is considered to be more effective in removing heat than the lower oil drain port.

Based on the above, the middle oil drain port is a better lubrication method over the tested range in terms of bearing temperature and dynamic torque. But in actual practice, the upper oil drain port method is employed to prevent salt water from intruding into the housing of the water jet pump.

4.3 Estimating dynamic torque in large-size spherical thrust roller bearings (experimental method)

Fig. 9 compares the measured dynamic torque results and those calculated where the lubrication viscosity is determined based on the oil drain port temperature. The calculation method relies on the experimental results obtained by Palmgren (and Harris) for dynamic torque[5), 6)]. The measured dynamic torque values and those obtained with the Palmgren equation are different. In this experiment (29480M), coefficients were calculated while considering the structure of the following equation which was based on measured results.

$$M = f_L \cdot d_m \cdot F_a + f_o \cdot d_m^3 \cdot \nu^a \cdot N^b + M_s \ (N\cdot m)$$

Here, d_m: Rolling element pitch diameter (mm)
F_a: Axial load (N)
N : Rotational speed (rpm)
ν: Lubrication viscosity (mm^2/s, = cSt)
f_L: Coefficient reflecting brg. type and load
f_o: Coefficient reflecting brg. type and lubrication method
M_s: Dynamic torque of the seal (N·m)

This estimation equation uses the oil drain port temperature as the representative temperature when determining the lubrication viscosity, ν. The reasoning behind this is as follows. For large bearings with forced recirculation of lubrication, the following trend exists: oil

drain port temperature > inner ring temperature > outer ring temperature. The oil drain port temperature is considered to be close to the bearing internal temperature which strongly affects the dynamic torque. The oil drain port temperature is taken to represent the oil temperature for the sake of ease and simplicity as it is easy to calculate the amount of heat removed by the oil and to take measurements in the field. Despite the recognition that there was a difference in the trend of the bearing temperature in the bearings with lower oil drain ports in this test, the oil drain port temperature was taken as the representative temperature in order to obtain the aforementioned advantages and unify the equations.

Also, in the estimation, for the increase of dynamic torque due to increase in oil amount the following sequence was considered: oil temperature decreases → viscosity increases → rolling & stirring resistance increase. However, another trend which is applied to jet lubrication was neglected, namely : increased oil amount → increased stirring resistance.

Each of the coefficients below was determined based on regressive calculations of test data.

$f_L \cdot d_m = 0.00014$

$a = 0.292$

$b = 0.573$

$f_o \cdot d_m^3 = 1.9123$ (lower side oil drain port)

$= 1.97114$ (middle oil drain port)

$= 3.60296$ (upper side oil drain port)

$M_s = 2.5$ (N·m)

These coefficient values were used to determine the calculated dynamic torque values in Fig. 10.

As for the calculation of the coefficients, the number of data points was 94, and the standard deviation was 1.90 (N·m) for the estimation equation (experimental calculation). Further, as for the appropriate ranges for the coefficients used in this estimation equation for spherical thrust roller bearing 29480M, they were: axial load 200 to 700 kN, rotational speed 300 to 800 rpm, lubrication oil ISO VG46 to VG100 or equivalent, and oil drain port temperature 50 to 90°C.

5. Conclusion

It was confirmed by experiment that it is possible to use these bearings in high-speed regions exceeding conventional limiting speeds. The new spherical thrust roller bearings with high-speed rotation specifications were used at high speeds: $(DH)^{0.5} = 187$ (D = 340 mm) size bearing at $(DH)^{0.5} \cdot N/f_1 = 480 \times 10^3$ and $(DH)^{0.5} = 362$ (D = 710 mm) size bearing at $(DH)^{0.5} \cdot N/f_1 = 355 \times 10^3$. Also, investigation into the optimum lubrication method for this case was conducted and estimation equations were established to calculate the bearing dynamic torque for a 29480M bearing.

Henceforth, it is believed possible to expand the high-speed range of large-size spherical thrust roller bearings. So NSK is considering the need to confirm the upper speed limit for large-size spherical thrust roller bearings and establish a dynamic torque estimation equation for general use to meet our customers' requirements.

References:

1) NSK Large-Size Rolling Bearing Catalog, No. 125a, NSK Ltd., (1994) B310.
2) Nishimura, H., "Actual Use of Techno-Super-Liner," Magazine of International Traffic Safety, 17-1 (1991), 42 - 49.
3) Hasegawa, Y., "Super-High-Speed Fully-Merged Hydrofoil Boat," "Jetfoil," Magazine of Welding Association, 61-7 (1992), 43 - 48.
4) Endoh, H., "Present Situation of Techno-Super-Liner Development," Magazine of Welding Association, 61-7 (1992), 29 - 34.
5) Palmgren, A., "Ball and Roller Bearing Engineering," S. H. Burbank and Co. (1945) 36.
6) T. Harris, "Rolling Bearing Analysis 3rd ED.," John Wiley and Sons, (1966) 508.

Tomoyuki Aizawa

Yukio Satoh

High-performance Ball Bearings for Automotive Alternator Applications

Kenji Ohkuma and Masao Koshigaya
Ball Bearing Technology Department, Bearing Technology Center

ABSTRACT

This report describes the latest ball bearing technology for automotive alternators. Since compact alternators appeared on the auto market, the ball bearings used in them have presented difficulties. These difficulties have been overcome by technical breakthroughs such as a new theory about the process for ball bearing flaking and the development of a special grease with a unique ability to prolong bearing life dramatically by easing shock and vibration. Additionally, NSK Super-NBR contact seals have been created to take the place of polyacrylic rubber seals used at approximately 140°C. Other advances in technology for bearing components have also been achieved.

An unwavering commitment to the continuous improvement of alternator bearings will enable NSK to remain a leader in the industry.

1. Introduction

Bearings for automotive alternators, which are exposed to external and worn-brush dust particles and muddy water, while being operated at high and low speeds under high temperatures and high loads, are required to satisfy rigid performance requirements, as well as be highly reliable. Particularly, the operating conditions of small fan-type alternators, which have been mass-produced for 10 years, have become increasingly severe of late. The specifications for the bearings used in these alternators, after undergoing various theoretical analyses and experimental verifications, have evolved in response to these more exacting operating conditions.

This paper reports on the main specifications established to date for automotive alternator bearings.

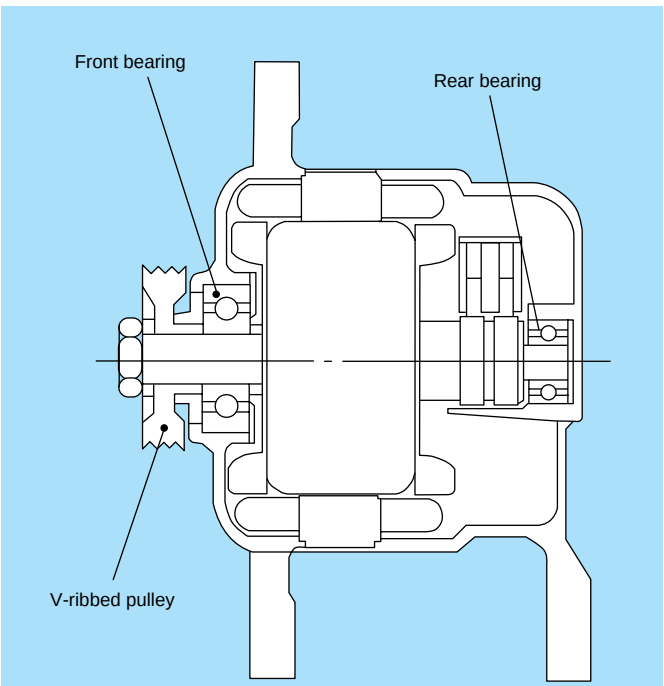

Fig. 1 Cross-section of an automotive alternator

2. Environment of Alternator Bearings

With engine performance becoming higher and alternators getting smaller, the running speed of alternators that formerly ranged from a maximum of 15 000 to 18 000 rpm is now required, in certain cases, to achieve a level in excess of 20 000 rpm. Installation of air conditioning and ABS increases the installation density in the engine space, and thereby contributes to rises in the ambient temperature in which alternator bearings must function. Additionally, the increasing popularity of RVs and the widening use of motor vehicles in tropical areas

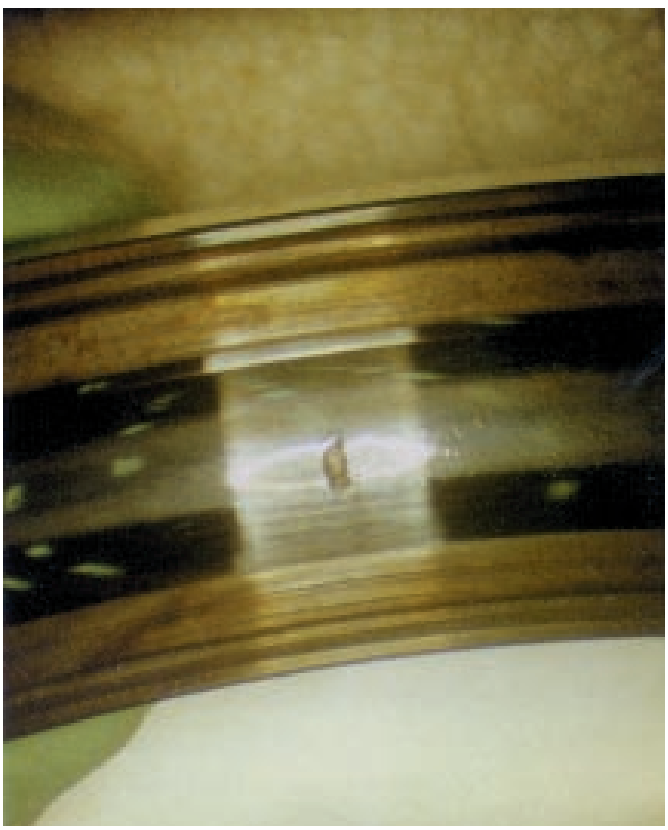

Photo 1 Outer ring flaking

and deserts have resulted in stricter requirements for alternators and naturally, the bearings they contain.

The use of a V-ribbed pulley for driving an alternator, as shown in Fig. 1, caused early flaking in the outer ring of the bearing (Photo 1). This flaking occurred only in the outer ring of the front bearing and caused structural change in the area where it occurred. The flaking was considered attributable to bending stress repeatedly applied to the outer ring. A special type of grease was developed to reduce this bending stress, and the problem was solved[1),2)].

3. Features of Alternator Bearings

Various improvements have been made in bearing design and manufacturing technologies to meet the rigid requirements mentioned in the foregoing section, and bearings designed specifically for automotive alternators have been developed.

The following sections describe the features of these alternator bearings.

Table 1 Boundary dimensions of alternator bearings

Units: mm

Bearings		Bore diameter	Outside diameter	Width
Front	B15-86	15	47	14
	B17-99	17	52	17
	B17-102	17	47	14
	6305	25	62	17
Rear	NCB8-85	8	23	14
	NCB10-50	10	27	11
	NC6202	15	35	11
	NCB15-69	15	35	13

3.1 Performance requirements and features of NSK alternator bearings

Fig. 2 shows the performance requirements for alternator bearings, NSK's corresponding design targets, and the resulting bearing specifications.

3.2 Boundary dimensions of bearings

An automotive alternator has two bearings: one is the front bearing on the fixed side which carries a majority of the belt load, and the other is the rear bearing located near the brush on the free side. The boundary dimensions

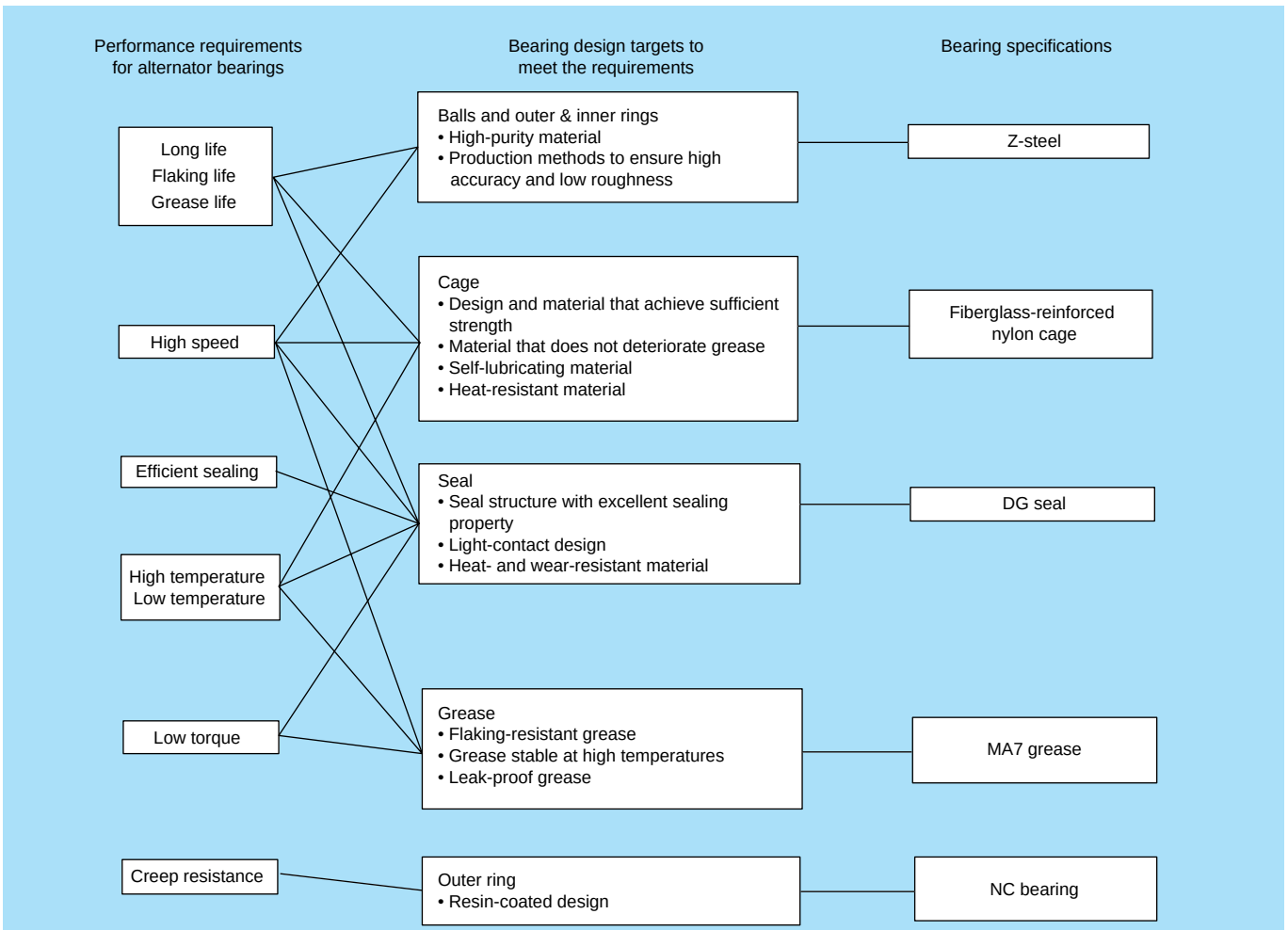

Fig. 2 Bearing specifications corresponding to expected features of automotive alternators

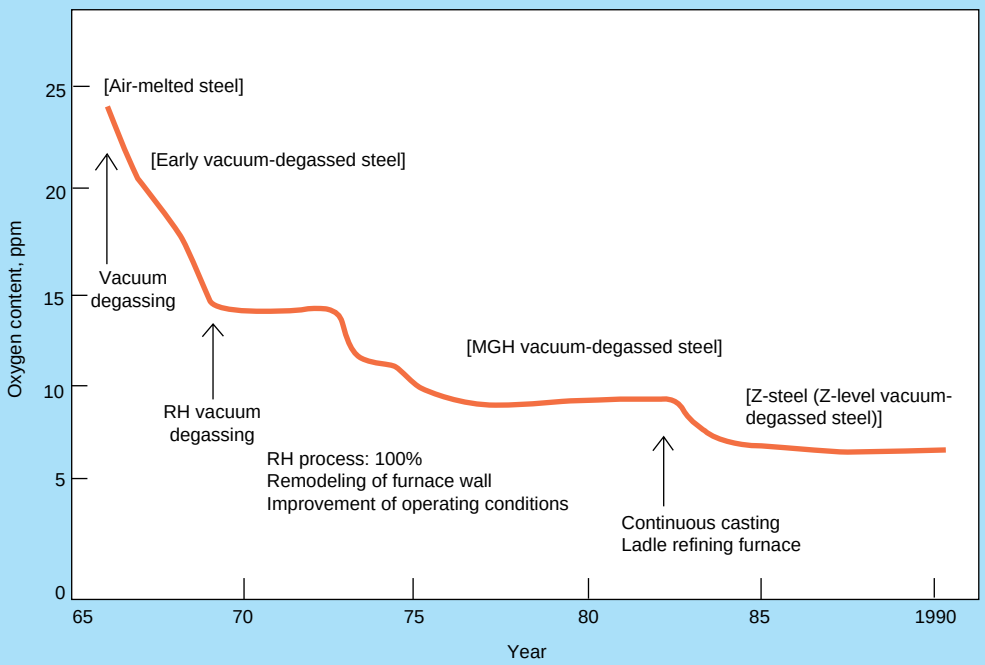

Fig. 3 Reduction of oxygen content in NSK bearing steels

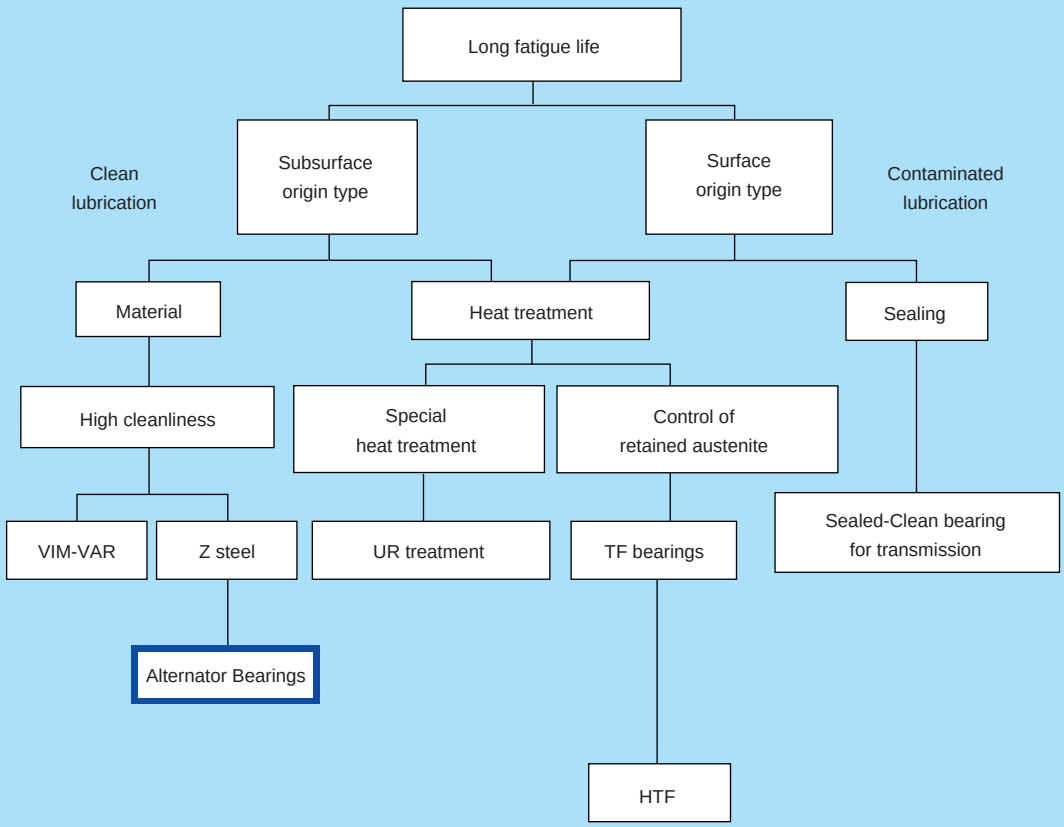

Fig. 4 NSK long-life bearing technologies

of these two bearings are in many cases special dimensions which differ from standard ones because of alternator performance requirements and space limitations (Table 1).

B17-102, shown in Table 1, is most often used for the front application. Its boundary dimensions are the same as those of a standard 6303 bearing, but its outer ring is approximately 30% thicker in order to minimize its deformation during rotation to prevent early flaking[3].

3.3 Bearing materials

The purity of the bearing steel used to make outer and inner rings was remarkably improved in the 1980's, as shown in Fig. 3.

High-purity steel has been the preferred material for alternator bearings. At present, the oxygen content in this steel is as low as approximately 6 ppm.

Fig.4 outlines the technologies behind the long life of NSK alternator bearings.

3.4 Seal structure

Alternator bearing seals are required to perform in a wide range of high and low speeds while being exposed to the external environment. Accordingly, a light-contact rubber seal is often used. NSK uses the DG seal that has excellent sealing and high-speed performance (Table 2 and

Table 2 Seal type and characteristics

Seal type	Conventional seals	Seals for alternator bearings
	DU	DG
Seal structure	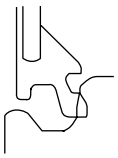	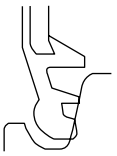
Torque	Fair	Excellent
Water resistance	Good	Excellent
Grease sealing	Good	Excellent

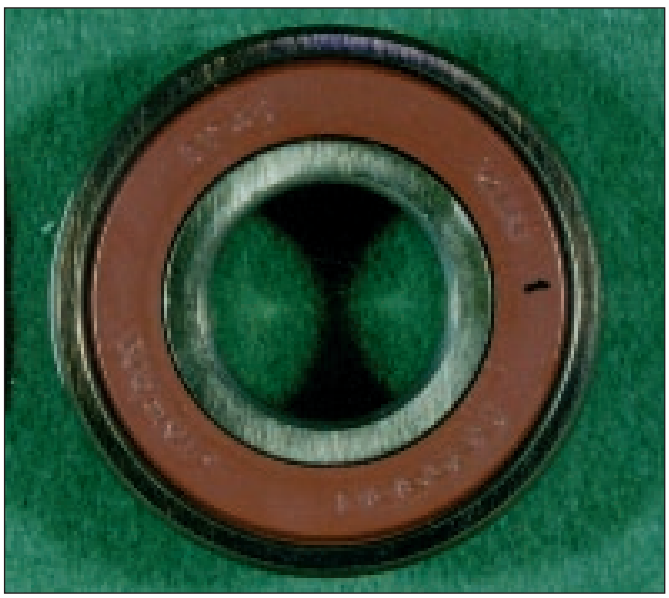

Photo 2 Appearance of NSK Super-NBR after evaluation

Test bearings: B17-102AT1X
DDG EA2H
DDU EA2H
(Outside dia.: 47, bore dia.: 17, width: 14 mm)

Test method: Left to stand at 100°C for 1 hour, and then submerged 20 cm in water for 10 minutes

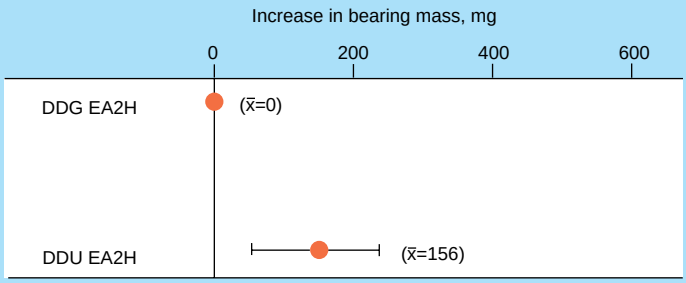

Fig. 5 Seal type and water resistance

Table 3 Comparison of physical characteristics of rubbers

			NSK Super-NBR		Nitrile		Acrylic		Fluoro	
Normal	Hardness, JIS-A		71		67		72		74	
	Tensile strength	(N/cm²)	107		166		123		153	
	Elongation	(%)	590		655		240		260	
Aged in air	Hardness change	(pts)	6	○	13	△	2	○	0	○
	Change in tensile strength	(%)	3	○	-36	△	9	○	17	○
	Change in elongation	(%)	-41	△	-61	×	0	○	2	○
Aged in grease 150°C	Hardness change	(pts)	-9	○	-12	○	-5	○	-2	○
	Change in tensile strength	(%)	-9	○	-44	△	-3	○	-7	○
	Change in elongation	(%)	6	○	-14	○	20	○	6	○
	Volume change	(%)	11.8	○	10	○	13	○	4	○

* Aged in air: Fluoro rubber at 170°C, other rubbers at 150°C, for 72 hrs.
* Aged in grease: Urea ester grease, for nitrile and NSK Super-NBR, 130°C, 72 hrs.
* Symbols in table: ○: excellent △: good ×: poor

Table 4 Seal rubber material and characteristics

		Nitrile		Acrylic	Fluoro
		NSK Super-NBR	NBR		
Water resistance		Good	Good	Fair	Good
Grease resistance	Ester	Excellent	Excellent	Poor	Excellent
	Ether	Excellent	Excellent	Excellent	Excellent
	PAO	Excellent	Excellent	Excellent	Excellent
	Urea	Excellent	Excellent	Excellent	Fair

Fig. 5).

The DG seal consists mainly of nitrile and acrylic rubber. For higher-temperature applications, however, NSK has developed Super-NBR, a nitrile rubber with heat resistance approximately 20°C higher than the conventional nitrile type.

Features of NSK Super-NBR

(1) Heat resistance between that of nitrile and acrylic rubber.
(2) Improved sealing performance in the temperature range in which the conventional type of nitrile rubber is used.
(3) Lower cost than acrylic rubber.

The physical properties of NSK Super-NBR in normal conditions are similar to those of the ordinary type of nitrile rubber as shown in Tables 3 and 4, and have good compatibility with the main constituents (thickener: urea, base oil: PAO or ether) of most typical greases for alternators.

Fig. 6 shows the relationship between the temperature at and time until which the initial hardness of a dumbbell test piece increases by 20 points for several types of rubber in an air-aging test as per JIS. As this figure indicates, NSK Super-NBR has 20°C higher heat resistance than the conventional heat-resistant NBR. Table 5 and Photo 2 show the results of a running test of B17-102DDG

Table 5 Evaluation of NSK Super-NBR seal mounted on bearing

	Hardness change	Wear	Appearance
NSK Super-NBR	+ 7.0 points	Negligible	Good
NBR	+ 8.0 points	Negligible	Good

Tested bearings: B17-102DDG
Conditions: 10 000 rpm × 196 N × 500h at 140°C (NSK Super-NBR)
120°C (NBR)

Table 6 Physical properties of polyamids

		Nylon 46	Nylon 66
Tensile strength	(MPa)	172	154
Tensile elongation at break	(%)	3.8	4.3
Bending strength	(MPa)	237	210
Flexural modulus	(MPa)	7 580	7 350
Notched impact strength	(J/m)	110	79
Heat deformation temperature	(°C)	285	244

alternator bearings with conventional NBR and NSK Super-NBR seals. The results provide further indication that NSK Super-NBR rubber has excellent heat resistance.

3.5 Cage

Fiberglass-reinforced plastic (nylon 66) cages are used to meet the high-speed requirements of alternator bearings. However, for higher temperatures and speeds in recent applications which require improvements in the openings (deformations) of the cage pockets, nylon 46 and PPS (polyphenylene sulfide) cages have been developed (Table 6).

3.6 Grease

Recently, alternators are designed to be more compact for higher speeds and require their bearings to run at 20 000 rpm or higher while withstanding bearing temperatures from 130 to 150°C. Naturally, the grease

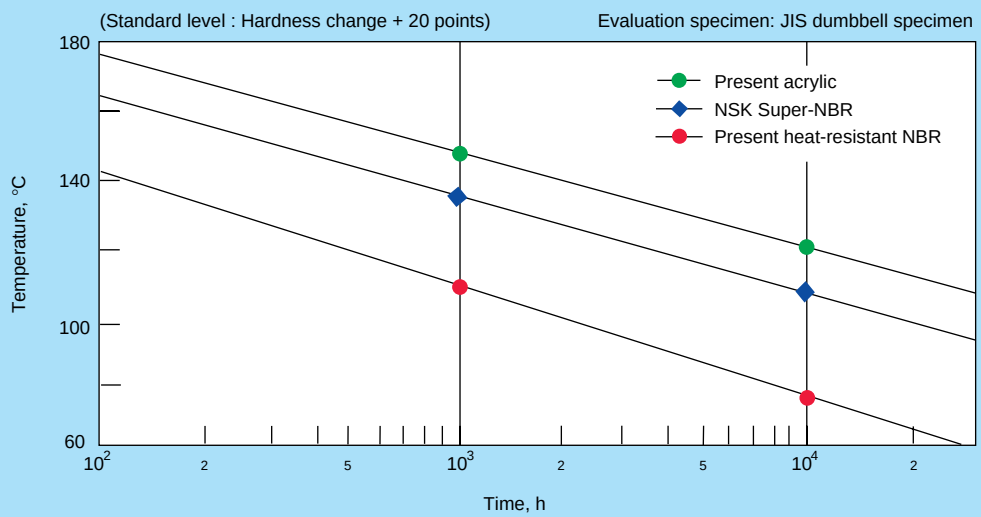

Fig. 6 Relationship between hardness change and life of rubbers

Table 7 Characteristics of grease for automotive alternator bearings

		MA7	Conventional grease	Test method
Appearance		Light-brown buttery	Light-brown buttery	—
Thickener		Diurea compound A	Diurea compound B	—
Base oil		Synthetic ether oil	Synthetic hydrocarbon oil	—
Base oil kinematic viscosity (mm^2/s)	40°C	100	47.3	JIS K2283
	100°C	13	7.9	
Worked consistency, 25°C		290	250	JIS K2220 (5.3)
Dropping point (°C)		240	260, min.	JIS K2220 (5.4)
Corrosiveness (copper strip,100°C, 24 h)		Passed	Passed	JIS K2220 (5.5B)
Evaporation (%, 99°C, 22h)		0.15	0.34	JIS K2220 (5.6B)
Oil separation (%, 100°C, 24h)		0.5	0.3	JIS K2220 (5.7)
Oxidative stability (MPa, 99°C, 100h)		0.02	0.025	JIS K2220 (5.8)
Worked stability (25°C, 10^5W)		336	364	JIS K2220 (5.11)
Water wash-out (%, 79°C, 1h)		0.8	2	JIS K2220 (5.12)
Low-temperature torque (–30°C) (mN·m)	Starting	304	157	JIS K2220 (5.14)
	Running	206	29	

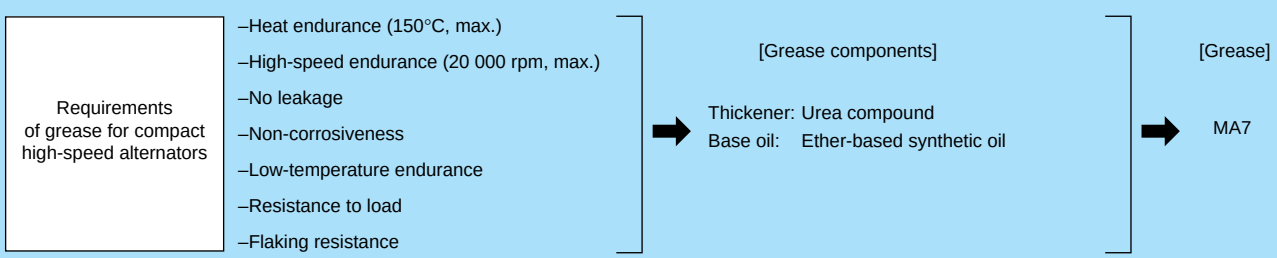

Fig. 7 Expected Grease Characteristics

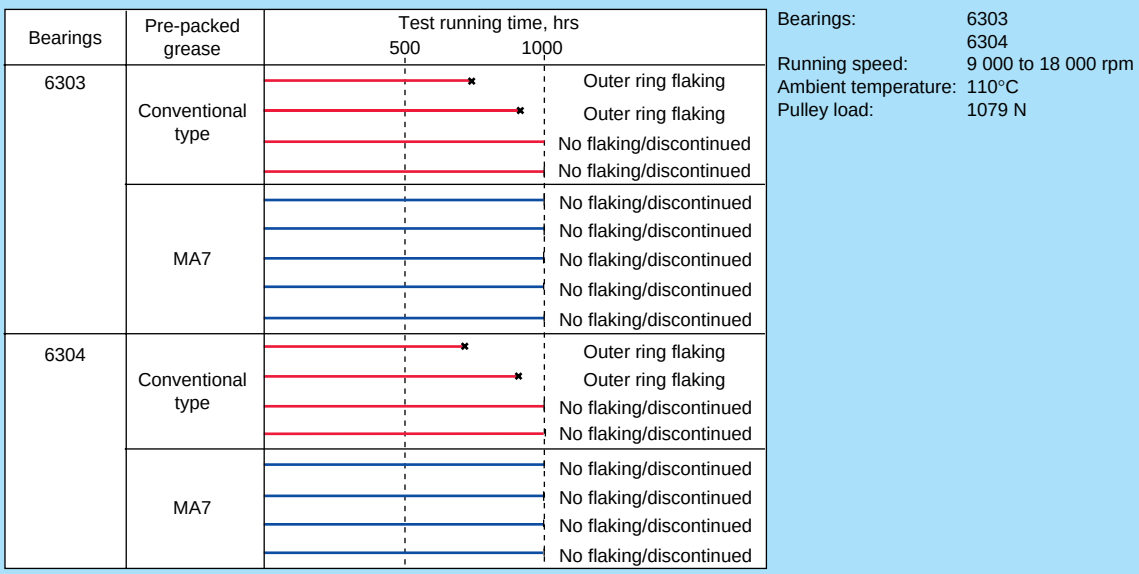

Fig. 8 Rolling-contact fatigue life bench test under up-down cyclic revolution

Table 8 Estimated residual life of grease after usage

No.	Running distance, km	Bearing	Grease residual life, km	Grease life (running distance + residual life), km
1	165 000	Equivalent to 6303, MA7	250 000	415 000
2	130 000	↑	340 000	470 000
3	155 000	↑	250 000	405 000
4	140 000	↑	450 000	590 000
5	130 000	↑	380 000	510 000

Photo 3 Bearing interior after running

used for lubricating these bearings must be able to perform reliably at such high temperatures and speeds. Greases composed of a urea-based thickener and a synthetic hydrocarbon base oil have often been used. At present, however, a urea/ether grease (MA7) has been developed which solves the problem of early flaking of the outer rings peculiar to bearings for alternators (Fig. 7).

Table 7 compares typical properties of MA7 grease and a conventional type of grease for alternators.

Fig. 8 shows the results of a fast acceleration/ deceleration bench test of grease-lubricated bearings in actual alternators. Flaking occurred between 700 and 900 hours of operation in the outer rings of samples of both the 6303 and 6304 bearings lubricated with a conventional type of grease while no flaking occurred during the same period in those lubricated with MA7 grease[4), 5)].

Table 8 shows the estimated residual life of grease collected from used automotive alternator bearings. In the analysis, each sample showed life exceeding 400 000 km.

Photo 3 shows the appearance of a bearing after use in an alternator.

4. Conclusion

Some technical breakthroughs have been achieved which have contributed to automotive alternator bearing specifications being what they are today. The most noteworthy among them was the development of a new grease which eliminated the peculiar problem of early flaking of the outer rings of alternator front bearings. This breakthrough has greatly improved the life of automotive alternator bearings. In the future, it will be important to develop and produce smaller alternator bearings with greater cost efficiency by fully utilizing such life-extending measures, and to make various improvements in response to requirements for higher-temperature, high-speed performance. It should also be noted that the knowledge and experience garnered in the process of developing alternator bearings can also be applied effectively to bearings for other applications under rigid operating conditions. Research and development of alternator bearings to meet the escalating requirements of our customers is ongoing at NSK.

References:

1) Murakami, Y. et al, “Study on Fatigue Mechanism of Bearings for Automotive Alternators,” NSK Technical Journal No. 656, (1993) 1-14. [in Japanese]
2) Murakami, Y., Naka, M., Iwamoto, A. and Chatell, G., “Long Life Bearings for Automotive Alternator Applications,” SAE Technical Paper Series 950944, (1995).
3) Takemura, H., Murakami, Y. and Furumura, K., “Rolling Fatigue under Bending Stress,” Preprints of JAST Tribology Conference, (1993). [in Japanese]
4) Naka, M., et al, “Rapid Acceleration/Deceleration Test of Automotive Accessory Bearings,” Preprints of JAST Tribology Conference, (1993). [in Japanese]
5) Kaneda, et al, “Evaluation of Grease Characteristics under Elasto-hydrodynamic Lubrication,” Preprints of JAST Tribology Conference, (1994). [in Japanese]

Kenji Ohkuma

Masao Koshigaya

Analysis of Steering Column Vibration

Kenji Fujikawa
Automotive Parts Technology Department, Automotive Technology Center

ABSTRACT

Presently, requirements for reducing noise, vibration and harshness (NVH) in automobiles are more stringent than ever. One form of NVH is the vibration of steering systems which occurs sometimes at high speeds or when the engine is idling. In order to reduce this vibration, accurately assessing the resonant frequency of steering systems is critical. This paper explains a method for achieving this with steering systems mounted in actual vehicles.

1. Introduction

When you are driving a car or its engine is idling, you may sometimes perceive appreciable vibration of the steering wheel. The main causes of this vibration ("steering vibration") are the vibrating force of the periodic explosions occurring in the engine and the rotational vibrating force from the tires being out of balance. The former can be the cause of steering vibration when the engine is idling, while the latter can be so when the car is running at high speeds. In recent years, with control of noise, vibration and harshness (NVH) becoming an important consideration for the commercial value of vehicles, controlling steering vibration has become an important requirement.

The steering system, consisting of a steering column and a steering wheel, is mounted on instrument panel reinforcements as shown in Fig. 1. Effective ways to reduce steering vibration are to reduce the vibration forces and, as far as possible, to keep the resonant frequency of the steering system away from the resonant frequency of the vehicle body and the frequencies of the aforementioned vibration forces. For this reason, it is important to ascertain, by actual measurement or estimation, the resonant frequency of the steering system in actual vehicles.

The following sections present first, a few examples of commonly-used methods for measuring or analyzing resonant frequencies, and then, a natural frequency estimation method based on a substructure synthesis method using a personal computer.

2. Measuring and Analytical Methods

2.1 Method which regards the steering system as mounted on a rigid body

This is the most fundamental method, treating the steering system as mounted on a rigid jig as shown in Fig. 2 (a). The steering wheel is made to vibrate by blows from a rubber hammer, and the responses are measured with an accelerometer. Fig. 2 (b) shows a spectrum of measured responses. The peak of the spectrum denotes the resonant frequency of the steering system.

As this method is relatively easy, it is often used for the evaluation of steering column systems. However, since the steering column mounts in vehicles are somewhat resilient, the resonant frequency of the steering system in an actual vehicle is considerably lower than that determined by this method. It would be best if the resonant frequency of the steering column of every vehicle could be measured when it is actually mounted, but this is impractical, particularly when vehicles of a new model are being developed with their bodies as yet unfinished. The question then becomes how to estimate the resonant frequency by a bench test simulating an actual vehicle.

The following sections describe methods for estimating the resonant frequency of steering systems in actual vehicles.

2.2 Method taking the rigidity of the steering system mount into account (1)

In this method, with the lower steering column mount fixed to the measuring apparatus and the steering wheel supported with a weak spring as shown in Fig. 3 (a), the mobility of the upper steering column mount is measured and drawn, and a mobility diagram of the upper vehicle mount is drawn over the steering system mobility diagram. Generally, in a logarithmic graph as shown in Fig. 4, the mobility diagram based on the mass forms a straight line declining to the right, while the mobility diagram based on the spring forms a straight line rising to the right[1]. The intersection between the two lines is the resonant frequency of the spring-mass system.

Fig. 3 (b) shows the mobility lines of the steering column mounts of two car models, A and B. The rigidity of the steering column mount of model A is lower than that of B. The higher the rigidity, the lower the line shifts parallel, resulting in the shifting of the intersection of the line with the steering column mobility diagram toward the right, i.e., toward higher frequency. In order to increase the resonant frequency, therefore, it is important to increase the rigidity of the mount on the vehicle body and create a design which effectuates either the shifting of the mobility diagram of the steering system upwards or the shifting of the anti-resonant frequency on the steering mobility diagram to the right.

This mobility-based method works relatively well for steering systems not significantly affected by the rigidity of the lower mount, but can produce errors for those where

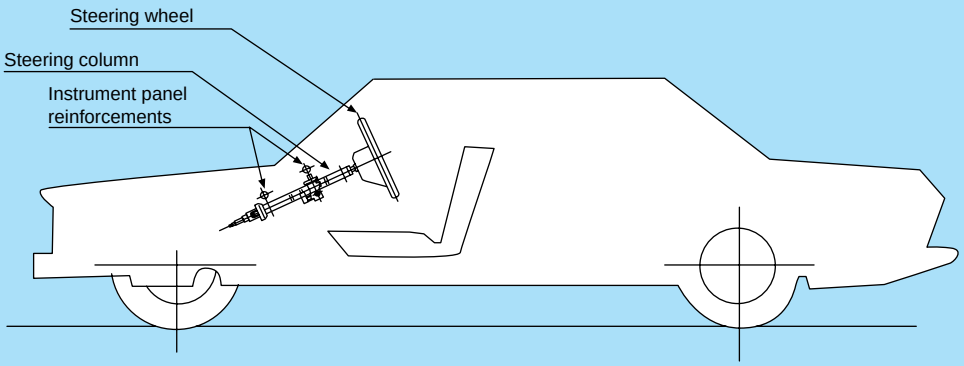

Fig. 1 Body of a car

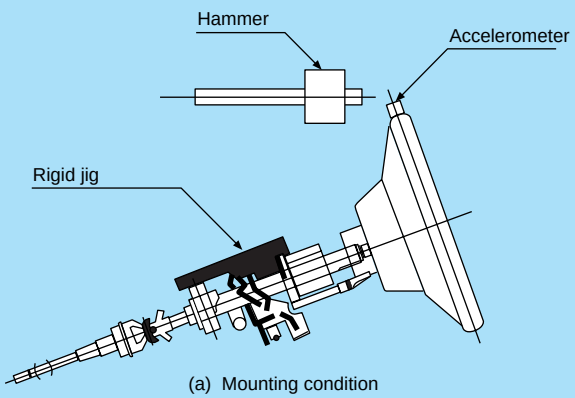

(a) Mounting condition

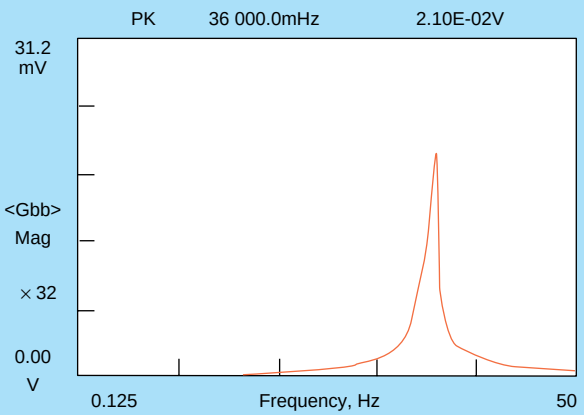

(b) Spectrum

Fig. 2 Test using a rigid jig

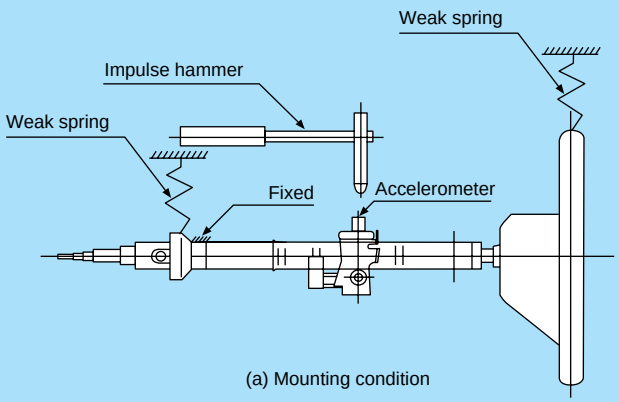

(a) Mounting condition

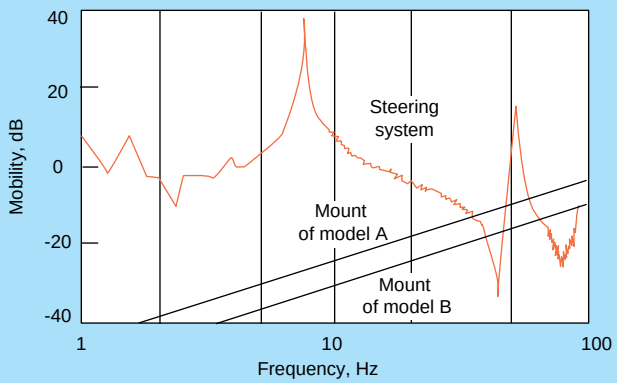

(b) Mobility chart

Fig. 3 Mobility method

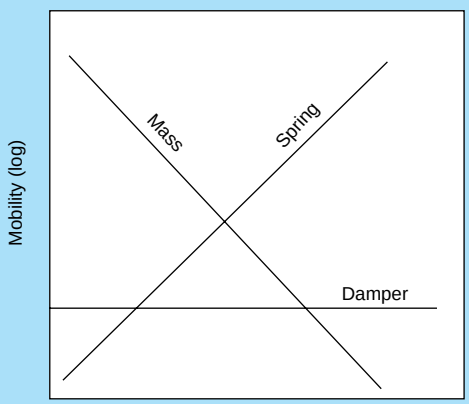

Fig. 4 Mobility

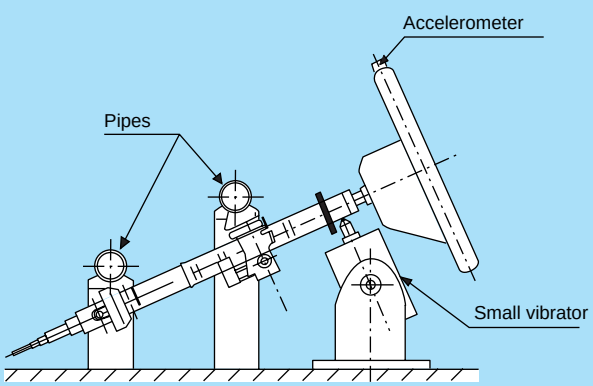

Fig. 5 Test using two pipes

the rigidity of the lower mount is not negligible.

The following section describes the measuring method that takes the effect of the rigidity of the lower mount into account.

2.3 Method taking the rigidity of the steering system mount into account (2)

In this method, a steering system is attached to two pipes which are regarded as instrument panel reinforcements, the steering column is vibrated by a small vibrator, and responses of the steering column are measured as shown in Fig. 5. The flexural rigidity of the upper and lower pipes can be adjusted to the rigidity of an actual vehicle by adjusting the pipe supports. Vibration within a certain range of frequencies including the resonant frequency is applied by a constant vibrating force, and the acceleration responses of the steering wheel are measured.

This method is effective for accurately estimating resonant frequency only if the pipe supports are properly adjusted so the rigidity of the pipes matches the rigidity of the instrument panel reinforcements. To ensure proper pipe rigidity, however, many adjustments of the pipe supports usually need to be made requiring a lot of time.

The following section describes a simple technique, based on a substructure synthesis method, for estimating the resonant frequency in actual vehicles in a relatively short time.

3. Analysis by Substructure Synthesis Method

3.1 Substructure synthesis method

This method divides a complicated vibration system consisting of many components into simple vibration subsystems, analyzes or measures the vibration characteristics of these subsystems, and estimates the characteristics of the entire vibration system by synthesizing the vibration characteristics of the subsystems. This method is simple and easy because only individual subsystems, not entire systems which can't be analyzed or tested, need to be considered.

The substructure synthesis method is subdivided into a transfer function synthesis method, a mode synthesis method and a characteristic matrix synthesis method. The transfer function synthesis method is further subdivided into an explicit method of solution and a dynamic rigidity combination method. The following sections describe a process we developed for estimating the resonant frequency of steering systems in actual vehicles using the dynamic rigidity combination method.

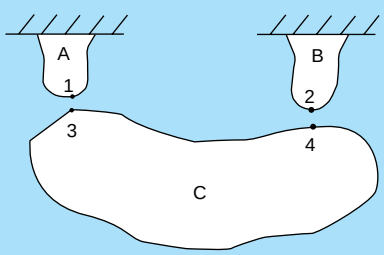

Fig. 6 Substructure synthesis method

3.2 Dynamic rigidity combination method

Suppose that subsystems A and B are joined to subsystem C at points 1 and 3, and 2 and 4, respectively.

Letting X_i equal the displacement response at each point,

G_{ij} equal compliance at each point, and

K_{ij} equal dynamic rigidity at each point,

we then get:

$$\begin{Bmatrix} X_1 \\ X_2 \end{Bmatrix} = \begin{bmatrix} G_{11} & O \\ O & G_{22} \end{bmatrix} \begin{Bmatrix} F_1 \\ F_2 \end{Bmatrix} \quad (1)$$

$$\begin{Bmatrix} X_3 \\ X_4 \end{Bmatrix} = \begin{bmatrix} G_{33} & G_{34} \\ G_{43} & G_{44} \end{bmatrix} \begin{Bmatrix} F_3 \\ F_4 \end{Bmatrix}$$

Multiplying both sides of Eq. (1) by a dynamic rigidity matrix gives:

$$\begin{Bmatrix} F_1 \\ F_2 \end{Bmatrix} = \begin{bmatrix} K_{11} & O \\ O & K_{22} \end{bmatrix} \begin{Bmatrix} X_1 \\ X_2 \end{Bmatrix} \quad (2)$$

$$\begin{Bmatrix} F_3 \\ F_4 \end{Bmatrix} = \begin{bmatrix} K_{33} & K_{34} \\ K_{43} & K_{44} \end{bmatrix} \begin{Bmatrix} X_3 \\ X_4 \end{Bmatrix}$$

By combining subsystems A and B and subsystem C, as in the finite element method, we get:

$$\begin{Bmatrix} F_{e1} \\ F_{e2} \end{Bmatrix} = \begin{bmatrix} K_{11}+K_{33} & K_{34} \\ K_{43} & K_{22}+K_{44} \end{bmatrix} \begin{Bmatrix} X_1 \\ X_2 \end{Bmatrix} \quad (3)$$

We now can find displacement responses by inverting the dynamic rigidity matrix of Eq. (3).

When we estimate the resonant frequency in an actual vehicle, subsystems A and B in Fig. 6 correspond to the steering mounts of the vehicle, and subsystem C to the steering system.

3.3 Results of estimation

Using a personal computer programmed as described

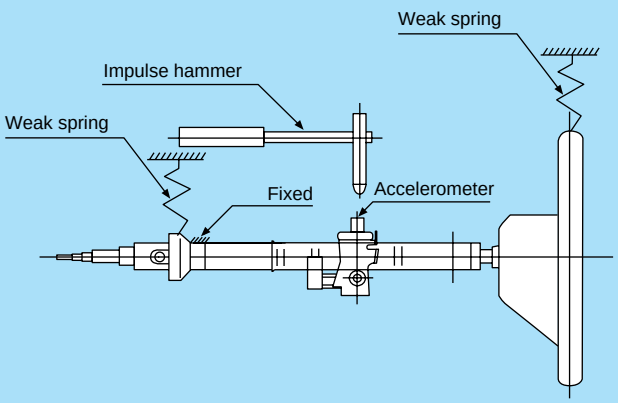

Fig. 7 Test method

above, we estimated the resonant frequency of a steering system. In the experiment, we suspended a steering column system with weak springs as in Fig. 7 and measured the transfer functions G_{33} to G_{44} of the steering system. Fig. 8 shows examples of the measurements.

In modal analysis, modal parameters are generally extracted from measured transfer functions. In the program being described, however, measured transfer functions were used as they were.

The rigidity K_{11} and K_{22} of the mounts can be obtained by actual measurement of the vehicle steering column mounts or by analysis using the finite element method (FEM).

Thus, by using values obtainable by measurement or analysis as described above, the resonant frequency in actual vehicles can be estimated. An example of the synthesized transfer function is shown in Fig. 9. The first peak denotes the point of resonance of the 1st order.

Table 1 compares estimated and measured values. The measured values are values measured by the method described in Section 2.3 above. Indicating the validity of this estimation method, the estimated and measured values in the table show good agreement with each other.

When this estimation method is used, data obtained by measurement can be stored in the memory of a personal

Table 1 Comparison of estimated and measured resonant frequencies

Car model	Rigidity at fixture (N/mm)		Resonant frequency (Hz)	
	Upper	Lower	Estimation	Measurement
A	1 400	3 300	31.5	31.8
	2 900	2 900	35.0	34.8
B	2 900	2 300	34.0	33.8
C	2 000	2 000	29.5	29.9
	2 900	2 900	31.3	31.1

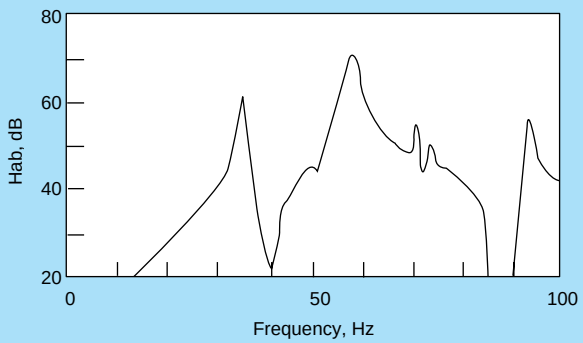

Fig. 9 Estimated transfer function

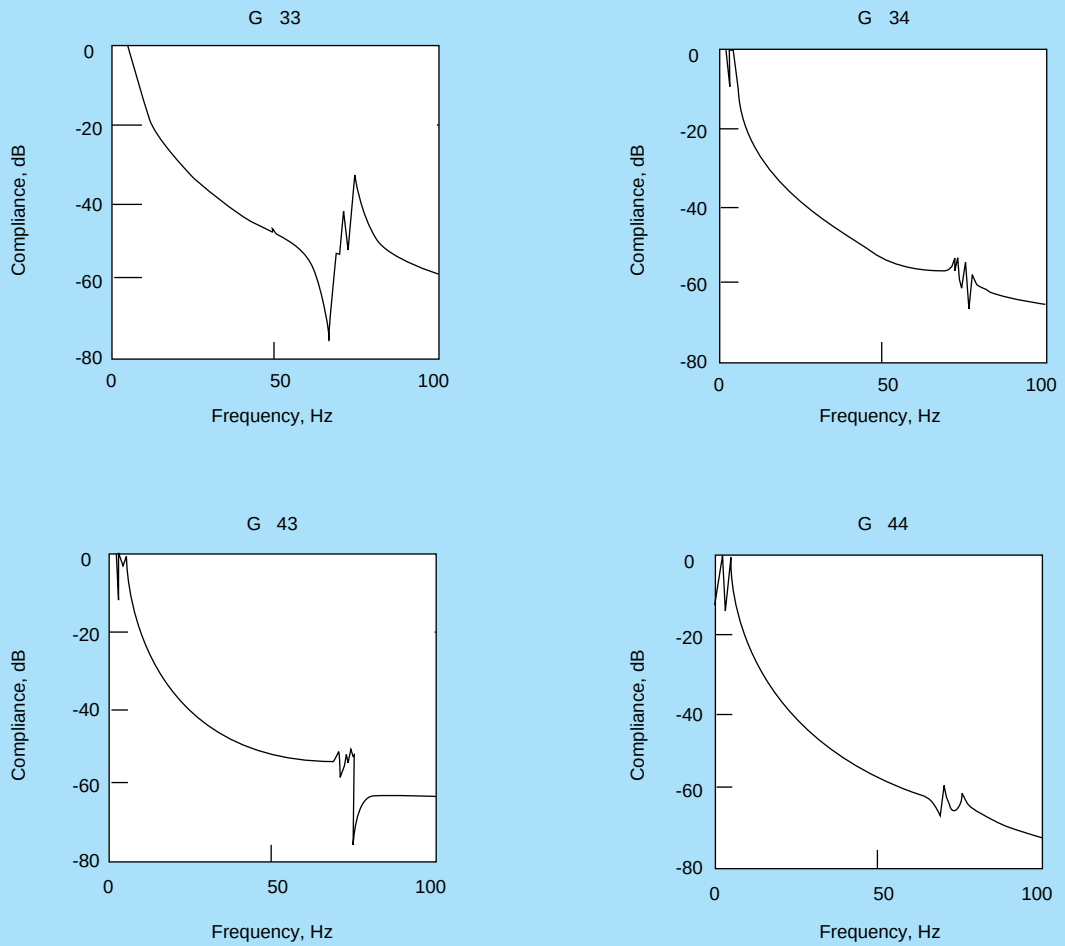

Fig. 8 Transfer function measurement results

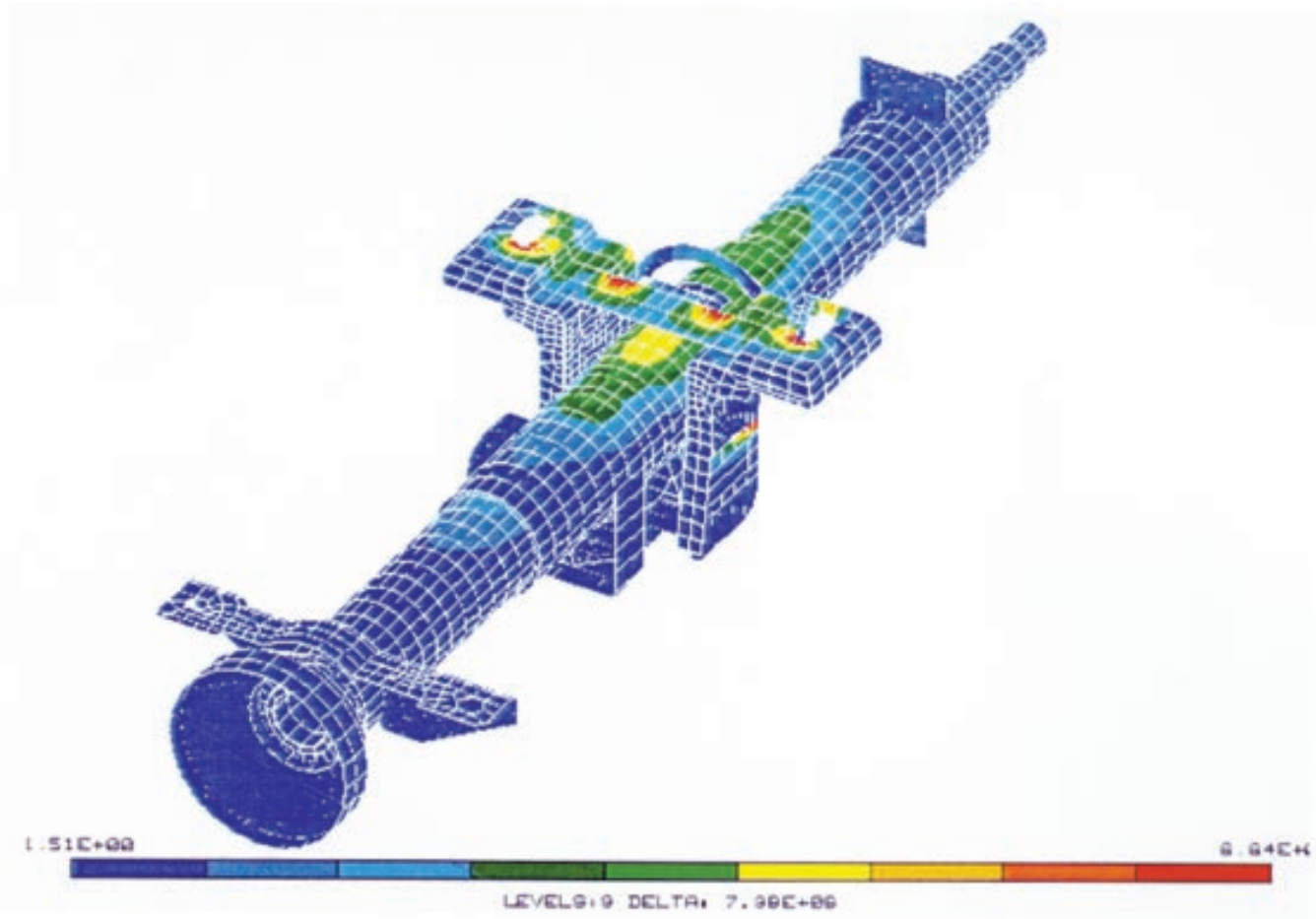

Fig. 10 FEM analysis (first mode)

computer. Even if the rigidity of the steering system mounts of the vehicle are changed due to design alterations, the resonant frequency after the change can be easily estimated, without the need for re-measurement, by entering the new rigidity values into the PC.

4. Conclusion

This report has presented some methods for measuring and estimating the resonant frequency of automotive steering systems. Analytical approaches using FEM are also often used nowadays in many fields. The Automotive Parts Technology Department at NSK also uses static and dynamic analyses for various products.

Fig. 10 shows an example of steering column vibration analysis using FEM. Advantages of FEM analysis include that it shows the locations of stress concentrations and insufficient rigidity, and cuts product development time and cost by reducing prototype production.

Research and development has been actively undertaken at NSK in pursuit of low-cost, lightweight and highly rigid steering columns.

References:

1) Taniguchi, O., "Vibration Engineering Handbook," Yokendo (1985), 668 - 674. [in Japanese]
2) Nagamatsu, A. and Ohkuma, M., "Substructure Synthesis Method," Baihukan (1991). [in Japanese]

Kenji Fujikawa

EA Spherical Roller Bearings

NSK's spherical roller bearing line-up has included the standard CD type with pressed-steel cages and the high-capacity H type with plastic cages.

However, NSK recently introduced EA spherical roller bearings which have the advantages of both types and, moreover, incorporate performance improvements making them the next generation of spherical roller bearings.

This article presents NSK's new EA spherical roller bearings.

Photo 1 EA spherical roller bearing

1. Design Concept of EA Bearings

The newly conceptualized and designed interior of EA bearings (Photo 1) offers outstanding features which fulfill the exacting requirements of today's industry. (Patented in the U.S.A., the U.K. and Germany. Patent pending in Japan.)

Fig. 1 compares the interior designs of EA and CD spherical roller bearings.

2. Features of EA Bearings

(1) High Capacity and Long Life

In CD bearings, a guide ring controls roller movement. However, this function in EA bearings is assumed by the cage, thus allowing the omission of the guide ring. The optimum design of the cage and inner and outer rings provides space for larger and more rollers. As a result, the load capacity is increased 10 to 20% and the bearing life is extended 30 to 80%.

Fig. 2 compares the load capacities of EA and CD bearings.

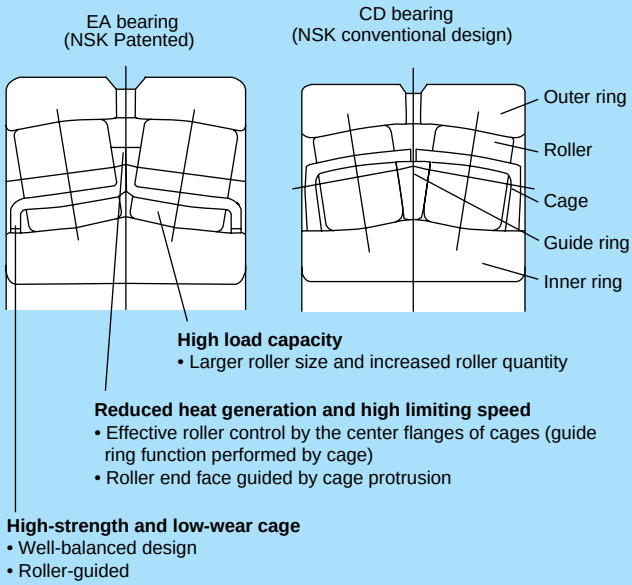

Fig. 1 Bearing interior design comparison

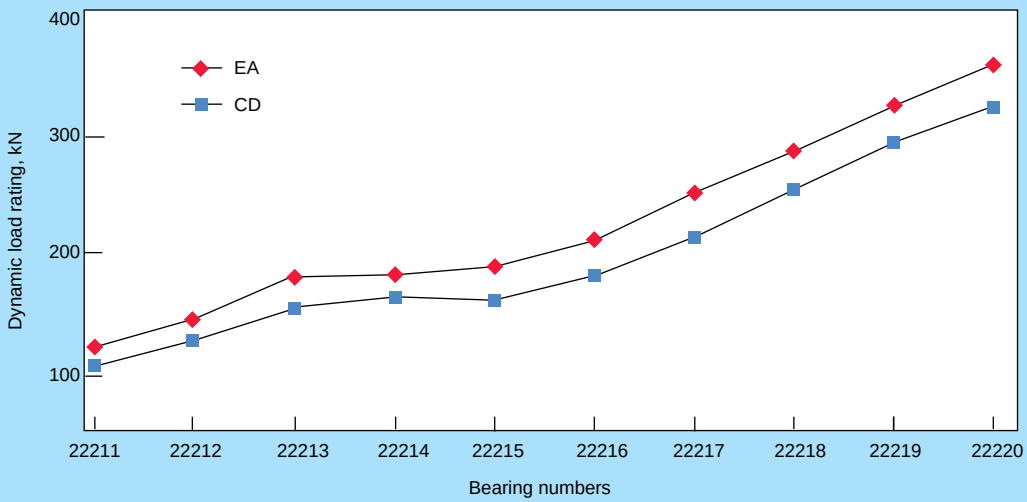

Fig. 2 Dynamic load ratings of 222XX Series

(2) Low Temperature Rise and High Limiting Speed

The cages for both rows, which contact and support each other at the back face of the center flanges, have their rotation maintained and guide the roller end faces with support from the flanges. The clearance tolerance of the cage is specified to be small so that the motion of the rollers is precisely controlled and heat generation is minimized even without the guide ring used in previous types.

Due to the above and the optimum design of the rollers and outer and inner rings, the temperature rise of EA bearings is minimal. As a result, the limiting speed is greatly increased compared to conventional spherical roller bearings.

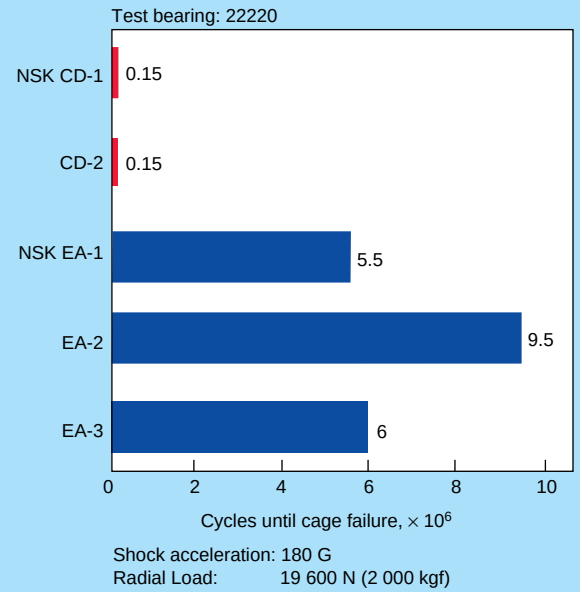

Fig. 4 Results of cage strength test

Fig. 3 compares the limiting speeds of EA and CD bearings.

(3) High-strength and Low-wear Cage

Effectively using the space vacated by the guide ring, a strong and well-balanced cage was created through detailed study of optimum cage design using structural analysis. A severe test of the strength of these cages has shown their toughness and durability.

Fig. 4 shows EA and CD cage strength test results.

The high accuracy and resulting drastic reduction in cage wear of these roller-guided pressed cages was made possible by improvements in press processing technology.

(4) High-temperature Specifications

Special heat treatment for the outer and inner rings is standard and the bearing can be used up to 200°C.

The maximum operating temperatures are as follows:

EA ·····200°C
CD ·····120°C
H ·····120°C

3. Conclusion

New EA spherical roller bearings are tough, high-capacity bearings which were created incorporating advanced analysis technology, press processing improvements, and severe evaluation tests. As a result, the bearings represent the next generation of spherical roller bearings for CD and H-type replacements. Mass production of these bearings is under way at NSK as we look to increase their sales in various industries.

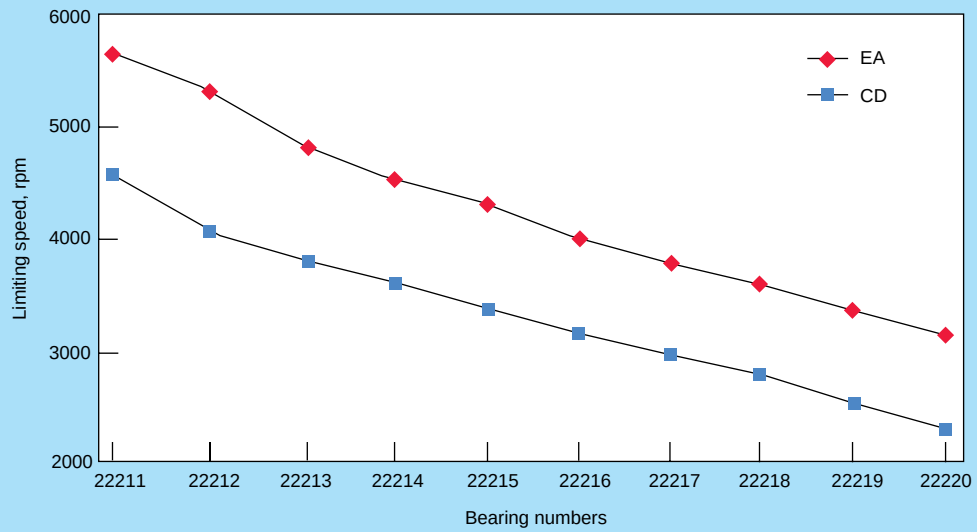

Fig. 3 Limiting speed of 222XX Series with oil lubrication

New LA Series Linear Guides for Machine Tools

NSK has been marketing LY Series linear guides to the machine tool industry for fifteen years. LY Series linear guides have been widely used as guiding mechanisms for machine tools thanks to their highly rigid 4-point-contact structure and proper frictional resistance which enables vibration damping.

However, remarkable improvements in the speed, accuracy and reliability of machine tools have necessitated increases in the rigidity and load-carrying capacity of linear guides. In response to this, NSK has developed LA Series linear guides (Photo 1) with much higher rigidity and load capacity than the existing LY Series.

This article presents the new LA Series linear guides.

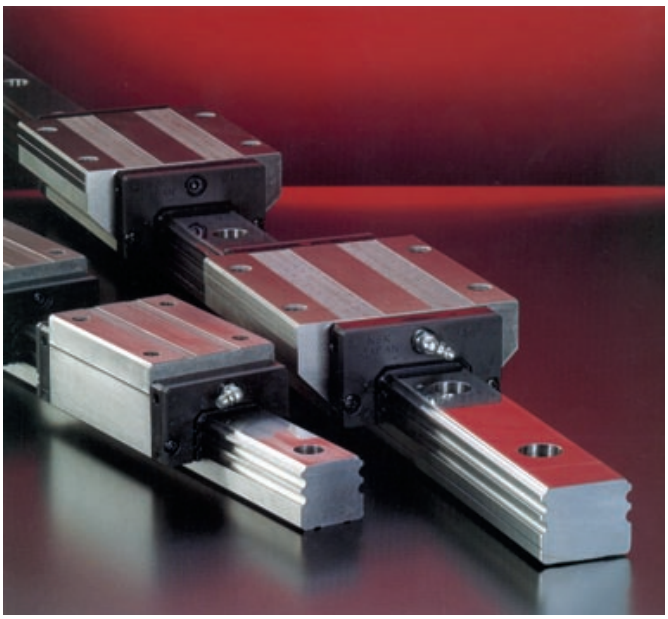

Photo 1 New LA Series Linear Guides for Machine Tools

1. Features

The design of LA Series linear guides for machine tools retains the advantageous 4-point-contact structure of the LY Series while incorporating improvements to achieve higher performance and reduced friction. Features include:

(1) Higher Rigidity and Higher Load Capacity
Through the inclusion of a third groove on each side, rigidity and load capacity are 1.4 to 1.5 times higher than the LY Series.

(2) Lower Friction Force
By achieving a better balance between 4-point and 2-point contact, friction force is 50-60% of that of the LY Series.

(3) Standardized
LA Series linear guides have the same mounting dimensions as previous series which are becoming standard in the market.

In Fig. 1, LY and LA Series cross-sections and groove shapes are compared.

LA Series linear guides have three grooves on each side for a total of six. The upper and lower grooves on either side are circular arc grooves, and the ratio between the groove and ball radii has been made smaller thereby achieving higher rigidity and load capacity with limited frictional resistance. On the other hand, the retention of the 4-point-contact gothic-arch-type middle groove means that appropriate friction force and highly precise measurement and grinding are secured.

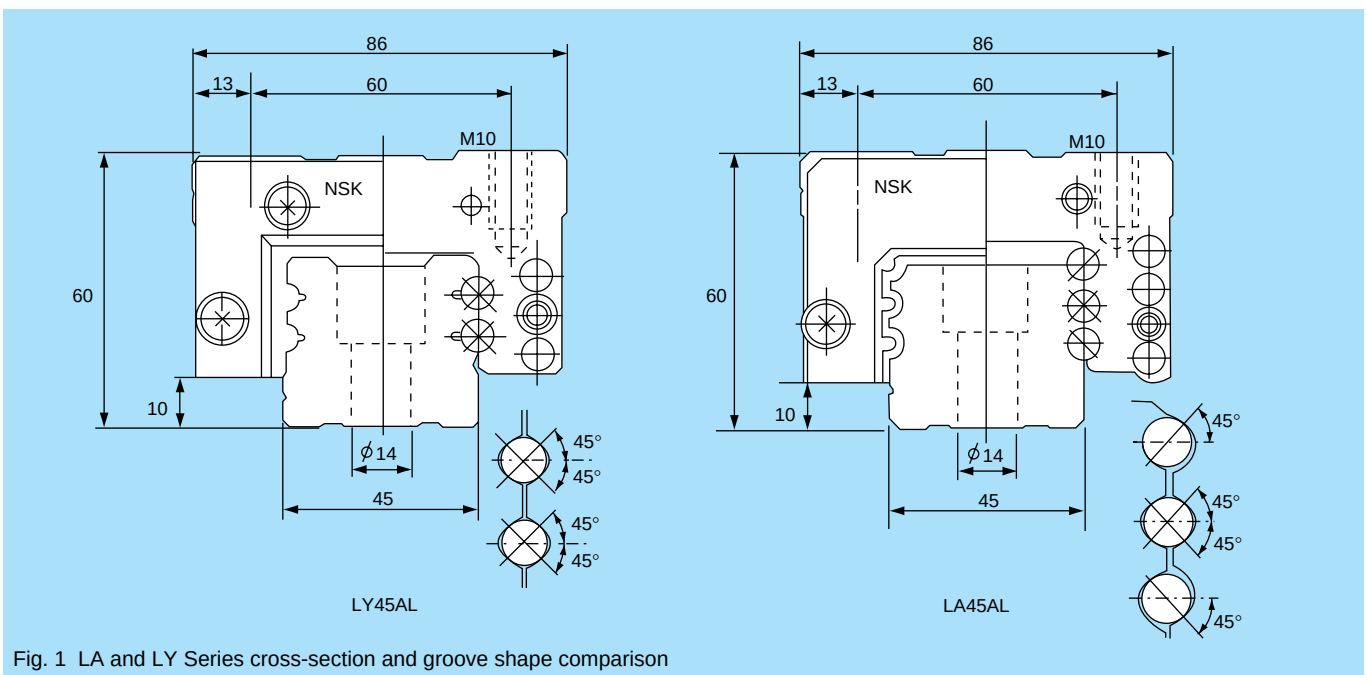

Fig. 1 LA and LY Series cross-section and groove shape comparison

Table 1 LA and LY Series characteristics comparison

		LA45 long type P5Z4	LY45 long type P5Z4
Ball diameter D_a	(mm)	6.35	6.35
Contact angle		45°	45°
Number of contact points		4	4
Dynamic load rating C	(kN)	89	63
Static load rating C_0	(kN)	166	103
Preload F_p	(N {kgf})	7750 {790}	4410 {450}
Calculated rigidity (N/μm {kgf/μm})		1640 {167}	1100 {112}
Friction rating	(N {kgf})	66 to 93 {6.7 to 9.5}	108 to 157 {11 to 16}

Table 2 Types of LA Series linear guides (High load/Ultra-high load)

Shape code	AN/BN	AL/BL	EL/GL	FL/HL
Shape	Square		Flanged	
	Higher	Lower		
Model No.	Tapped mounting holes			Drilled mounting holes
LA30	○		○	○
LA35	○	○	○	○
LA45	○	○	○	○
LA55	○	○	○	○
LA65	○		○	○

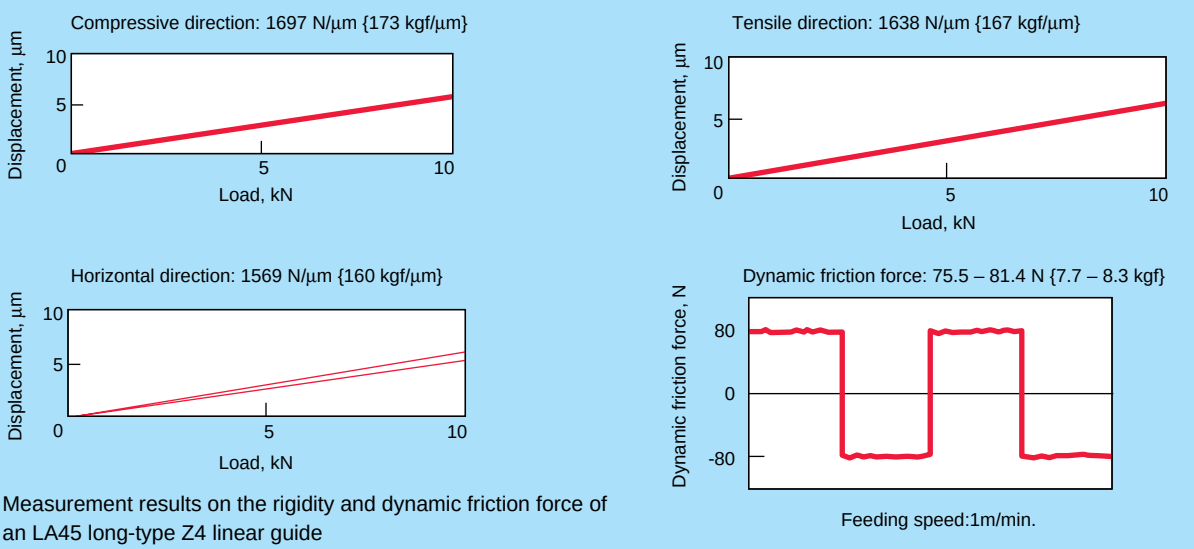

Fig. 2 Measurement results on the rigidity and dynamic friction force of an LA45 long-type Z4 linear guide

In addition, as in the LY Series, the contact angle is 45°, making the load capacity and rigidity nearly the same in every direction. As a result, loads applied from diverse directions can be sustained without adversely affecting overall balance.

Even though the LA Series uses balls as rolling elements, its unique groove structure makes rigidity and load capacity equivalent to linear roller bearings.

Table 1 compares characteristics of the LA and LY Series.

Fig. 2 shows measurement results on the rigidity and frictional resistance of an LA45 long-type linear guide. As can be seen, the goals behind the development of the LA Series have been achieved.

2. Available Ball Slide Types

There are two types of ball slide in the LA Series: flanged and square. The mounting holes for flanged-type ball slides are either tapped or drilled while those of square ones are tapped only.

Square ball slides are available in two assembly heights: the higher N type and the lower L type (except certain model numbers). Also, in addition to the standard high-capacity type, a special longer ultra-high-load capacity type is available.

Table 2 lists the various ball slide configurations of LA Series linear guides.

3. Accuracy and Preload

Similar to the LY Series, there are four accuracy classes in the LA Series: P3 (ultra precision), P4 (super precision), P5 (precision) and P6 (semi precision). Also, there are two kinds of preload: Z3 (medium preload) and Z4 (heavy preload).

4. Conclusion

We have presented here our new LA Series linear guides with high rigidity and load capacity equivalent to linear roller bearings. We are confident that the linear guides of this series will be used widely as the guiding mechanisms for the ever-faster, ever-more accurate machine tools of today and the future.

P Series Robot Modules

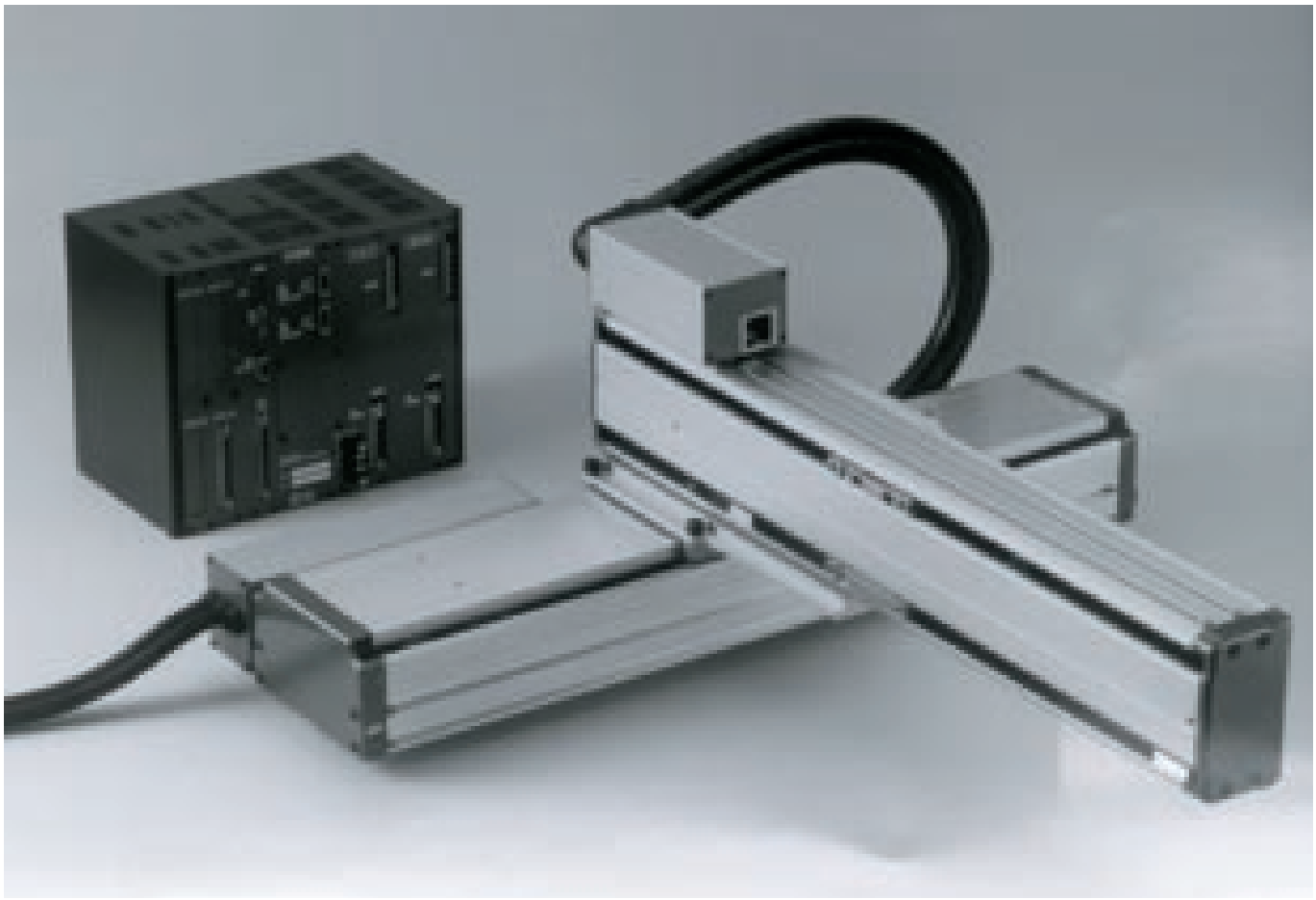

Photo 1 P Series Robot Module

NSK's mono-axis robots, "Robot Module™", are widely acclaimed due to their outstanding features which include: the great variety of Cartesian-type robots made possible through various combinations of module main unit, controller, cable and other components; the wide range of available strokes; high load capacity; and high resistance to dust attained by the innovative, specially-designed seal belt. The latest addition to NSK's robot module line-up, the P Series (Photo 1), has a newly-conceptualized and designed module main unit and controller. In this article, the features and specifications of the P Series are presented.

1. Features

The P Series was designed with easy operation and excellent cost performance in mind for labor-saving applications which were previously cost-prohibitive such as transporting light to medium loads, small component assembly, and sealing.

1.1 Easy operation

(1) The new absolute value encoder makes returning to the home position unnecessary in normal operation.
(2) Among competing products in the 40 kg mass capacity class, the P Series robot module with the indirect motor mount specification has the shortest overall length.
(3) Use of high-load capacity grease makes replenishment unnecessary for 15 000 km of operation in clean environments with ambient temperatures ranging from 0 to 40°C.
(4) The new design allows PCB units in the controller to be changed making maintenance easier.
(5) The brake which is standard with some models can stop the robot module quickly making the robot safer and more reliable.
(6) P Series Robot Modules are equipped with all the safety and reliability features required in today's workplace and meet all CE Marking Directives.

1.2 Performance

(1) In a two-axes combination system configuration, the PH module, structurally sound with its two linear guides, becomes the X or lower axis, and the PM module, with its lightweight frame and high rigidity, becomes the Y or upper axis. As a result, high precision operation and reduced tact time are achieved.
(2) State-of-the-art technology such as multi-tasking, 3-dimensional arch motion, and sinusoidal acceleration and deceleration enables a wide variety of functions and excellent performance.

Table 1 Module main unit variations

Ball screw lead (mm)	Motor mounting	Brake	Maximum speed (m/s)	Transportable mass (kg)	
				PH module	PM module
20	Straight	None	1.2	Horizontal 40	Horizontal 20
20	Indirect	None	1.2	Horizontal 40	Horizontal 20
10	Straight	None	0.6	Horizontal 80	Horizontal 40
10	Straight	Attached	0.6	Vertical 25	Vertical 8

Table 2 Module main unit specifications

	PH module	PM module
Stroke (mm)	100~800 (in steps of 100)	100~800 (in steps of 100)
Rolling transportable moment* (N•m)	113	19
Pitching transportable moment* (N•m)	97	25
Yawing transportable moment* (N•m)	66	22
Repeatability (mm)	±0.02	±0.02
Motor output (w)	200	100

* Transportable moment represents the value at which the fatigue life becomes 10 000 km when moment in a single direction is continuously applied.

Table 3 Controller Specifications

Number of controlled axes		1 to 4
Power supply		Single phase AC200V/220V±10% or 100V/110V±10%
Program capacity		5000 steps/128 programs
Max. number of points		4000
Program command	Movement	Return to home, PTP, 3-axes linear/circular interpolation, continuous path, arch motion, 2-axes palletizing
	Sequence, Other	General input/output, timer, conditional/ unconditional jump, repeat, sub-routine, interrupt
Control function		Feed-forward compensation, digital filter
Input/ Output	Exclusive inputs	Servo-on, emergency/cycle/temporary stop, program selection/start, alarm clear
	Exclusive outputs	Preparation and return-to-home complete, alarm, cycle stop, hold, program operation restart, mode condition
	General input/output	16 points in + 16 points out expandable to 64 points (32 points for the mono-axis model)
PC interface program (sold separately)		[For Windows 95] Program data upload/download, off-line program editing, printing, direct operation

2. Specifications

There are two module main units in the P Series, the PH module and the PM module. Each module is available in four types characterized by ball screw lead, motor mounting position, maximum speed, load capacity and whether or not a brake is attached. Strokes from 100 to 800 mm are available in 100 mm-steps for each type.

Please see Table 1 for the module main unit variations, Table 2 for the module main unit specifications, and Table 3 for the controller specifications.

3. Conclusion

When speaking about industrial robots, vertically articulate-type robots or SCARA-type robots are imagined, but recently the use of mono-axis robots mainly for labor-saving applications is increasing due to their relatively low cost and the variety of Cartesian-type robots they make possible. Fully automated production lines are often constructed exclusively with mono-axis robots.

NSK's P Series Robot Modules with absolute encoders were developed focusing on easy operation and excellent cost performance. We believe they meet the exacting demands of today's industry for labor-saving equipment.

Rack-type Tilt-wheel Steering Columns

Tilt-wheel steering columns are popular nowadays in the United States because they are easy for drivers to adjust to a comfortable driving position and move out of the way when getting into or out of a vehicle.

Up to now, NSK has been producing friction-type and gear-type tilt-wheel steering columns. Recently added to this product line is a low-cost and highly rigid rack-type tilt-wheel steering column which has been adopted for use in vehicles produced inside and outside Japan.

This report describes NSK's rack-type tilt-wheel steering columns.

1. Construction

Fig. 1 illustrates its construction. The wheel tilt can be locked and unlocked by engaging and disengaging, respectively, the movable rack, which is attached to the bottom center of the aluminum die-casted upper bracket, and the fixed rack, which is attached to the bottom of the lower bracket. In its locked position, the lever is pulled to the left in Fig. 1 by the spring which keeps the pin in the movable rack pushed up so that the movable rack is kept engaged with the fixed one.

When the lever in Fig. 1 is drawn up, the pin in the movable rack is driven down thereby disengaging the upper and lower racks and unlocking the steering wheel so that it can be adjusted to a desired tilt position. Releasing the lever after adjusting the steering wheel allows the spring to lock the steering wheel automatically. The pressure angle of the engagement of the two racks is set at smaller than the angle of friction.

2. Features

(1) Since the pressure angle of the engagement of the two racks is set smaller than the angle of friction, the racks cannot be disengaged unless the lever is pulled. This has permitted the elimination of many of the parts that were formerly needed around the lever, resulting in the steering column taking up less space in the downward direction.

(2) The construction of the tilt pin and of both of the rack-to-bracket joints has been improved to ease assembly.

(3) The vibration characteristics and the overall rigidity of the steering column are better than conventional types because of the aluminum die-casted upper bracket and the improved rigidity of the racks and other parts.

3. Performance

3.1 Inertance* (vibration rigidity)

To avoid resonance between the steering column and the vibration of a vehicle when idling or operating at high speed, it is important that the inertance of the steering column be low.

As shown in Fig. 2, the rack-type tilt-wheel steering column has inertance of 33 dB/35 Hz, approximately 3.5 dB/35 Hz lower than that of our gear-type tilt-wheel steering column which is already credited with being highly rigid.

*Inertance: When a periodic vibration force having an amplitude of F is working on a point of an elastic body, measuring by A the periodic responses of acceleration caused by F gives a transmission characteristic between F and A. A/F is termed inertance.

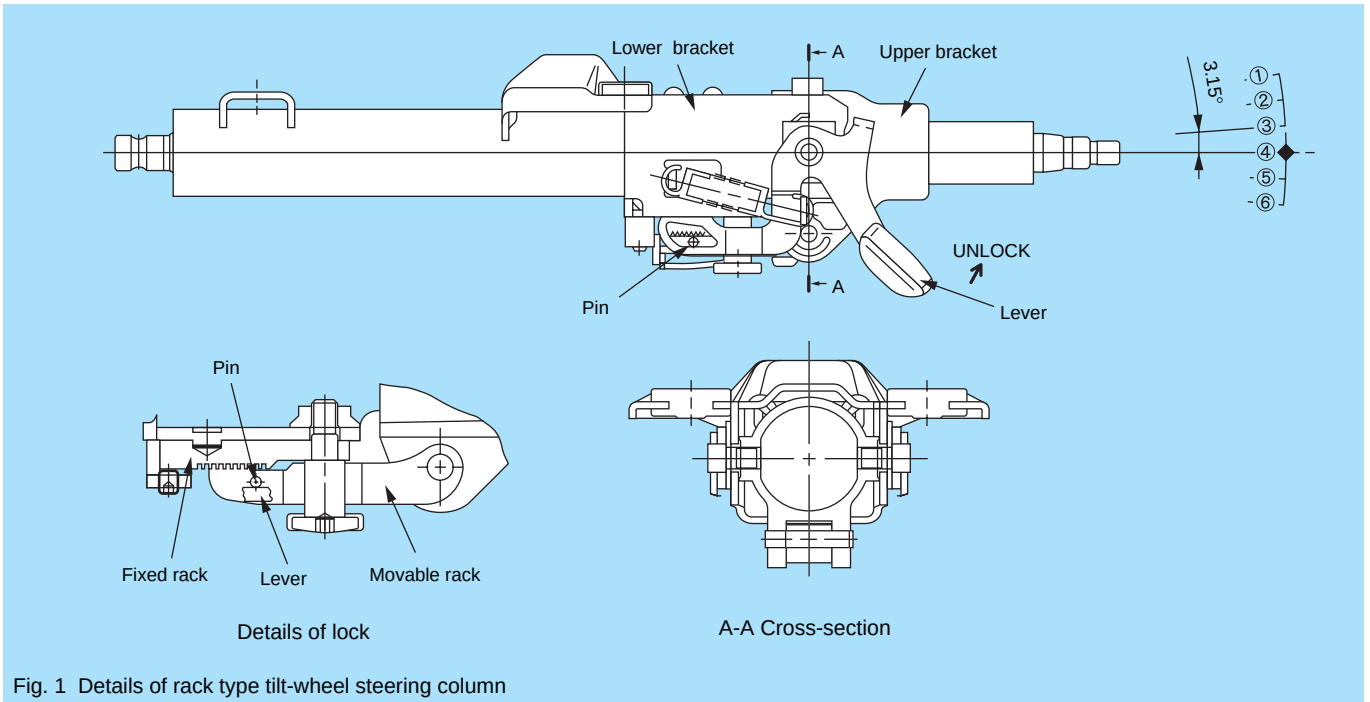

Fig. 1 Details of rack type tilt-wheel steering column

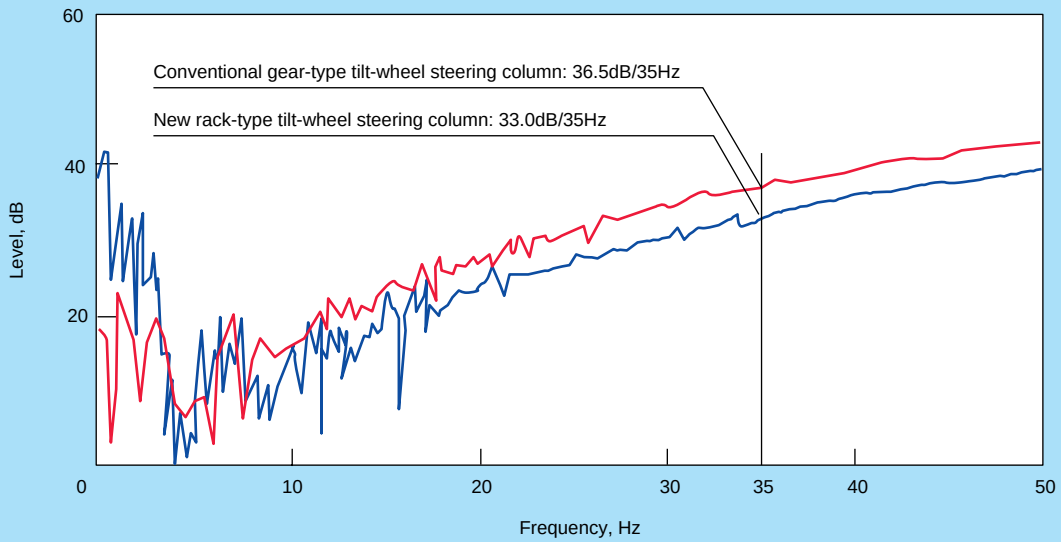

Fig. 2 Bench test inertance measurements (Vibration characteristics)

Table 1 Results of durability tests

Test item	Test conditions	Result
Tilt operation durability	A cycle consisting of [locking at lower tilt position → jerking up → locking at upper tilt position → pulling back] was repeated 2×10^4 times	No cracking occurred
Bending durability	±490 N was applied to the steering wheel 10^5 times	No cracking occurred
Vibration durability	Vertical acceleration of ±2.5 G was applied to the steering wheel 10^7 times	No cracking occurred
Collision test	Air bag: FMVSS 208 (conducted on actual vehicle)	Satisfied FMVSS 208

3.2 Main specifications

(1) Tilt lock intervals: 3.15°
(2) Number of lock positions: 6
(3) Tilt lever operating angle range: 10°
(4) Tilt lever operating force: 34 N, max.
(For tilt lever whose length from the tilt center is 90 mm)

3.3 Durability test results

Table 1 shows test results which demonstrate that rack-type tilt-wheel steering columns have sufficient durability for practical applications.